This dissertation has been
microfilmed exactly as received 67-3975

HARDWICKE, Norman Lawson, 1924-
THE MECHANISM OF PARTIAL OXIDATION OF METHANE AT HIGH PRESSURES.

The University of Oklahoma, Ph.D., 1967
Engineering, chemical

University Microfilms, Inc., Ann Arbor, Michigan

Downloaded from SHAREOK. Persistent Handle URL: https://hdl.handle.net/11244/2132

THE UNIVERSITY OF OKLAHOMA

GRADUATE COLLEGE

THE MECHANISM OF PARTIAL OXIDATION OF METHANE AT HIGH PRESSURES

A DISSERTATION

SUBMITTED TO THE GRADUATE FACULTY

in partial fulfillment of the requirements for the degree of

DOCTOR OF PHILOSOPHY

BY

NORMAN LAWSON HARDWICKE

Norman, Oklahoma

1966

THE MECHANISM OF PARTIAL OXIDATION

OF METHANE AT HIGH PRESSURES

APPROVED BY

C. M. Sliepcevich

R. D. Daniels

F. Mark Townsend

R. L. Darrington

DISSERTATION COMMITTEE

ABSTRACT

Although research on combustion mechanisms has been going on for over a century, a general mechanism for oxidation of the simplest hydrocarbon, methane, does not exist. It is known that one or more chain reactions occur, but the specific free radical mechanism has not been found.

The objective of this work was to obtain data on the thermal oxidation of methane at very high pressure, and, with data available in the literature, propose a mechanism for the reaction.

Experiments were conducted at pressures of approximately 15,000, 50,000 and 100,000 psi. and at temperatures of 250- > 420°C. Oxidations were run in the presence of alumina and in the presence of Pyrex-porcelain in order to determine the effects of these materials on the course of the reaction. Residence times ranged from essentially zero to 60 minutes. Oxygen concentration in the methane was maintained at about 8.2 mole percent.

It was found that no change in reaction rate or product distribution occurred after successive experiments with the same experimental conditions in the presence of alumina in the nickel alloy reactor. Pyrex, however, decreased in activity with time, and the Pyrex cylinder

used for the internal heater core shattered after a large number of experiments.

Methanol, carbon dioxide, formaldehyde, formic acid, methyl formate and water increased with increasing pressure, temperature and residence time. At short residence time and temperatures less than 285°C carbon monoxide was not a product at any of the pressures investigated. Once formed carbon monoxide increased rapidly with temperature and residence time. It was concluded that carbon dioxide, carbon monoxide and methanol are made by different reactions. The controlling mechanisms shift with temperature. Formaldehyde appears not to be as important an intermediate at high pressure as at low pressure.

The induction period observed for carbon monoxide at temperatures above 285°C is believed to be due to one free radical specie, $CH_3O\dot{O}$, being complexed at any surface in the reactor. The paramagnetic nature of oxygen may be the key factor. A certain charge or radical concentration may have to be built up at the surface before this particular free radical specie can go into solution (dense phase) and be available for the chain reactions forming carbon monoxide and methanol. However, the free radical complexed at the wall is believed to be capable of reacting with oxygen, forming carbon dioxide, water, $\dot{O}H$ radical and a little performic acid.

Compressibility factors and activity coefficients for methane containing small amounts of oxygenated compounds

were calculated at 50,000 and 97,000 psi. and 550°K. The overall energy of activation was estimated to be 40-46 kcal./mole. Values published in the literature vary from 25 to 96 kcal./mole, with values around 45 kcal./mole obtained in recent years.

ACKNOWLEDGEMENTS

The author gratefully acknowledges the guidance and assistance given by his committee -- Dr. C. M. Sliepcevich, Dr. H. H. Rowley, Dr. F. M. Townsend, Dr. J. L. Lott and Dr. R. D. Daniels. Consultations with Dr. S. E. Babb are gratefully acknowledged.

Mr. E. L. Johnson, Jr., assisted throughout the experimental work, and his contribution is gratefully acknowledged. Mr. A. Koohyar also provided able assistance in obtaining some of the data during the summer of 1965 and his contribution is gratefully acknowledged.

Messrs. J. L. Morrison, W. F. Porter, and C. W. Burns of the Research Institute Central Research Shop were instrumental in maintaining the equipment as needed. Mr. J. E. Fox of the Chemical Engineering Shop and Messrs. J. C. Hood, G. J. Scott and J. Edmondson of the Physics Shop were very helpful in coping with some of the equipment problems.

This work was supported in part by Grant GK-857 from the National Science Foundation. The Monsanto Company provided a tuition scholarship and the University of Oklahoma, a research assistantship.

Autoclave Engineers, Inc., supplied much of the special equipment, and the advice of Mr. W. W. Robertson is particularly acknowledged.

Norman Lawson Hardwicke

TABLE OF CONTENTS

Page

LIST OF TABLES x

LIST OF ILLUSTRATIONS xi

Chapter

I. INTRODUCTION 1

II. FREE RADICAL THEORY 3

III. PRIOR WORK 12

Subatmospheric and Atmospheric Pressure
High Pressure

IV. MECHANISMS PROPOSED BY PREVIOUS INVESTIGATORS 28

V. EXPERIMENTAL EQUIPMENT 43

Feed Section
Compression Section
Reaction Section
Product Collection Section
Auxiliaries
High Pressure Cell

VI. EXPERIMENTAL PROCEDURE 68

Feed Preparation and Storage Prior to Reaction
Conducting the Reaction
Sample Collection

VII. ANALYTICAL EQUIPMENT, PROCEDURES AND CHEMICALS USED 76

Analytical Equipment
Analytical Procedures
Chemicals Used

Page

VIII. DISCUSSION OF RESULTS 85

The Effect of Temperature (Alumina Heater Core)
The Effect of Temperature (Pyrex Heater Core)
The Effect of Time (Alumina Heater Core)
The Effect of Time (Pyrex Heater Core)
Occurrence of Acetone
The Reaction Rate Constant
Proposed Mechanism

IX. CONCLUSIONS 144

NOMENCLATURE 147

LITERATURE CITED 149

APPENDICES . . . . .

A. Summary of Experimental Results 153
B. Calibration of Chromatographs 160
C. Check of Analytical Methods for Formaldehyde, Formic Acid and Methanol 168
D. Curve for Correction of Formaldehyde in the Presence of Acetone 170
E. Sample Calculation of Material Balance 172
F. Calculations for Wet Test Meter 174

LIST OF TABLES

Table		Page
1.	The Relative Reactivity of $\dot{O}H$ and $H\dot{O}_2$ Radicals with Methane and Carbon Monoxide and Formaldehyde	21
2.	Variation of the Order of Reaction with Respect to Oxygen and Methane in the Rate Equation	38
3.	Operating Conditions for Chromatographs	80
4.	Compressibility Factors and Activity Coefficients for Methane at 15,000, 50,000, and 97,000 psi.	129
5.	The Effect of Temperature and Pressure On the Ratio $\frac{H_2O}{CO_2 + CO + CH_3OH}$	142
6.	Summary of Experimental Results at High Pressure	154
7.	Material Balances	156
8.	Summary of Product Data	158

LIST OF ILLUSTRATIONS

Figure		Page
1.	Disappearance of Reactants and Formation of Products at 235 mm Hg Pressure	13
2.	Formation of Formaldehyde and Hydrogen Peroxide at 235 mm Hg Pressure	13
3.	Reaction Rates for Oxidation of Methane in Reactors with Treated Surfaces	17
4.	Disappearance of Oxygen and Formation of Products at 106 atm. Pressure	23
5.	Effect of Temperature on Residence Time	25
6.	Flow Diagram of Feed Section	44
7.	Feed Storage Vessels	48
8.	Flow Diagram of Compression Section	50
9.	200,000 psi. Compression Cylinder	52
10.	200,000 psi. Equipment Inside the High Pressure Cell	55
11.	Flow Diagram of the Reaction and Product Collection Sections	57
12.	200,000 psi. Reactor	59
13.	Internal Heater (Alumina) Attached to Top Cover	61
14.	Oil Bath and Accessories	63
15.	Liquid Product Collection Section	66
16.	Vapor Phase Chromatograph	77

Figure Page

17. The Effect of Temperature on Concentrations at 15,000 psi., Alumina Core 88

18. The Effect of Temperature on Concentrations at 50,000 psi., Alumina Core 90

19. The Effect of Temperature on Concentrations at 97,000 psi., Alumina Core 93

20. The Effect of Temperature on Product Formation at 15,000 psi., Alumina Core . . . 94

21. The Effect of Temperature on Product Formation at 50,000 psi., Alumina Core . . . 96

22. The Effect of Temperature on Product Formation at 97,000 psi., Alumina Core . . . 98

23. The Effect of Alumina and Pyrex Cores at Various Temperatures and 15,000 psi.. . . . 100

24. The Effect of Alumina and Pyrex Cores at Various Temperatures and 50,000 psi. 103

25. The Effect of Alumina and Pyrex Cores at Various Temperatures and 98,000 psi. 105

26. The Effect of Alumina and Pyrex Cores on Product Formation at 15,000 psi. 106

27. The Effect of Alumina and Pyrex Cores on Product Formation at 50,000 psi. 107

28. The Effect of Alumina and Pyrex Cores on Product Formation at 98,000 psi. 108

29. The Effects of Alumina and Pyrex Cores on Methanol Formation 110

30. Concentrations at Various Residence Times at 97,000 psi., Alumina Core 111

31. Formation of Products at Various Residence Times at 97,000 psi., Alumina Core 114

32. Concentrations at Various Residence Times at 50,000 psi., Pyrex Core 115

33. Formation of Formic Acid and Methyl Formate at 50,000 psi., Pyrex Core 116

Figure Page

34. Concentrations at Various Residence Times, Pyrex Core 118

35. Methanol Formation at Various Residence Times, Temperatures and Pressures 119

36. Concentrations under Adiabatic Conditions Pyrex Core 121

37. Correlation of the Reaction Rate Constant with Temperature for Methane, Order m = 2, and Oxygen, Order n = 0.5 124

38. Correlation of the Reaction Rate Constant with Temperature for Methane, Order m = 2, and Oxygen, Order n = 0 126

39. Correlation of the Reaction Rate Constant with Temperature for Methane, Order m = 0, and Oxygen, Order n = 0 127

40. Correlation of the Compressibility Factor with Volume at Various Pressures 130

41. Correlation of the Reaction Rate Constant with Temperature Corrected for Pressure, m = 0, n = 0 132

42. Correlation of the Reaction Rate Constant with Temperature for m = 2, n = -2 133

43. Correlation of the Reaction Rate Constant with Temperature Pressure, m = 2, n = -2 . . 134

44. Chromatographic Calibration Curve for Oxygen 162

45. Chromatographic Calibration Curve for Carbon Monoxide 163

46. Chromatographic Calibration Curve for Carbon Dioxide 164

47. Chromatographic Calibration Curve for Methanol 165

48. Chromatographic Calibration Curve for Methyl Formate 166

49. Chromatographic Calibration Curve for Acetone 167

50. Curve to Correct Concentration of Formaldehyde in Presence of Acetone 171

THE MECHANISM OF PARTIAL OXIDATION OF METHANE AT HIGH PRESSURES

CHAPTER I

INTRODUCTION

In the latter half of the nineteenth century research work was underway to determine the mechanism of hydrocarbon combustion. By 1910 good data had been obtained, and yet there was no single reaction or set of reactions which seemed to represent the oxidation process accurately. The results of work using methane were as difficult to interpret as those obtained during oxidation of the higher hydrocarbons.

It was not until almost twenty years later that it was concluded that hydrocarbon oxidation proceeds via a chain mechanism. During the intervening years a large amount of work has been done, mostly in the Soviet Union and Great Britain, to specify the method of initiation, propagation, and termination of the chains. Today many of the peculiarities of the oxidation mechanism are known, but a mechanism which applies to the oxidation of even methane over a wide range of conditions does not exist.

Most of the progress over the years has been made due to work to prove or disprove a particular mechanism.

Much research has been done, for instance, during the past seven years to strengthen the mechanism for methane oxidation proposed by the eminent Soviet scientist, Semenov. Based on work at the University of Oklahoma, Semenov's mechanism is open to question, indicating that more fundamental work is needed.

Most of the research concerning the oxidation of methane has been done at low pressure and relatively high temperature. Thermal oxidations have not been conducted at low temperature because the rate of reaction is too slow. However, some photo-initiated and catalyzed work has been carried out at low temperature and pressure, and the results have proved very valuable. It was concluded that adequate reaction rates for thermal oxidation could be obtained at low temperature by use of very high pressures.

The objective of the present work was to obtain data on the thermal oxidation of methane at very high pressure, and, with data already available, to propose a mechanism for the reaction.

Experiments were conducted at pressures of approximately 15,000, 50,000 and 100,000 psi., at temperatures of 250- > 420^{o}C and at residence times of essentially zero to 60 minutes. Oxygen concentration was constant at about 8.2 mole percent. Oxidations were conducted in the presence of alumina and Pyrex-porcelain in order to determine the effects of these materials on the reaction.

CHAPTER II

FREE RADICAL THEORY

Earlier it was stated that the oxidation of methane proceeds via one or more chain mechanisms. The occurrence of a chain mechanism in organic chemistry implies reactions of free radicals. The free radical is an energy-rich entity in that it is deficient one or more protons, but it is not deficient in electrons. Electrons in the outer orbitals are unpaired. One of the free radicals which can be derived from methane is the methyl radical, $\dot{C}H_3$. It is one of the key radicals in the oxidation of methane.

The reactions of free radicals differ from those of stable molecules in that the energy of activation, ΔE, in the rate (Arrhenius) equation is very low. Whereas molecular reactions have energies of activation of the order of 60-100 kcal./mole, the maximum energy of activation of a free radical with a molecule is of the order of 10 kcal/mole. The energy of activation of one free radical reacting with another is even lower, sometimes being zero. Under this condition reaction rate depends only on probability related factors such as concentration and spatial configuration and not on energy considerations. When two

free radicals collide at a right angle, no energy barrier prevents them from forming a stable compound because no transfer of electrons is involved.

Several types of distinctive reactions are known for free radicals. These are initiation, propagation, chain transfer, degenerate branching and termination. Two other reactions occur during polymerization of organic monomers, intramolecular and intermolecular chain branching, but these reactions are improbable in methane oxidation.

Chain reactions must have a means of starting, and this step is usually referred to as initiation. Initiation can occur when a peroxide or hydroperoxide decomposes into free radicals. The initiation step in a hydrocarbon oxidation process is represented by the reaction of oxygen with the hydrocarbon to form two free radicals. An example using methane is

$$O_2 + CH_4 \rightarrow \dot{C}H_3 + H\dot{O}_2 \qquad (2\text{-}1)$$

The activation energy for this type of initiation could be as high as 100 kcal./mole since it is a molecular reaction. Another method of initiation is a chain reaction in itself. In this case one free radical only is needed to form a peroxide or hydroperoxide which can later be the source of free radicals. This type of reaction consumes reactant molecules, contains a propagation step, and leads to formation of final product. An example, theorized by Lott (29) for the oxidation of methane at high pressure is:

1. $\dot{C}H_3 + O_2 \rightarrow CH_3O\dot{O}$
2. $CH_3O\dot{O} + CH_4 \rightarrow CH_3OOH + \dot{O}H$ (2-2)
3. $\dot{O}H + CH_4 \rightarrow H_2O + \dot{C}H_3$

The methyl hydroperoxide is formed in step two and is available as an initiator for another free radical reaction. The third step forms the final product and the radical needed to form more intermediate in the first step, which forms more hydroperoxide, etc. Reactions of free radicals are very rapid, since little energy is required. In some cases the heat of reaction, derived from the propagation step, is high, and the reaction rate accelerates due to a temperature increase.

Usually the propagation step does not include an initiation step. The following is a propagation scheme proposed by Semenov (50) which is believed to occur in methane oxidation:

1. $\dot{O}H + CH_4 \rightarrow H_2O + \dot{C}H_3$
2. $\dot{C}H_3 + O_2 \rightarrow CH_3O\dot{O}$ (2-3)
3. $CH_3O\dot{O} \rightarrow HCHO + \dot{O}H$

The energy of activation for propagation is usually six to nine kcal./mole.

A third type of free radical reaction is chain transfer. In this case a hydrogen atom is removed or abstracted from a molecule by a free radical, and the unpaired electron configuration passes to the molecule losing the hydrogen. In effect the molecule becomes a free radical, while the free radical becomes inactive or is terminated. This process is not considered a termination step, however, because

a free radical is not lost. The new radical formed may be less or more active than the one deactivated. Hydrogen abstraction would occur between a methyl radical and ethane in the following manner

$$\dot{C}H_3 + H_3C\text{-}CH_3 \rightarrow CH_4 + H_3C\text{-}\dot{C}H_2 \qquad (2\text{-}4)$$

The energy of activation of chain transfer is usually seven to ten kcal./mole.

Degenerate branching is a molecular reaction between a stable intermediate product and one of the initial reactants in which the rate of free radical formation is greater than in the initiation mechanism described in equation (2-1). In methane oxidation the following degenerate branching reaction could occur

$$O_2 + HCHO \rightarrow H\dot{C}O + H\dot{O}_2 \qquad (2\text{-}5)$$

Each $H\dot{C}O$ and $H\dot{O}_2$ radical is considered to be a chain initiator. The rate of reaction of oxygen with formaldehyde (intermediate product), however, is much greater than the rate of reaction of oxygen with methane.

Termination is defined as the permanent loss of a free radical. Free radicals can terminate at the surface of the reacting vessel, or two free radicals can react with each other and form one or two stable compounds. The former case is referred to as unimolecular termination and the latter as bimolecular. The energy of activation for termination is usually less than one kcal./mole. Bimolecular termination can be via a combination reaction

$$\dot{HCO} + \dot{OH} \rightarrow HCOOH, \qquad (2\text{-}6)$$

or via disproportionation, where two compounds are formed

$$\dot{CH}_3 + H_3C\dot{C}H_2 \rightarrow CH_4 + H_2C{=}CH_2 \qquad (2\text{-}7)$$

It is well known that acetylene and ethylene, for instance, are products of methane oxidation at very high temperatures and short residence times. Only a small fraction of the unsaturated products are made in this way, however. Most are made by ionic reactions.

At high pressure, where there is less chance for diffusion of the free radicals to the walls, bimolecular termination predominates over, but not to the exclusion of, unimolecular termination.

Two important reference terms in chain reactions are the chain length, ν, and the number of active chains, n_o. The rate at which chains are generated is given as w_o. The overall rate of a chain reaction, w, is equal to the product of the chain length and the number of chains generated.

$$w = \nu w_o \qquad (2\text{-}8)$$

The chain length is then

$$\nu = \frac{w}{w_o} \qquad (2\text{-}9)$$

In order to determine the number of active chains, assume that free radicals are produced in a given reactor of unit volume at a rate w. Free radicals are terminated in the reactor at a rate $g_1 n_o$, where g_1 is the rate constant of termination. Thus, the instantaneous rate of active chains

is given by

$$\frac{dn_o}{dt} = w - g_1 n_o \qquad (2\text{-}10)$$

The solution for n_o is

$$n_o = g_1 w + ce^{-g_1 t} \qquad (2\text{-}11)$$

where c is the integration constant. With the initial condition that $n_o = 0$ at $t = 0$, the integration constant is

$$c = -g_1 w_o$$

Thus

$$n_o = \frac{w_o}{g_1}(1 - e^{-g_1 t}) \qquad (2\text{-}12)$$

After sufficient time has elapsed following the formation of the first chain, the exponential term approaches zero and Equation (2-12) reduces to

$$n_o = \frac{w_o}{g_1} \qquad (2\text{-}13)$$

The above equation will hold so long as the decrease in the concentration of initial reactants does not affect the propagation step.

An example of a complete chain mechanism is given below. Relationships will be derived which yield the chain length, the rate constant of initiation and the overall rate constant.

1.	$X_1 + X_2 \rightarrow Y_1 + Y_2$	k_1
2.	$Y_1 + X_1 \rightarrow P_1 + Y_3$	k_2
3.	$Y_3 + X_2 \rightarrow P_2 + Y_1$	k_3
4.	$Y_1 + Y_3 \rightarrow P_3$	k_4
5.	$Y_2 \xrightarrow{\text{wall}}$ termination	k_5

(2-14)

where

X_i = reactant in reaction

Y_i = free radical in reaction

P_i = product of reaction

The initiation, propagation and termination steps are readily identified as equation 1, equations 2 and 3, and equations 4 and 5, respectively.

The corresponding rate equations for this set of chemical equations are:

$$1.\quad \frac{d[Y_1]}{dt} = k_1[X_1][X_2] + k_3[X_2][Y_3] - k_2[X_1][Y_1] - k_4[Y_1][Y_3]$$

$$2.\quad \frac{d[Y_2]}{dt} = k_1[X_1][X_2] - k_5[Y_2]$$

$$3.\quad \frac{d[Y_3]}{dt} = k_2[X_1][Y_1] - k_3[X_2][Y_3] - k_4[Y_1][Y_3] \qquad (2\text{-}15)$$

$$4.\quad -\frac{d[X_1]}{dt} = k_1[X_1][X_2] + k_2[X_1][Y_1]$$

$$5.\quad -\frac{d[X_2]}{dt} = k_1[X_1][X_2] + k_3[X_2][Y_3]$$

where

[ ] = concentration

These equations can be handled as any set of simultaneous equations. Unfortunately the individual equations are nonlinear, and the difficulty in finding a classical solution is obvious. Certain features of the system are known, however. The number of chains initiated depends on the number of molecules X_1 and X_2 which react.

$$w_o = k_1[X_1][X_2] \qquad (2\text{-}16)$$

The overall reaction rate, w, in the case being considered is given by either Equation 4 or Equation 5 of Set (2-15). Thus

$$w = - \frac{d[X_1]}{dt} \tag{2-17}$$

or

$$w = - \frac{d[X_2]}{dt} \tag{2-18}$$

These reaction rates are equal in the present case since both equations comprise the chain mechanism and the free radicals concerned terminate to form the product, P_3. The overall reaction rate is also given by Equation (2-8). Substituting Equation (2-16) in Equation (2-8), the overall reaction rate is

$$- \frac{d[X_1]}{dt} = - \frac{d[X_2]}{dt} = \nu k_1 [X_1][X_2] \tag{2-19}$$

In the present instance, it is possible to determine the kinetic chain length by noting that P_2 is formed in the chain reaction and that the radicals, Y_1, and Y_3, terminate to form P_3. Therefore,

$$\nu = \frac{[P_2]}{[P_3]} \tag{2-20}$$

Substitution of Equation (2-20) in Equation (2-19) gives the following equation which can be used to determine the initiation rate constant, k_1,

$$- \frac{d[X_2]}{dt} = \frac{[P_2]}{[P_3]} k_1 [X_1][X_2] \tag{2-21}$$

Inspection of Equation (2-21) shows that the overall reaction rate constant, k, is

$$k = \frac{[P_2]}{[P_3]} k_1 \qquad (2\text{-}22)$$

In the case assumed, it is possible to determine three important constants of the chain reaction--the chain length, the rate constant for the initiation reaction and the overall rate constant for the reaction.

Another method for solution of the rate equations for a chain reaction is the quasi steady state method. Although the quasi steady state method was not used in the case illustrated, it can be applied in many cases. If an intermediate product is made in sufficient concentrations to be measured and the intermediate reacts with one of the initial reactants, the quasi steady state method can be used. In this method the reaction rates of the free radicals are assumed to be much faster than the reaction rate of the intermediate product. The rate expressions for the free radicals are set equal to zero, i.e.,

$$\frac{d[Y_i]}{dt} = 0 \qquad (2\text{-}23)$$

It is thus possible to solve the simultaneous rate equations, such as those given in Set (2-15), by equating radical concentrations to the intermediate product concentration.

CHAPTER III

PRIOR WORK

Early research into the oxidation of hydrocarbons was done to elucidate non-chain mechanisms and valuable data were collected. Subsequently experimental work was done to develop a chain mechanism specifically for methane oxidation. Thus far the results are inconclusive.

Subatmospheric and Atmospheric Pressure

Virtually all of the work has been done at atmospheric and subatmospheric pressure. Some of the data of Karmilova, Enikolopyan and Nalbandyan (21) are shown plotted in Figures 1 and 2. The pressure and temperature were 235 mm Hg and 472°C, respectively. A hydrofluoric acid-treated quartz reactor was used, and the O_2:CH_4 ratio was 2:1. These plots are typical of those in the literature; they show the disappearance of the oxygen and methane, the formation of the products and the change in total pressure relative to time. Under these conditions the major products are water, carbon monoxide and carbon dioxide. An important characteristic of the oxidation of methane at atmospheric pressure is the increase in carbon monoxide concentration to a moderate value and then the slow decrease as carbon dioxide increases

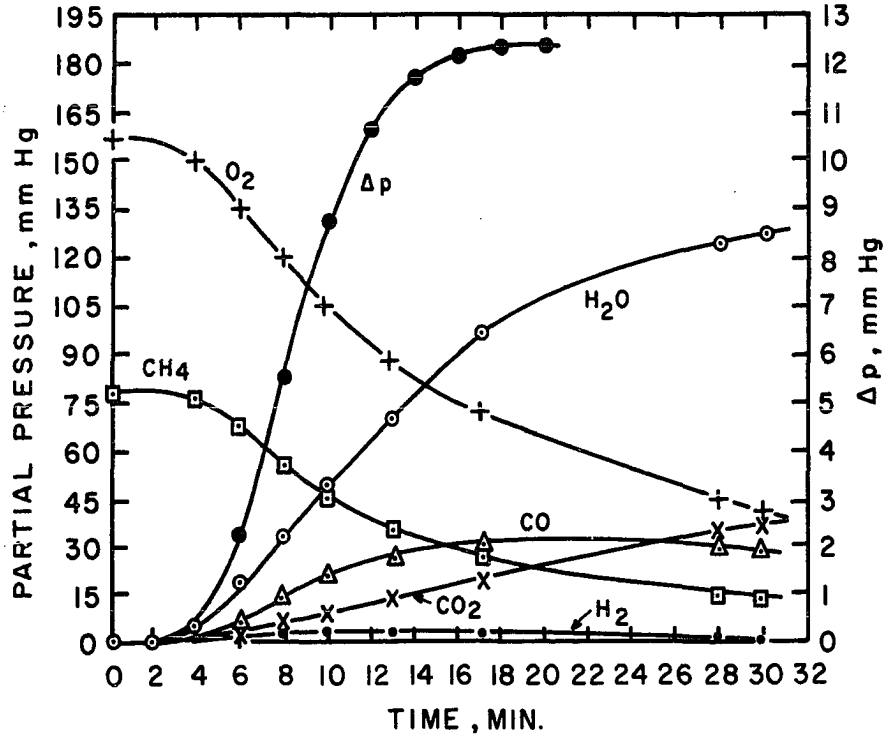


Figure 1. Disappearance of Reactants and Formation of Products at 235 mm Hg Pressure [from L. V. Karmilova, N. S. Enikolopyan and A. B. Nalbandyan (21)].

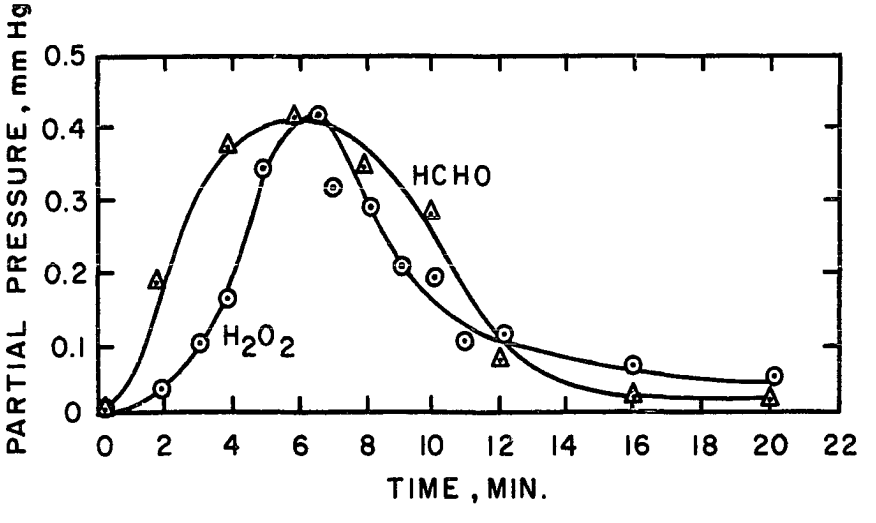


Figure 2. Formation of Formaldehyde and Hydrogen Peroxide at 235 mm Hg Pressure [from L. V. Karmilova, N. W. Enikolopyan and A. B. Nalbandyan (21)].

almost linearly. This trend has been interpreted to mean that part of the carbon monoxide is being oxidized to carbon dioxide (23).

In Figure 2 the formation of formaldehyde (HCHO) indicates a maximum with time. Other workers have also reported an initial increase in formaldehyde (4, 5), but they found that the concentration was essentially constant to the end of the reaction time. This leveling out of the formaldehyde concentration led to the acceptance at one time of formaldehyde as the key intermediate in the oxidation of methane at low pressures and at temperatures above $350^{o}C$.

The formation of hydrogen peroxide is also shown in Figure 2. The presence of hydrogen peroxide was definitely proved when it was isolated from the reaction mixture (37). If formaldehyde plays a key role in the oxidation of methane, the increase of hydrogen peroxide to a maximum could mean that it also influences the reaction rate.

The presence of organic peroxides or hydroperoxides has not been detected under the conditions described earlier. At low temperatures, about $150^{o}C$, photo-initiation has given high yields of hydroperoxides, however (24). In another study by Fisher and Tipper (10) methane was oxidized by the photo-decomposition of acetone. The main products were carbon monoxide, carbon dioxide, water, formaldehyde and methanol. The latter two products reached a maximum concentration and the methanol appeared late in the experiment.

After several experiments at 395°C, the rate depended on retreatment of the reactor surface. Appreciable amounts of hydrogen peroxide and methyl hydroperoxide were present when the reactor surface was activated by washing with nitric acid, and a large amount of methanol was made.

The decomposition of methyl hydroperoxide formed at 395°C was believed by Fisher and Tipper (11), to form formaldehyde, methanol, water and probably oxygen. The ratio of formaldehyde to methanol was given as 1.0 with an activated surface and 4.0 with a deactivated surface. The half life of the hydroperoxide was estimated to be 30 seconds with an activated surface and 5-10 seconds with a deactivated one. Some tagged acetone $(C^{14}H_3)_2CO$, was used in this work, and some $C^{14}H_4$ was found. This result led to the conclusion that there was some hydrogen abstraction by the methyl radical.

At low pressure an induction period, τ, is characteristic of the oxidation of methane. From Figure 1, it is seen that the induction time is about four minutes. The time varies with temperature but to a greater degree with the surface characteristics of the reactor, such as total surface and surface to volume ratio. It also varies with some additives. Norrish and Foord (42) and Norrish and Reagh (43) found that the rate of reaction is almost decreased to zero if the reactor diameter is less than 3.0 mm, and the rate increases as the diameter increases up to about 16 mm. A greater increase has little further

effect on the rate. Fort and Hinshelwood (12) and Bone and Gardner (5) found packing a quartz vessel with quartz chips greatly reduced the rate of reaction and increased the induction period. The induction period was increased from 14 to 62 minutes when the surface to volume ratio was increased by a factor of two by packing the vessel. This effect was confirmed by van Meerssche (35) who found that the maximum reaction rate is inversely proportional to the surface to volume ratio.

The most comprehensive work on the effect of the nature of the surface on the oxidation of methane was done by Walsh and Hoare and their coworkers (6, 7, 8, 16, 18). The different surfaces investigated consisted of: heat treated silica, lead oxide coated silica, silica washed with hydrofluoric acid and hydrochloric acid, sodium hydroxide washed after hydrofluoric acid treatment, treatment by gases and a reactor aged only by conducting a number of experiments in it. A plot of the results of four of the surfaces is shown in Figure 3. The activity, in decreasing order, is: new silica vessel, aged by reaction, heat treated and lead oxide treated. The new vessel apparently has little capability of terminating any of the free radical species. This type of curve is different from those obtained with the less active surfaces. After a short induction time, the reaction proceeds at a high, essentially constant rate until one of the reactants is depleted. Hoare (16) emphasizes that with the results

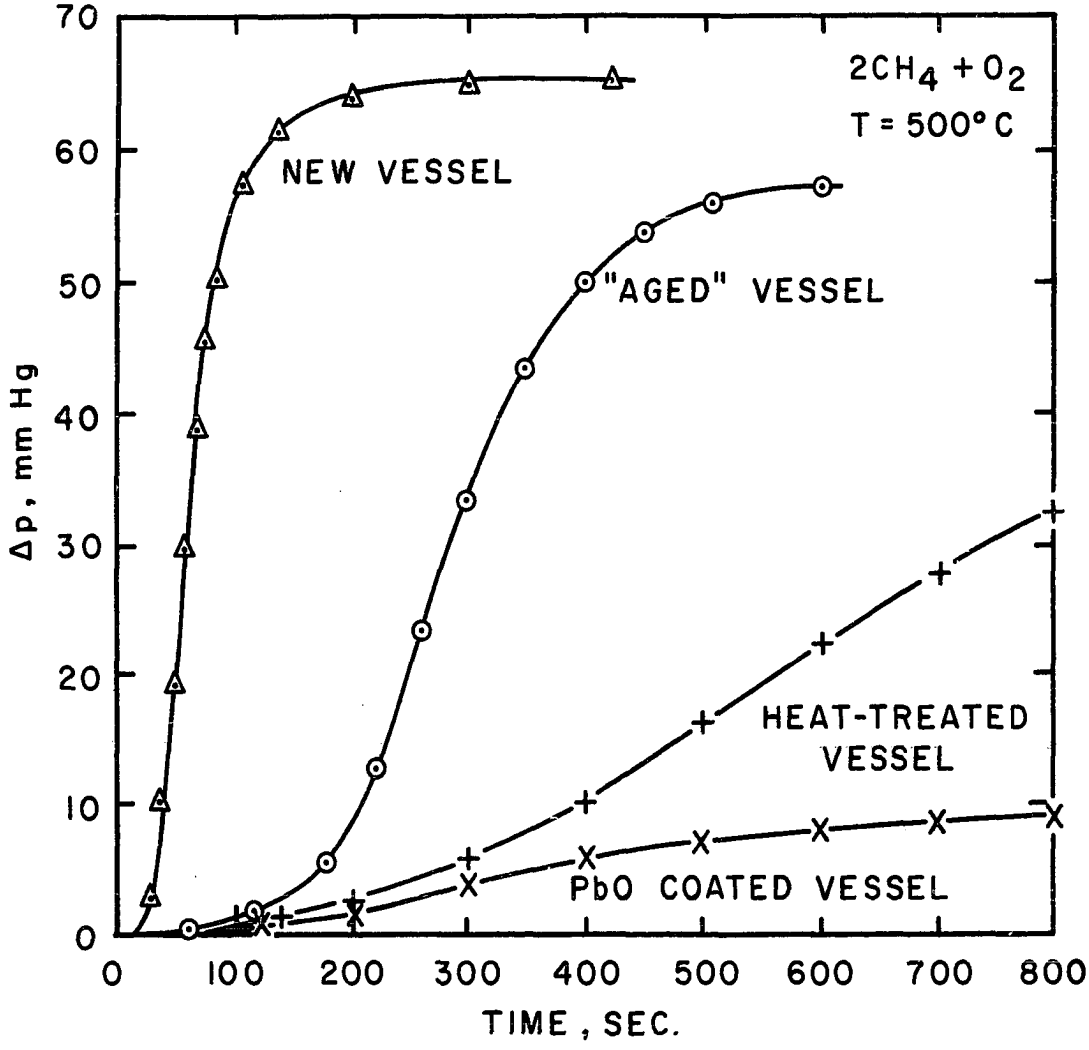


Figure 3. Reaction Rates for Oxidation of Methane in Reactors with Treated Surfaces [from D. E. Hoare (16)].

obtained on the effect of the state of the surface on the oxidation of methane, it is clear why conflicting results appear in the literature. When using a silica-containing reactor, for instance, devitrification occurs, and the surface must be reactivated.

Gudkov (14) investigated the oxidation of methane by air in a stainless steel reactor packed with quartz, porcelain, firebrick, high alumina-content firebrick or silica gel. Quartz gave the highest conversion, but porcelain gave the highest yield of formaldehyde--0.25 mole/mole of methane consumed.

Stadnik and Gomonai (51) investigated the oxidation of methane in a flow system at 500°C and at 700-800°C. A quartz reactor was used. In some experiments the quartz surface was partly covered with brass, copper or platinum. It was found that the formaldehyde concentration increased with an increase in the percentage of quartz surface exposed. They also essentially duplicated the work of Hoare and Welsh (16), (18) and reported the same ranking of the activity of the surfaces.

The effect of the nature of the surface on the oxidation of methane was also investigated by Mari, Letort, Niclause and Dzierzynski (33). They postulated that water formed during the reaction is at least partly responsible for the change in the surface activity of the reactor and that formaldehyde is not the only factor in auto-acceleration of the slow oxidation of methane.

Various additives, other than known activators such as oxides of nitrogen, have been used in the oxidation of methane. Gardner and Bone (5) added formaldehyde and found that the induction time was reduced. When the equilibrium amount of formaldehyde that occurs during the oxidation was added, the induction time was completely eliminated. Karmilova, Enikolopyan and Nalbandyan (22) investigated the effect of hydrogen peroxide and water on the kinetics of methane oxidation. They concluded that hydrogen peroxide accelerates the reaction by shortening the induction period and that neither hydrogen peroxide nor water play a part in any degenerate branching reaction.

In a study by Gudkov (13) a two stage reaction was carried out, and formaldehyde was removed after the first stage. It was reported that when formaldehyde was removed, less carbon monoxide and carbon dioxide were made. When oxygen was injected between stages, the formaldehyde concentration went up 10-12 percent, but the carbon monoxide and carbon dioxide increased by 50 percent.

Mantashyan and Nalbandyan (31) report oxidation of methane carried out at very low oxygen pressure--3.0 mm. The reaction was initiated by light. In addition to formaldehyde, formic acid was obtained. Initiation via ozone and photo-initiation were used in a study by Kleimenov and Nalbandyan (25) at low temperature. The kinetic results were the same using both methods of initiation. They propose a mechanism in which methyl hydroperoxide is an

intermediate. Schneider (47) reported ethane, ethylene and acetaldehyde as being among the products of methane oxidation. A quartz reactor was used, and temperatures of 676, 724, and 770°C were investigated.

The oxidation of methane was carried out by Avramenko, Kolesnikova and Kutnetsova (2) in water vapor using a high voltage spark as initiation. The main products were carbon monoxide, water and formaldehyde. Small amounts of methanol were also found at 240 and 276°C.

Kinetics of the slow oxidation of methane was studied by Hsien-Cheng Yao (19). It was concluded that the oxidation is zero order with respect to oxygen and methane when the partial pressure of oxygen is less than that of methane. In a later paper, Hsien-Cheng and Ruof (20) reported on the thermal oxidation at 400-480°C. Below 416-430°C they found that the rate depends only on the initial pressures of methane and oxygen. The rate is unaffected by total pressure, diluents or the addition of about an equimolar amount of formaldehyde. The rate expression is:

$$W = A \exp(-30{,}200/RT)[CH_4^{\,o}]^2[O_2^{\,o}]$$

where $CH_4^{\,o}$ and $O_2^{\,o}$ are the initial concentrations. Above 430°C the rate is accelerated by the addition of diluents and formaldehyde, and the rate is higher than for the expression given above. They suggested that formaldehyde is not the rate controlling intermediate at low temperatures.

Data were obtained on the oxidation of methane initiated at 670°C by nitrogen oxides by Kompaneets and

Moshkina (27). Semenov's scheme (50) was used to treat the data. Michael and Glass (36) used a time-of-flight mass spectrometer to identify ions from the high temperature oxidation of methane and acetylene in a shock tube. Ions present in high concentration are $C_3H_3^+$, H_3O^+, $H_3O^{\cdot}H_2O^+$ and CH_3O^+. In both oxidations the first ion observed is $C_3H_3^+$. A Langmuir probe was used to measure the ion concentrations and the rate of formation of ions.

Ratios of methane to oxygen of 5:1 and 1:10 were used by Blundell, Cook, Hoare, and Milne (3) to investigate the thermal oxidation at 500-750°C. They reported the following rates of reaction of the $\dot{O}H$ and $H\dot{O}_2$ radicals with carbon monoxide, methane and formaldehyde in the temperature range 500-525°C.

TABLE 1

THE RELATIVE REACTIVITY OF FREE RADICALS WITH SOME COMPOUNDS AT 500-525°C

Free Radical	CH_4	CO	HCHO
$\dot{O}H$	2.1	1.0	--
$\dot{O}H$	1.0	--	33
HO_2	--	1.0	340

at 650 and 750°C the ratio of the relative reactivity of the $\dot{O}H$ radical with CH_4 to the relative reactivity of the radical with CO was > 2.1.

High Pressure

Only two major studies of the batch oxidation of methane at pressures much greater than atmospheric are published. These are the work of Newitt and Haffner (39) and that of Lott (29).

The work of Newitt and Haffner was done at pressures up to 150 atm. and at temperatures of 335-400°C. The experimental procedure was to heat the reactor while it was under vacuum and then to charge it rapidly at the initial temperature. Results of an experiment at 106 atm. and 341°C initial temperature are shown in Figure 4. The methane to oxygen ratio was 8:1. In addition to the products found at atmospheric pressure, a large amount of methanol was made.

Although there was a rapid increase in temperature at the end of the reaction period, no accompanying large change in product concentration was observed. At atmospheric pressure the ratio to formaldehyde ratio was no more than 1.0, but the ratio under pressure of 106 atm. was well over 20.0. The individual values of carbon monoxide and carbon dioxide were not given. The ratio of carbon monoxide to carbon dioxide increased with time up to 12 minutes. When the reaction time was continued to 16.5 hours, the ratio dropped from 1.45 at 12 minutes to 0.13 at the end. The amount of methanol and formaldehyde also dropped after 12 minutes. In experiments at 150 atm. the methanol concentration was higher on average than at 106 atm.

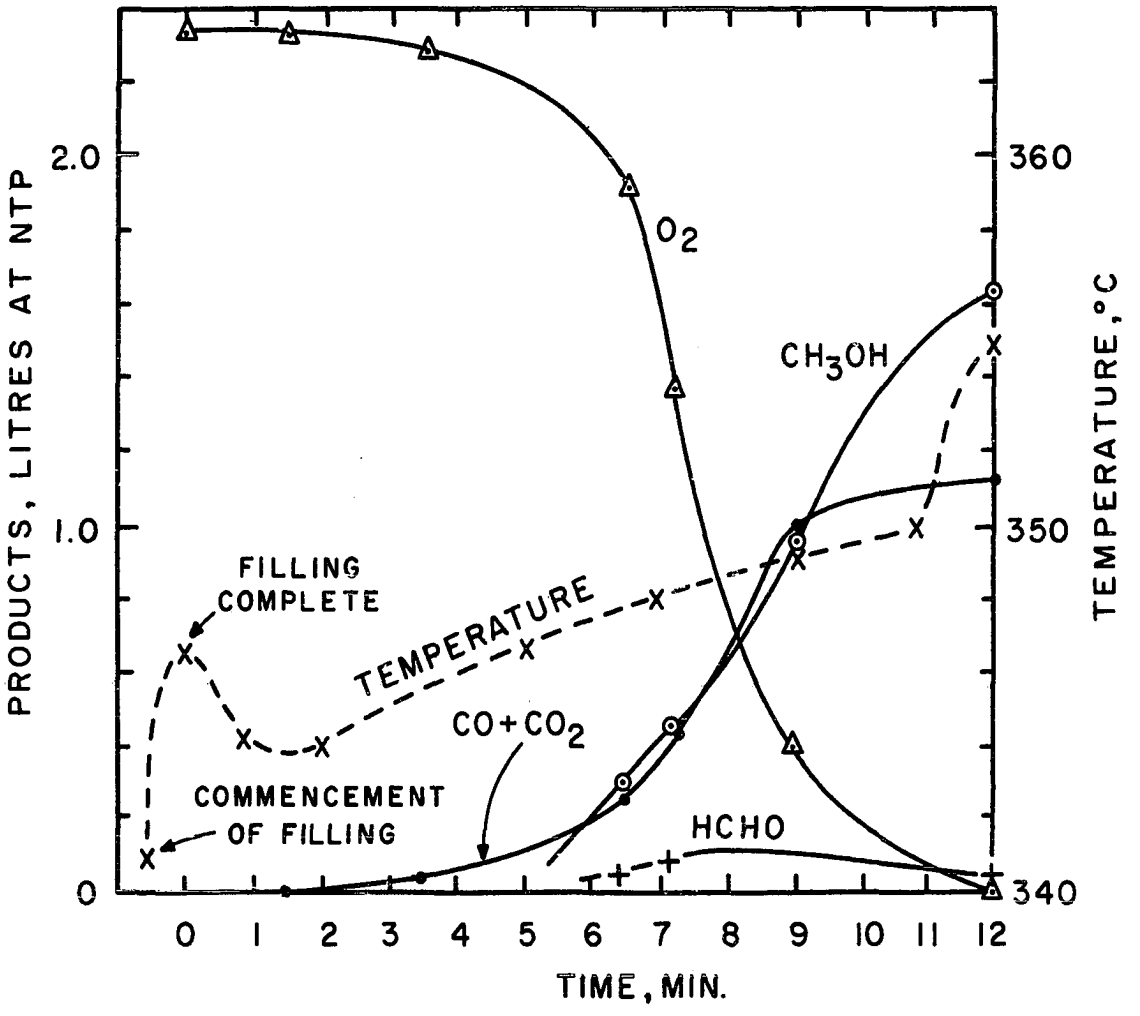


Figure 4. Disappearance of Oxygen and Formation of Products at 106 atm. Pressure [from D. M. Newitt and A. E. Haffner (39)].

The study of Lott (29) consisted of two parts. In the first part mixtures of methane and oxygen in a ratio of 10:1 were reacted at pressures of up to 1,020 atm. in a reactor made of 19-9DL stainless alloy. A temperature range of 289-340^{o}C was investigated, and residence times ranged from 0.25-140 minutes. The procedure was to heat the reactor to the desired temperature of the experiment, and then to admit the cold feed mixture to the reactor to the desired initial pressure. The time to the occurrence of the peak temperature was followed, and the reactor was depressured at this point.

The procedure was similar to that used by Newitt and Haffner. The time to maximum temperature is shown in Figure 5, which includes the data of Newitt and Haffner. The decrease in residence time as pressure increases becomes small above 10,000 psi. As pressure was increased from 5,400 to 15,000 psi., the maximum yield of methanol based on the methane consumed increased from 24.5 to 28.5 percent. In addition to the methanol the main products were carbon monoxide, carbon dioxide and water. Small quantities of formaldehyde, formic acid and methyl formate were also made.

The second part of the study by Lott consisted of experiments conducted up to 200,000 psi. The reactor and other high pressure equipment used is that described in this study. The internal heater consisted of nichrome wire, threaded through porcelain beads and wrapped around a Pyrex tube. The exterior of the heater was then coated with

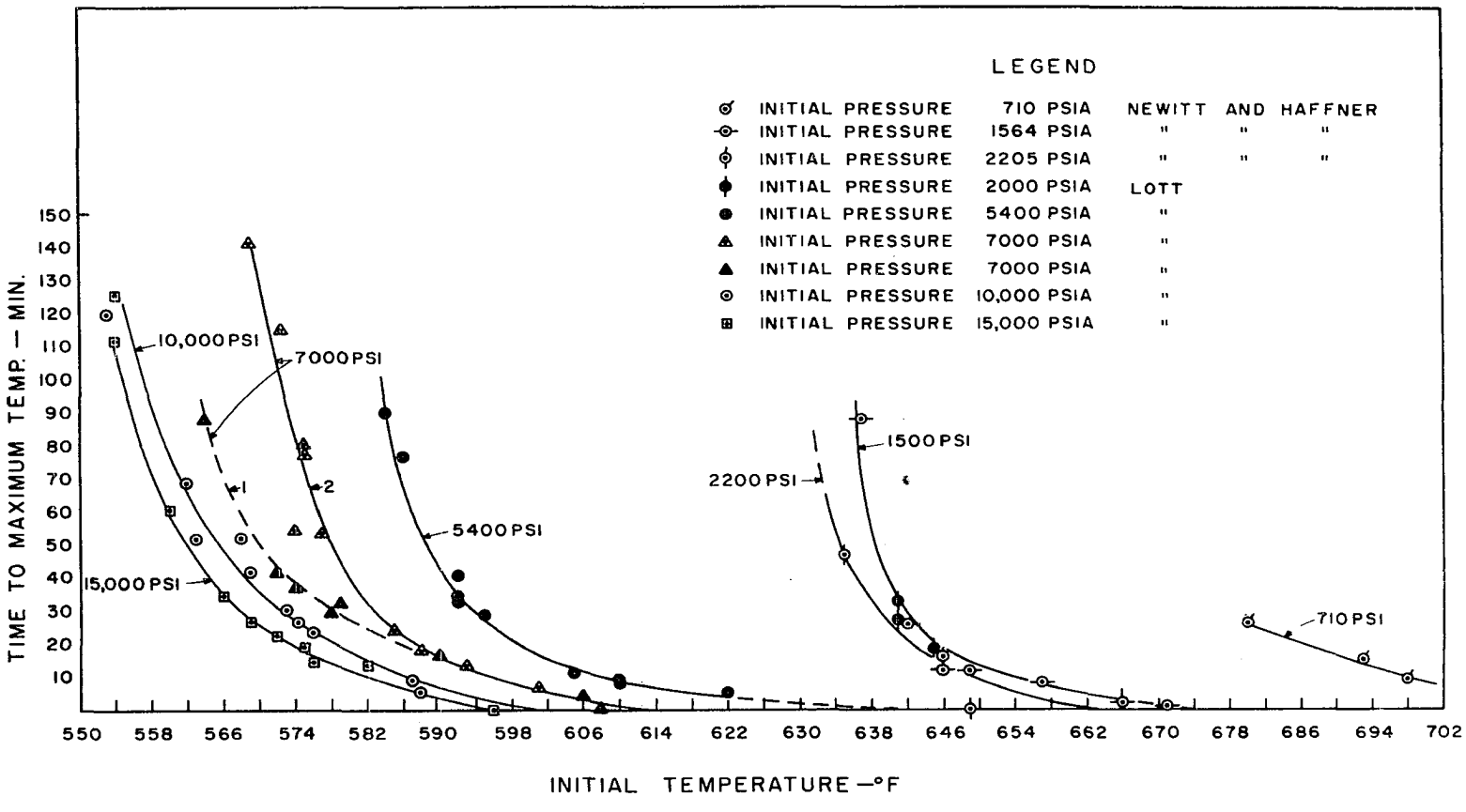


Figure 5. Effect of Temperature on Residence Time [from Lott (29) reproduced by permission.]

porcelain cement. The procedure for this equipment was different than described earlier for the work conducted at lower pressure by Lott. The oil bath was heated until the reactor internal temperature was within 40-50°C of the desired experimental temperature. The feed mixture was admitted to the compression cylinder and reactor and compressed via the compression cylinder to the desired pressure above 20,000 psi. After the valve between the compression cylinder and reactor was closed, the internal heater was turned on and the current adjusted to give the desired temperature.

A pronounced wall effect occurred in the experiments in the newly installed reactor. In some cases essentially isothermal reactions could be conducted, but runaway reactions occurred in others. The data show the highest yield of methanol of 40.5 percent at 50,000 psi. to be at a residence time of seven minutes. The yield then dropped with time to a level of 27 percent after 97 minutes.

Newitt and Szego report results of methane oxidation at 50 psi. pressure in a flow system (40). Methane, oxygen and nitrogen were stored at pressure well above the planned operating pressure, and bled through a needle valve at a constant rate to the reactor during an experiment. Results of a mixture of 90 percent methane, three percent oxygen and seven percent nitrogen showed a yield of 50 percent methanol based on methane usage at 430°C and 50 atms., while at 400°C the yield was only 12 percent. For a mixture

of 90 percent methane and five percent each of oxygen and nitrogen, the yield was 23 percent at 410°C and three percent at 400°C. The residence time was 30 seconds at the lower temperature and only six seconds at the higher temperature. The formaldehyde concentration was fairly constant in each case.

CHAPTER IV

MECHANISMS PROPOSED BY PREVIOUS INVESTIGATORS

During the nineteen thirties several chain mechanisms were proposed for the oxidation of hydrocarbons. Two of these schemes, by Semenov (49) and Norrish (42, 44), were for methane oxidation. They proposed chain reactions propagated via carbon and oxygen diradicals. Semenov's 1934 scheme was rather sketchy, but he considered the chain reaction to be:

$$\begin{aligned} &1.\ \ddot{O} + CH_4 \longrightarrow \ddot{C}H_2 + H_2O \\ &2.\ \ddot{C}H_2 + O_2 \longrightarrow HCHO + \ddot{O} \end{aligned} \qquad (4\text{-}1)$$

Formaldehyde was then considered to react with oxygen forming carbon dioxide, carbon monoxide and water. Chain termination was believed to be caused by destruction of the oxygen diradical at the wall, forming molecular oxygen.

The 1936 scheme proposed by Norrish and Foord (42) was somewhat more specific about the role of formaldehyde:

$$\begin{aligned} &1.\ CH_4 + O_2 \longrightarrow HCHO + H_2O \qquad k_1 \\ &\quad HCHO + O_2 \longrightarrow HCOOH + \ddot{O} \\ &2. \qquad\qquad\qquad\qquad\qquad\qquad\quad k_2 \\ &\quad HCOOH + \ddot{O} \longrightarrow H_2O + CO \end{aligned}$$

$$
\begin{aligned}
&3.\ \ddot{O} + CH_4 \longrightarrow \ddot{C}H_2 + H_2O && k_3\\
&4.\ \ddot{C}H_2 + O_2 \longrightarrow HCHO + \ddot{O} && k_4\\
&5.\ HCHO\ \text{oxidation} \longrightarrow CO + H_2O && k_5\\
&6.\ HCHO + \ddot{O} \longrightarrow X && k_6\\
&7.\ \ddot{O} + CH_4 + X \longrightarrow CH_3OH + X' && k_7\\
&8.\ \ddot{O} + \text{surface} \longrightarrow \tfrac{1}{2}O_2 && k_8
\end{aligned}
\qquad (4\text{-}2)
$$

where X is an intermediate (unspecified).

The authors theorized that the first oxygen diradicals are formed from traces of formaldehyde at the wall. As methane and oxygen are consumed via chain reactions 3 and 4, the formaldehyde concentration steadily increases. Most of the carbon monoxide and water was presumed to be formed by equation 2. However, it was considered possible that carbon monoxide and water could be formed via equation 5. They also provided a mechanism for formation of methanol, which was known to be a product of methane oxidation at high pressure. Chain breaking occurs by loss of the oxygen diradical at the wall.

The data obtained were found to fit the following equation for the rate of consumption of methane

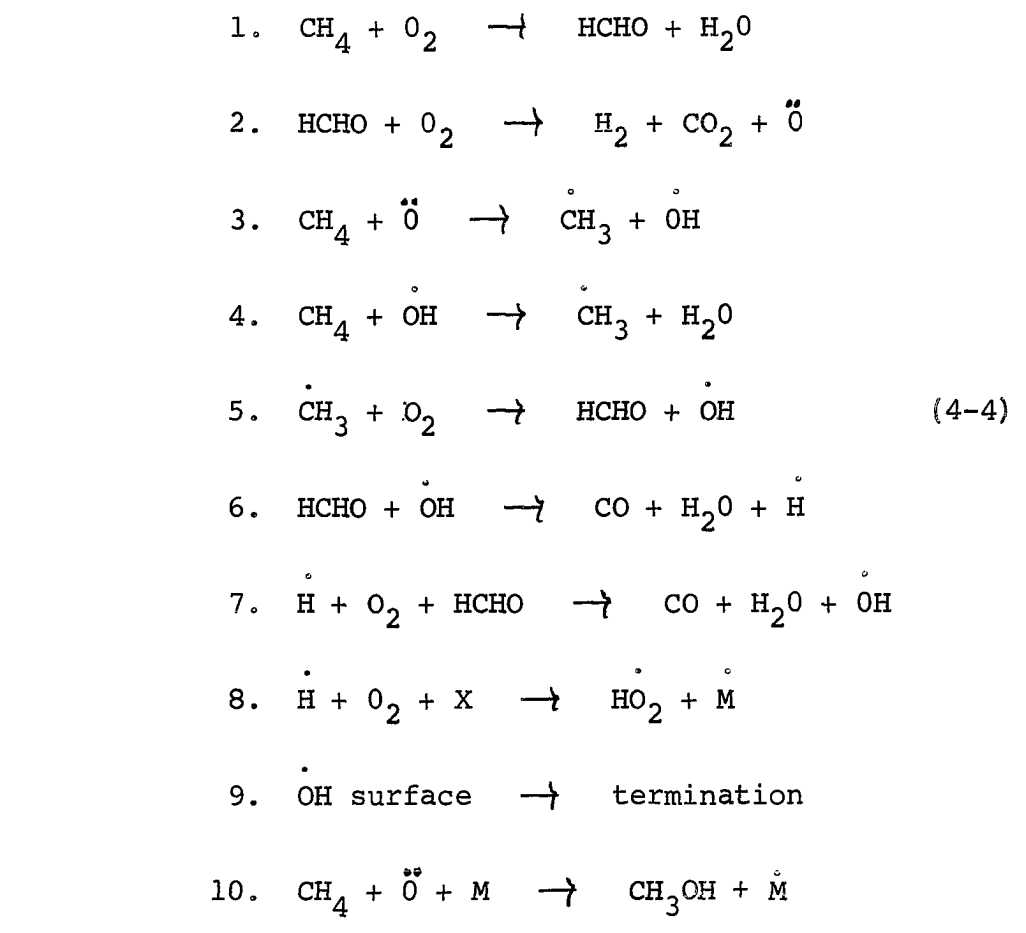
$$
-\frac{d[CH_4]}{dt} = \frac{k_2 k_3^{\,2}}{k_6}\,\frac{[CH_4]^2\,[O_2]Pd}{k_7 S} \qquad (4\text{-}3)
$$

where P = total reactor pressure

d = reactor diameter

S = state of activity of the reactor surface

By 1948 Norrish (41) had modified the mechanism:



(4-4)

Norrish's mechanism of 1948 has been questioned by at least two authors (48, 28). Because of the reactions which result in a volume increase, it would not seem to apply at high pressure.

Semenov presented a new mechanism for the oxidation of methane in 1958 (58). The oxygen and methylene diradicals

were no longer included; the reaction steps involve mono-radicals only:

$$
\begin{aligned}
&0 \quad CH_4 + O_2 \rightarrow \dot{C}H_3 + \dot{H}O_2 \\
&1 \quad \dot{C}H_3 + O_2 \rightarrow HCHO + \dot{O}H \\
&2 \quad \dot{O}H + CH_4 \rightarrow H_2O + \dot{C}H_3 \\
&2' \quad \dot{O}H + HCHO \rightarrow H_2O + \dot{H}CO \\
&3 \quad HCHO + O_2 \rightarrow \dot{H}CO + \dot{H}O_2 \\
&4 \quad \dot{H}CO + O_2 \rightarrow CO + \dot{H}O_2 \\
&5 \quad \dot{H}O_2 + CH_4 \rightarrow H_2O_2 + \dot{C}H_3 \\
&5' \quad \dot{H}O_2 + HCHO \rightarrow H_2O_2 + \dot{H}CO \\
&6 \quad \dot{O}H \text{ wall} \rightarrow \text{termination} \\
&7 \quad \dot{H}O_2 \text{ wall} \rightarrow \text{termination} \\
&8 \quad HCHO \text{ wall} \rightarrow \text{termination}
\end{aligned}
\tag{4-5}
$$

The corresponding rate equations for each of the free radicals and formaldehyde are:

$$1. \quad \frac{d[\dot{C}H_3]}{dt} = w_o + a_2 [\dot{O}H] + a_5 [\dot{H}O_2] - a_1 [\dot{C}H_3]$$

$$2. \quad \frac{d[\dot{O}H]}{dt} = a_1 [\dot{C}H_3] - a_2 [\dot{O}H] - a_2' [OH] - a_6 [\dot{O}H]$$

$$3. \quad \frac{d[\dot{H}CO]}{dt} = k_2' [HCHO] [\dot{O}H] + a_3 [HCHO] + k_5' [HCHO] [\dot{H}O_2] - a_4 [\dot{H}CO]$$

$$4.\quad \frac{d[\dot{HO}_2]}{dt} = w_o + a_3\,[HCHO] + a_4\,[\dot{HCO}] - a_5\,[\dot{HO}_2] - k_5'\,[HCHO]\,[\dot{HO}_2]$$

$$5.\quad \frac{d[HCHO]}{dt} = a_1\,[\dot{CH}_3] - k_2'\,[HCHO]\,[\dot{OH}] - a_3\,[HCHO] - k_5'\,[HCHO]\,[\dot{HO}_2] - a_8\,[HCHO] \qquad (4\text{-}6)$$

where

$$a_i = k_j\,[O_2] \text{ or } k_m\,[CH_4]$$

Semenov made the assumption that the free radicals have a very short existence and that formaldehyde has a relatively long reaction time. Therefore, the radical concentration is completely determined by the aldehyde concentration (assumption of quasi steady state). The first derivatives of the free radicals therefore become zero

$$\frac{d[\dot{CH}_3]}{dt} = \frac{d[\dot{OH}]}{dt} = \frac{d[\dot{HCO}]}{dt} = \frac{d[\dot{HO}_2]}{dt} = 0 \qquad (4\text{-}7)$$

For convenience Semenov did not include $\dot{HO}_2$ termination at the wall at this time. The linear products of constants and components also became equal to zero, of course, and the equations were solved in terms of formaldehyde, oxygen and methane concentrations only.

Substitution into the differential equation for formaldehyde gave

$$\frac{d[HCHO]}{dt} = \left\{ \frac{2a_2a_3}{a_6} [HCHO] - a_3 [HCHO] - a_8 [HCHO] \right\} - \frac{2a_3k_5'}{a_5} [HCHO]^2 - \frac{2k_2'k'_5a_3}{a_5a_6} [HCHO]^3 \quad (4\text{-}8)$$

By assuming that the chain length $\nu = 100$ and by making assumptions concerning some rate constants, k_i, Semenov estimated that

$$[HCHO]_{max} \tilde{=} \exp(-10{,}000/RT) \quad (4\text{-}9)$$

where $[HCHO]_{max}$ is the pseudo equilibrium concentration of HCHO.

The equation for the conversion of methane was next considered:

$$-\frac{d[CH_4]}{dt} = a_2 [\dot{O}H] + a_5 [\dot{H}O_2] \quad (4\text{-}10)$$

$$-\frac{d[CH_4]}{dt} = \left\{ k_2' [HCHO] + a_2 \right\} 2 \left\{ \frac{w_o + a_3 [HCHO]}{a_6} \right\} + w_o + 2a_3 (HCHO) \quad (4\text{-}11)$$

By making three simplifying assumptions, and by assuming that methane reaches its maximum rate of consumption where HCHO = $[HCHO]_{max}$ Semenov obtained the following result

$$-\frac{d[CH_4]}{dt} = \frac{2k_2k_3}{a_6}\left(\frac{k_2k_5}{k_2'k_5'}\right)^{\frac{1}{2}}[CH_4]^2\,[O_2] \qquad (4\text{-}12)$$

This equation is almost the same as that obtained by Norrish and Foord which was given earlier. Of course, Semenov had not intended to include surface, diameter and pressure effects.

The termination of $\dot{H}O_2$ radicals was next considered by Semenov, and he found that omission of this step did not change the results. It may be inferred that termination of $\dot{O}H$ radicals is the controlling termination step.

From 1959 to date a great amount of research has been done to confirm the theory and mechanism proposed by Semenov in 1958.

In 1961 two articles were published by Mari and coworkers in which the role of formaldehyde as the sole autoaccelerating factor was questioned (33, 34). They theorized that water forming at the walls of the reactor inhibited chain termination. It was stated that the mechanism appeared more complex than theorized by Semenov.

The work of Hsien-Cheng and Ruof (20) conducted at 400-480°C, tended to show that formaldehyde was not the only intermediate controlling reaction rate. These findings were significant because up to this time little work had been reported on thermal (uncatalyzed) oxidation of methane at temperature as low as 400°C. The Semenov scheme had been based on data obtained mainly in the temperature range of 500-700°C.

In 1965 Kompaneets and Moshkina (27) reported on results of their work at 670°C using nitrogen dioxide initiation. They used Semenov's mechanism to calculate rate constants. There was considerable difference in the values calculated and those obtained from published experimental data. Therefore they claimed that the Semenov mechanism is not applicable to the high temperature oxidation of methane.

It is well known that acetylene and ethylene are obtained as products from the oxidation of methane at temperatures of 1000°C and higher. Dwell times are very short. Schneider even reports that ethane, acetaldehyde and ethylene appear in the products during oxidation of methane in quartz at 675°C (47).

Knox in recent work investigated hydrocarbon oxidation at 300-400°C (26). Although this work is not specific to methane, it was stated that any hydrocarbon oxidation must provide for the conversion of $\dot{HO}_2$ to $\dot{OH}$. This conversion is believed to involve the cooxidation of an olefin, which was stated to be the primary product of most oxidations.

It appears necessary to include cracking and reforming reactions in the methane oxidation mechanisms above a certain temperature. This temperature may be as low as 675°C. Recent work tends to show that the mechanism of Semenov does not adequately describe the oxidation of methane at any temperature. However his approach to

determining the mechanism was novel and valuable since it stimulated a great amount of research.

Lewis and von Elbe (28) proposed the following mechanisms:

$$
\begin{aligned}
&1.\ HCHO + O_2 = \text{free radicals} \longrightarrow \dot{O}H \\
&2.\ \dot{O}H + \dot{C}H_4 \longrightarrow H_2O + \dot{C}H_3 \\
&3.\ \dot{C}H_3 + O_2 \longrightarrow HCHO + \dot{O}H \\
&4.\ \dot{O}H + HCHO \longrightarrow H_2O + \dot{H}CO \\
&5.\ \dot{H}CO + O_2 \longrightarrow CO + \dot{H}O_2 \\
&6.\ \dot{H}CO + O_2 + M \longrightarrow H\dot{C}(=O)O\dot{O} + M \\
&7.\ H\dot{C}(=O)O\dot{O} + HCHO \longrightarrow 2CO + H_2O + \dot{O}H \\
&8.\ \dot{O}H \xrightarrow{\text{wall}} \text{destruction} \\
&9.\ \dot{H}O_2 \xrightarrow{\text{wall}} \text{destruction} \\
&10.\ HCHO + O_2 \xrightarrow{\text{wall}} \text{destruction of HCHO}
\end{aligned}
\qquad (4\text{-}13)
$$

The chemical equations are of interest in that the performyl radical is included. The authors stated that at the high temperatures, ca.530°C, encountered in methane oxidation the performyl radical reacts with formaldehyde. At lower temperatures, ca. 370°C, encountered in oxidation of formaldehyde, however, performic acid itself was theorized to form. Minkoff and Tipper (38), in a discussion on formaldehyde oxidation, noted that thermal oxidation is slow at 250°C, and that above this temperature peroxidic compounds decompose rapidly at the walls.

In the Lewis and von Elbe scheme shown for methane oxidation, no equation was provided for the formation of carbon dioxide. They stated that the formation of carbon dioxide may be explained by further reaction of carbon monoxide with $\dot{O}H$. Evidence for a concurrent reaction of carbon monoxide and $\dot{O}H$ has been provided by Vanpée (53). Equation 7 of Set (4-12) would not seem likely at high pressure because of the twofold increase in volume. Yet most of the carbon monoxide is formed through this equation. Work on the oxidation of formaldehyde at 451°C with $C^{14}O$ as an additive has shown that only 3-5 percent of the carbon dioxide is formed from carbon monoxide (45). This result is in conflict with the findings of Karmilova et al. (23) for the oxidation of methane in which carbon dioxide was found to form from carbon monoxide. Certainly the source of carbon dioxide is not clear, and the inclusion of a separate reaction for its formation cannot be discounted.

By assuming steady state concentration of $\dot{O}H$ and HCHO, the following equation for methane consumption was obtained by Lewis and von Elbe

$$-\frac{d[CH_4]}{dt} = \frac{k_{40}k_{42}\,[CH_4]\,[O]}{2k_{50}} \cdot \frac{\frac{k_{40}}{k_{51}}\,[CH_4]\,[M_t]d^2 - \frac{k_{53}}{k_{42}}\,\frac{1}{d} - 1}{\frac{1}{2}\,\frac{k_{40}k_{49}}{k_{51}k_{44}}\,[CH_4]d^2 + 1} \qquad (4\text{-}14)$$

This equation is complex, and it is difficult to isolate the orders of methane and oxygen as shown below in the equation

$$w \tilde{=} k\,[CH_4]^m\,[O_2]^n \qquad (4\text{-}15)$$

Methane and oxygen concentrations, however, will remain at approximately first order. The equations of Norrish and Semenov, described earlier, have oxygen as first order and methane as second order. The following table, published by Enikolopyan (9), shows the wide variation in exponents which have been reported by various authors for equation (4-15).

TABLE 2

VARIATION OF THE ORDER OF REACTION WITH RESPECT TO OXYGEN AND METHANE IN THE RATE EQUATION

Temperature, °C	Vessel	m Order with Respect to Methane	n Order with Respect to Oxygen
376	Pyrex	2.3	0.5
416	Pyrex	2.0	0.5
467	Clean vessel	1.6	1.0
480	- - -	2.0	1.0
500	Quartz, treated by heating	2.4	1.0 - 1.6
570	- - -	1.4	2.4
617	- - -	0.11?	2.5
650	Quartz, treated by heating	0 - 0.7	2.3 - 2.7
666	- - -	- 0.14	3.8
750	- - -	- 0.4 → + 0.4	2 - 2.4

The order with respect to methane has varied from - 0.14 to 2.4, and the order for oxygen has varied from 0.5 to 3.8. The wide range of values shows that a simple relationship cannot portray the mechanism of methane oxidation. The equations are useful, however, in that trends are shown.

Shtern presents a scheme credited to Enikolopyan which was stated to be applicable to hydrocarbon systems in general (48):

$$
\begin{aligned}
&1.\ RH + O_2 \longrightarrow \dot{R} + \dot{H}O_2 \\
&2.\ \dot{R} + O_2 \longrightarrow R\dot{O}O \\
&3.\ R\dot{O}O + RH \longrightarrow ROOH + \dot{R} \\
&4.\ R\dot{O}O \longrightarrow R'CHO + R''\dot{O} \\
&5.\ R''\dot{O} + RH \longrightarrow R''OH + \dot{R} \\
&6.\ R''\dot{O} + R'CHO \longrightarrow R''OH + R'\dot{C}O \qquad (4\text{-}16) \\
&7.\ R'\dot{C}O + O_2 \longrightarrow R'\dot{O} + CO_2 \\
&8.\ R'\dot{O} + RH \longrightarrow R'OH + \dot{R} \\
&9.\ R'\dot{O} + R'CHO \longrightarrow R'OH + R'\dot{C}O \\
&10.\ \dot{O}H + RH \longrightarrow H_2O + \dot{R} \\
&11.\ ROOH \longrightarrow R\dot{O} + \dot{O}H \\
&12.\ R'CHO + O_2 \longrightarrow R'\dot{C}O + \dot{H}O_2 \\
&13.\ R\dot{O}O \xrightarrow{\text{wall}} \text{termination}
\end{aligned}
$$

14. $2R\dot{O}\dot{O} \longrightarrow$ termination

15. $\dot{R} \xrightarrow{\text{wall}}$ termination

The formation of alcohols higher than methanol and aldehydes higher than formaldehyde do not apply to methane oxidation. Two points are of special interest: the reaction of $R\dot{O}\dot{O}$ with hydrocarbon in equation 3 to form hydroperoxide and equation 7 in which carbon dioxide is formed. In Semenov's scheme the product of this reaction is carbon monoxide. For some reason Enikolopyan did not give an equation for the formation of carbon monoxide. One can only add that the mechanism is deficient without one.

In recent work Lott (29) proposed a mechanism for methane oxidation at high pressure:

$$
\begin{aligned}
&0. \quad CH_4 + O_2 \longrightarrow \dot{C}H_3 + H\dot{O}_2 \\
&1. \quad \dot{C}H_3 + O_2 \longrightarrow CH_3\dot{O}\dot{O} \\
&2. \quad CH_3\dot{O}\dot{O} + CH_4 \longrightarrow CH_3OOH + \dot{C}H_3 \\
&3. \quad CH_3OOH \longrightarrow CH_3\dot{O} + \dot{O}H \\
&4. \quad CH_3\dot{O} + CH_4 \longrightarrow CH_3OH + \dot{C}H_3 \qquad (4\text{-}17) \\
&5. \quad CH_3\dot{O}\dot{O} \longrightarrow HCHO + \dot{O}H \\
&6. \quad \dot{O}H + CH_4 \longrightarrow H_2O + \dot{C}H_3 \\
&7. \quad \dot{O}H + HCHO \longrightarrow H_2O + \dot{C}HO \\
&8. \quad HCHO + O_2 \longrightarrow \dot{H}C\dot{O} + H\dot{O}_2 \\
&9. \quad \dot{H}C\dot{O} + O_2 \longrightarrow H\dot{O}_2 + CO
\end{aligned}
$$

10. $HO \xrightarrow{\text{wall}}$ chain breaking

11. $CH_3OO \xrightarrow{\text{wall}}$ chain breaking

The scheme includes two chain reactions. One forms formaldehyde and water through equations 1, 5, and 6. The second forms methanol through equations 1, 2, 3, and 4. No equation is proposed for carbon dioxide formation, and it can be inferred that it comes from oxidation of the monoxide.

Comparative rate constants for equations 1, 2, and 5 were calculated by Lott. Methane and oxygen concentrations used were from results obtained at 2,000 psi. and 338°C.

$$w_1 = k_1 [O_2] [\dot{C}H_3] \qquad (4\text{-}18)$$

$$a_1 = k_1 [O_2] = 6.02 \times 10^7 \text{ sec}^{-1} \qquad (4\text{-}19)$$

$$a_2 = 5.9 \times 10^6 \text{ sec}^{-1} \qquad (4\text{-}20)$$

$$k_5 = a_5 = 8.56 \times 10^5 \text{ sec}^{-1} \qquad (4\text{-}21)$$

It is seen that a_5 is smaller than a_1 or a_2, indicating that the isomerization of the $CH_3\dot{O}O$ cannot be discounted in the mechanism. Semenov had assumed the isomerization was not controlling. It now seems advisable to picture the formation of formaldehyde as a two-step process. Reaction 2 competes with step 5 for $CH_3\dot{O}O$ radicals, and one would expect formaldehyde to be a less important intermediate

at high pressure than at low pressure. Lott thus postulated that the $CH_3\dot{O}O$ radical is the probable precursor to methanol. Either the methanol is formed as shown in reactions 2, 3 and 4 of Set (4-16), or it could be formed directly

$$CH_3\dot{O}O + 2CH_4 \longrightarrow 2CH_3OH + \dot{C}H_3. \qquad (4\text{-}22)$$

The three step mechanism was considered by Lott (29) to be the more probable.

CHAPTER V

EXPERIMENTAL EQUIPMENT

The equipment used was essentially that described in earlier work (29) but modified for the present study. In this equipment methane and oxygen were compressed to a high pressure and were reacted at a given temperature and for a given period of time. Samples of the gaseous and liquid products were then recovered for analysis.

Flow diagrams of sections of the system are shown in Figures 6, 8, and 11. These figures contain, respectively: (1) The Feed Preparation and Storage Section. (2) The Compression Section. (3) The Reaction and Product Collection Sections.

Feed Section

The function of the feed system was to store pure methane and oxygen in the proper proportions at room temperature and 5,500 psi. Methane and oxygen were supplied to the feed system directly from 1A size cylinders. Initial pressure in each was approximately 2,000 psi. A section of temporary copper tubing was used to connect the methane and oxygen cylinders to the feed inlet point of the system.

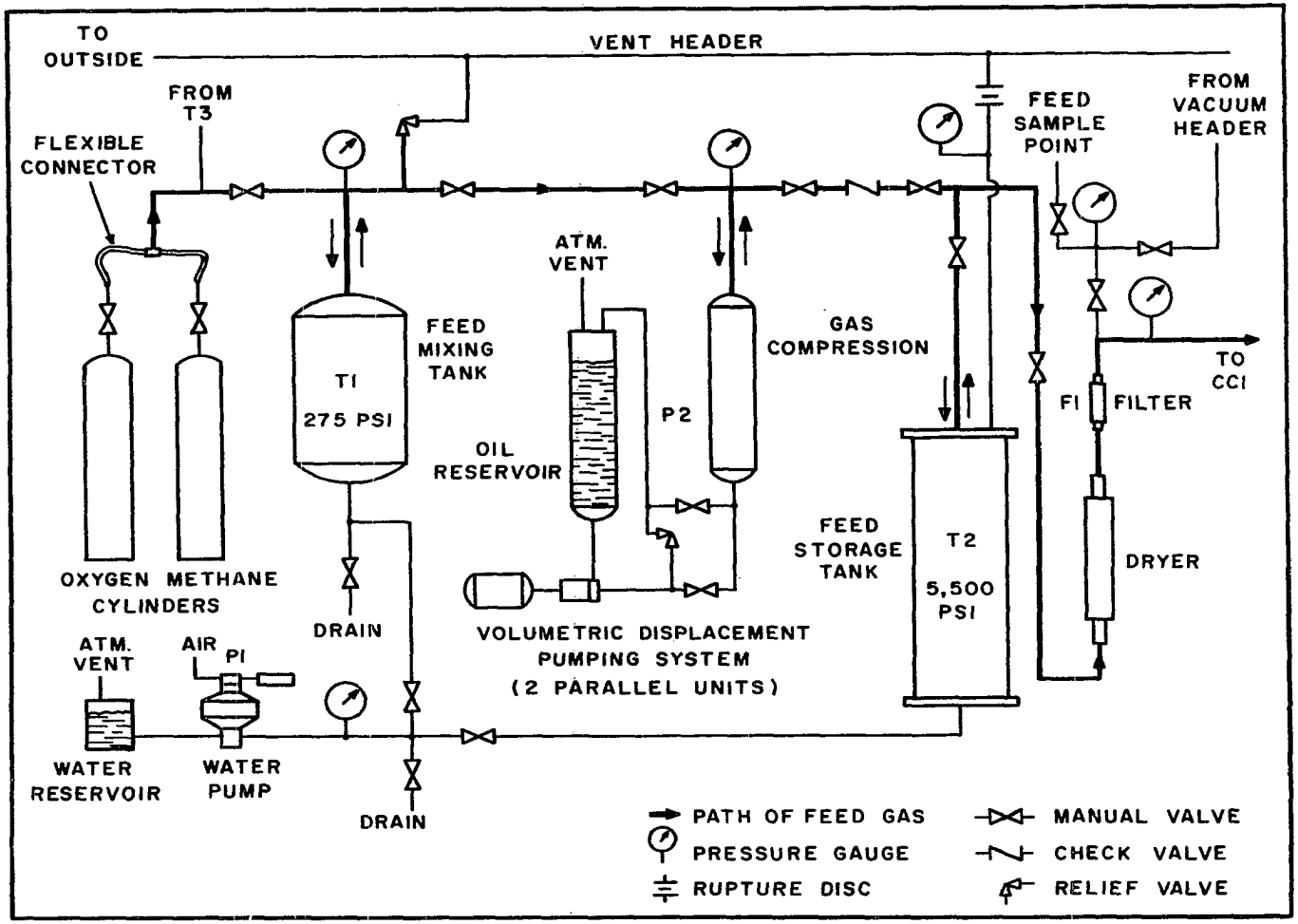


Figure 6. Flow Diagram of Feed Section.

The methane cylinder was equipped with a gas regulator which delivered a maximum pressure of 90 psig. A special regulator, required for use with pure oxygen, delivered the gas at a maximum pressure of about 150 psig. The hazards of using pure oxygen are well known. When connecting the copper tubing to the oxygen regulator, it was necessary to inspect and clean the copper tubing to make sure there was no oil present which could react explosively with the pure oxygen.

The methane and oxygen flowed from the cylinder to the feed mixing tank, T1. The vessel was cylindrical in shape with hemispherical ends and of nonshatterable construction. Connections were located at the center of each of the hemispherical ends. It was 24 in. O.D. and had a volume of 18,000 cu. in. The vessel was rated at 400 psig. and was equipped with a relief valve set at 375 psig. to discharge the contents of T1 into the one inch diameter vent header.

The feed gas in T1 was compressed from 100 psig. to 300 psig. by injecting water into the bottom of the tank. A Sprague air-driven pump, Model S-16C-100, was used for this purpose. The high pressure cylinder was made of brass and the plunger of stainless steel. A hard rubber O-ring, held between Teflon backup rings, was used as packing. Both check valves were of stainless steel. Maximum recommended pressure was 8,800 psi., and output was specified as 0.15 gpm at 5,000 psi. A 15-gallon glass jar

was used as a reservoir for water. A filter was installed between the reservoir and the pump.

From T1 the feed gas was transferred batchwise to the feed storage tank using the volumetric displacement pumping system, P2. This unit was designed and built at the University of Oklahoma. It consisted of two identical pumping units. While one cylinder was being used to compress the feed gas, oil was drained from the other and returned to its reservoir. Each pumping unit, then, consisted of a gas compression cylinder, an oil reservoir and a 0-10,000 psi. pressure gauge. Eight valves were required to direct the gas and oil to the proper points of the unit. One oil pump, a Seco, radial pump, Model 20LA-H, rated at 10,000 psi., was used to pump the oil alternately to the bottom of the gas compression cylinders. The pump, which was driven by a 3 hp electric motor was of the positive displacement type and was equipped with a relief valve set at 10,000 psi. Rated output of the oil pump was 0.5 gpm.

Feed gas for several runs was charged to the feed storage tank, T2. The vessel was 8 in. I.D. and 52 in. in internal length and was constructed by Autoclave Engineers, Inc. It was cylindrical in shape with the O.D. being 12 in. An end closure was located at only one end, and the seal was made using a hard rubber O-ring. The material of construction was 4340 steel. Two openings for 3/8 in. Autoclave Engineers (AE) cone fittings were located at the bottom of the tank and three were located in the top cover

(closure). The vessel was tested hydrostatically to 22,500 psi. The maximum working pressure was recommended as 15,000 psi. A rupture disc was installed in the top cover, designed to relieve when pressure in the vessel reached 20,000 psi.

A check valve was installed in the line between P2 and T2 to prevent the large volume of gas stored in T2 being inadvertently misdirected back to T1. All connections between T1, P2 and T2 were of 1/8 in. x 1/4 in. stainless steel tubing and connections were made to valves, etc., using Autoclave Engineers "Ermeto" fittings. The pressure rating of the fittings was 10,000 psi. Maximum working pressure of this part of the system was limited to 6,500 psi. Figure 7 shows T2 at the left and T1 at the right.

One of the bottom openings of T2 was piped to the discharge side of P1 in order that water could be pumped into the bottom of T2. Gas in T2 was normally stored over water and had to be dried before being compressed further. A Kuentzel bomb, located downstream from T2, was used as a dryer. The bomb was made of stainless steel and manufactured by Autoclave Engineers. Internal dimensions were 1 in. x 8 in. Pressure rating of the vessel was 10,000 psi. Drierite was used as drying agent and cheesecloth was also used as a partial filtering medium at the discharge side. In addition, a filter containing porous metal discs was installed downstream of the dryer. The filter was manufactured by Autoclave Engineers and was designed for 10,000

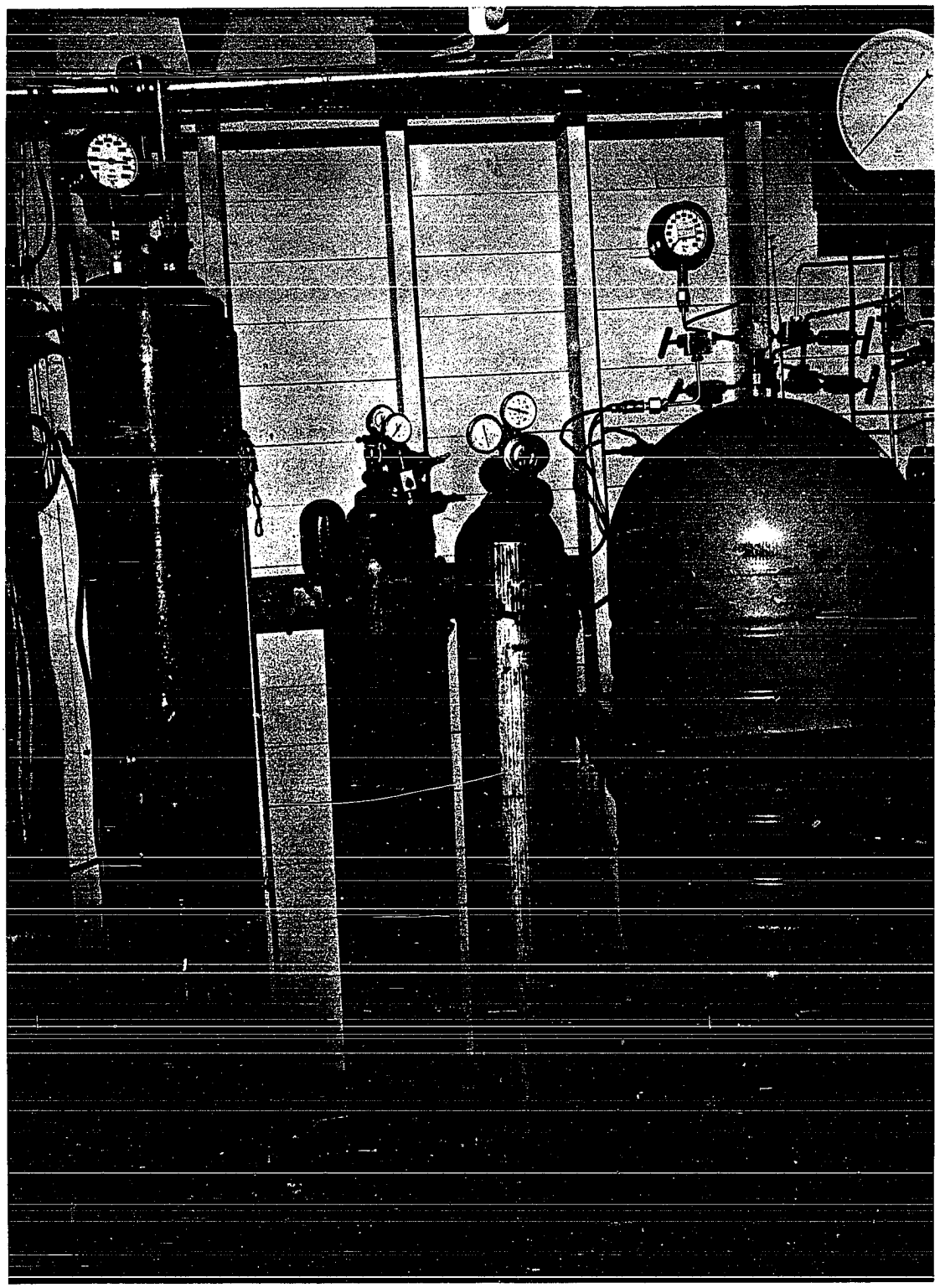


Figure 7. Feed Storage Vessels.

psi. maximum pressure. A connection was provided downstream of the filter as a sampling point for the feed.

Compression Section

The compression section received feed gas at room temperature and 5,500 psi. and delivered it to the reactor after compression at room temperature and pressure up to 150,000 psi. The compression section is shown in Figure 8.

Feed gas stored in T2 was dried and filtered and fed batchwise to the intermediate pressure compression cylinder, CC1. This compression unit was constructed at the University of Oklahoma using a high pressure cylinder procured from the University of Michigan. The dimensions of the cylinder were 1 5/16 in. I.D. and 16 in. internal length. The outside diameter was 3 in. and material of construction was 400 series steel. An end closure, sealed by an O-ring, was located at one end. The end closure had two AE cone connections for 9/16 in. diameter high pressure tubing. The other end had one opening for the same size tubing. An aluminum piston, 1 5/16 in. diameter x 1 5/16 in. long was used as a free piston between the feed gas and hydraulic fluid. A hard, oil-resistant O-ring was used on the piston as the sealing medium. The cylinder was installed vertically with the end closure being at the bottom. One of the bottom openings was connected to the discharge side of the oil pump, P3. The other opening was connected to the line leading to the oil reservoir. Maximum working pressure of CC1 was 25,000 psi.

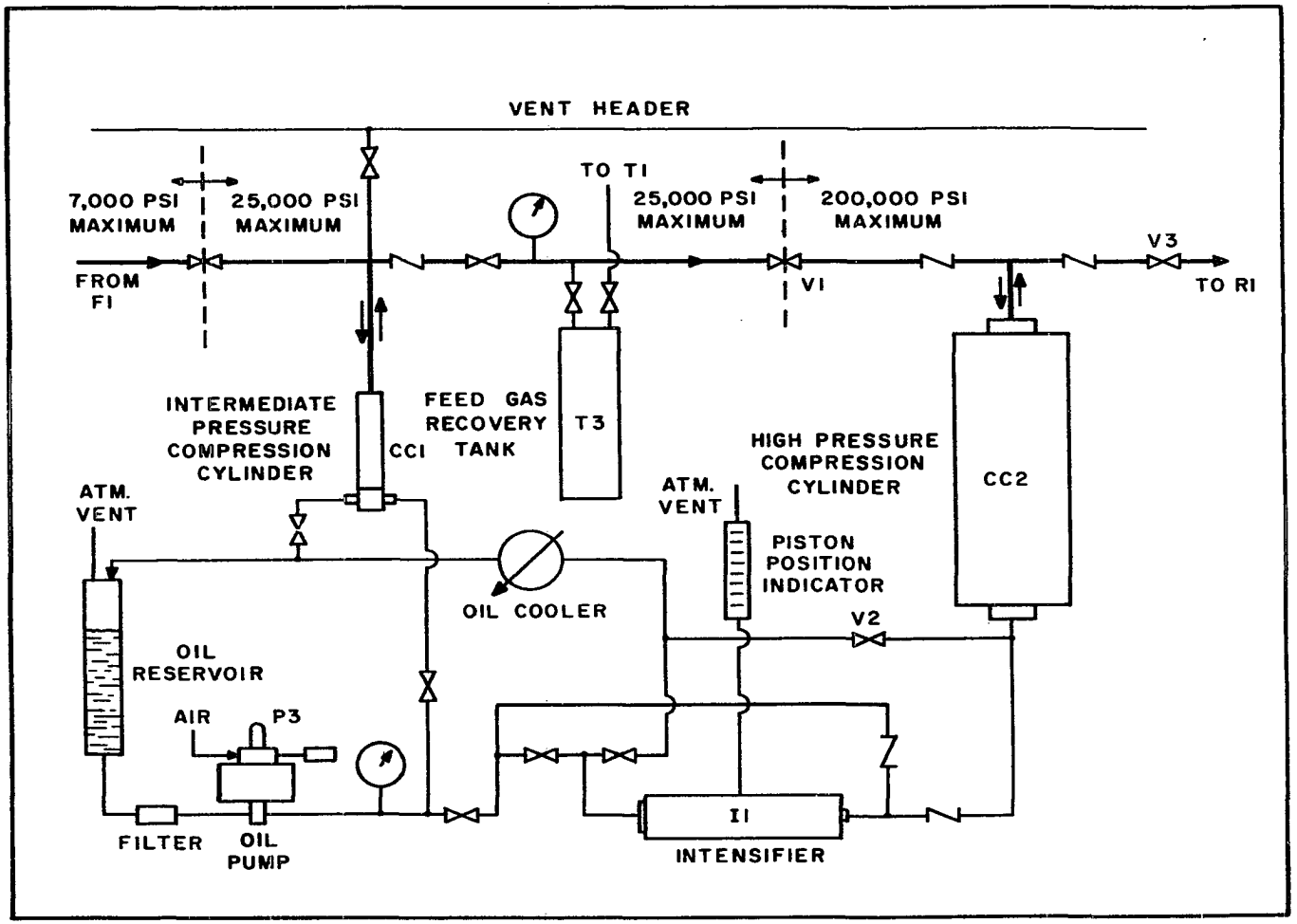


Figure 8. Flow Diagram of Compression Section.

The oil pump, P3, was used to pump hydraulic oil to the bottom of CC1. The pump was manufactured by S-C Corporation as Model 10-600. The high pressure cylinder was made of brass and the plunger of stainless steel. A Buna N O-ring with Teflon backup rings on either side was used as packing. Both suction and discharge check valves were of stainless steel. The pump was air operated and had a maximum working pressure on the hydraulic side of 30,000 psi. Plexol 201 obtained from Rohm and Haas Company was used as hydraulic fluid. Since the oil was recycled, it was filtered before being introduced to the suction check valve.

From CC1 the feed gas was pressured batchwise into the high pressure compression cylinder, CC2. This vessel, along with the reactor, was designed by personnel of the University of Oklahoma in collaboration with Autoclave Engineers, Inc. CC2 was a heavy-walled vessel of modified 4340 steel and triplex, shrunk-fit construction. Details of the design are given in reference 29. A photo of the vessel is shown in Figure 9.

The inside diameter of CC2 was two inches and overall length of the billet was 40 in. The outside diameter was 18 in., giving the highest wall ratio economically feasible--9:1. Modified Bridgman closures were provided at both ends. CC2 was installed in a vertical position as shown in Figure 9. A free piston made of brass was used in this cylinder to separate the hydraulic oil from



Figure 9. 200,000 psi. Compression Cylinder [from Lott (29) reproduced by permission].

the gas phase. The piston was fitted with oil-resistant, O-ring seals at the top and bottom of the piston. Double Teflon rings were used on either side of the O-rings. Maximum design pressure of CC2 was 200,000 psi., at which pressure it was tested hydrostatically. Due to the heavy weight of this unit, 2400 lb., it was supported on a metal stand with the weight distributed on a bottom plate 20 in. in diameter.

Gas flowing from CC1 to CC2 passed through a check valve and manually-operated valve rated at 30,000 psi. before the gas entered the first 200,000 psi.-rated component, a block valve shown as V1 in Figure 8. Between the 30,000 psi. valve and the block valve a line was installed to the feed gas recovery tank, T3. This tank was not in the line of flow; it was isolated from the system when feed gas was compressed. It served two functions. When a leak developed in the 200,000 psi. part of the system, the gas was recovered by bleeding it slowly backwards to T3. If not contaminated with product, the gas was recycled to T1. The second function of T3 was to serve as a surge volume for the 200,000 psi. part of the system in case the block valve, V1, leaked. This provision avoided the hazard of overpressuring the part of the system ahead of V1 which was rated at only 30,000 psi.

T2 was obtained from the University of Michigan. It was a 75 mm. cannon barrel converted to a high pressure vessel. Plugs were welded into both ends of the bore.

Two connections for 1/4 in. coned tubing were provided in one end. The vessel was tested and rated at 25,000 psi. As noted in this work it was used as an auxiliary vessel.

The tubing used for connections around CC1, P3 and T3 was 0.083 in. I.D. x 1/4 in. O.D. and no section had a pressure rating of less than 30,000 psi. The valves, tees, ells, etc., also were rated at 30,000 psi. minimum. However, CC1 was only rated at 25,000 psi. and a pressure gauge installed between CC1 and CC2 had a range of only 25,000 psi. In practice, pressure in this part of the system was limited to 22,000 psi.

Hydraulic oil was pumped into the bottom of CC2 using the intensifier, I1, a single acting compression device. The low pressure drive cylinder was powered by hydraulic oil pumped from P3. The cross-section of the high pressure cylinder was one-tenth that of the low pressure cylinder, giving an intensification ratio of 10:1. Figure 10 shows the intensifier at the bottom with P3 at the right and CC2 in the background.

The intensifier was designed and manufactured by Autoclave Engineers, Inc. The low pressure cylinder was of 4340 steel, and the high pressure cylinder of Vascomax 250 CVM, an 18 percent nickel Maraging steel manufactured by Vanadium-Alloys Steel Company. Hard rubber O-rings were used to seal the closures on both ends and to seal the high pressure and low pressure cylinders together. Low pressure packing was of chevron design made of Teflon.

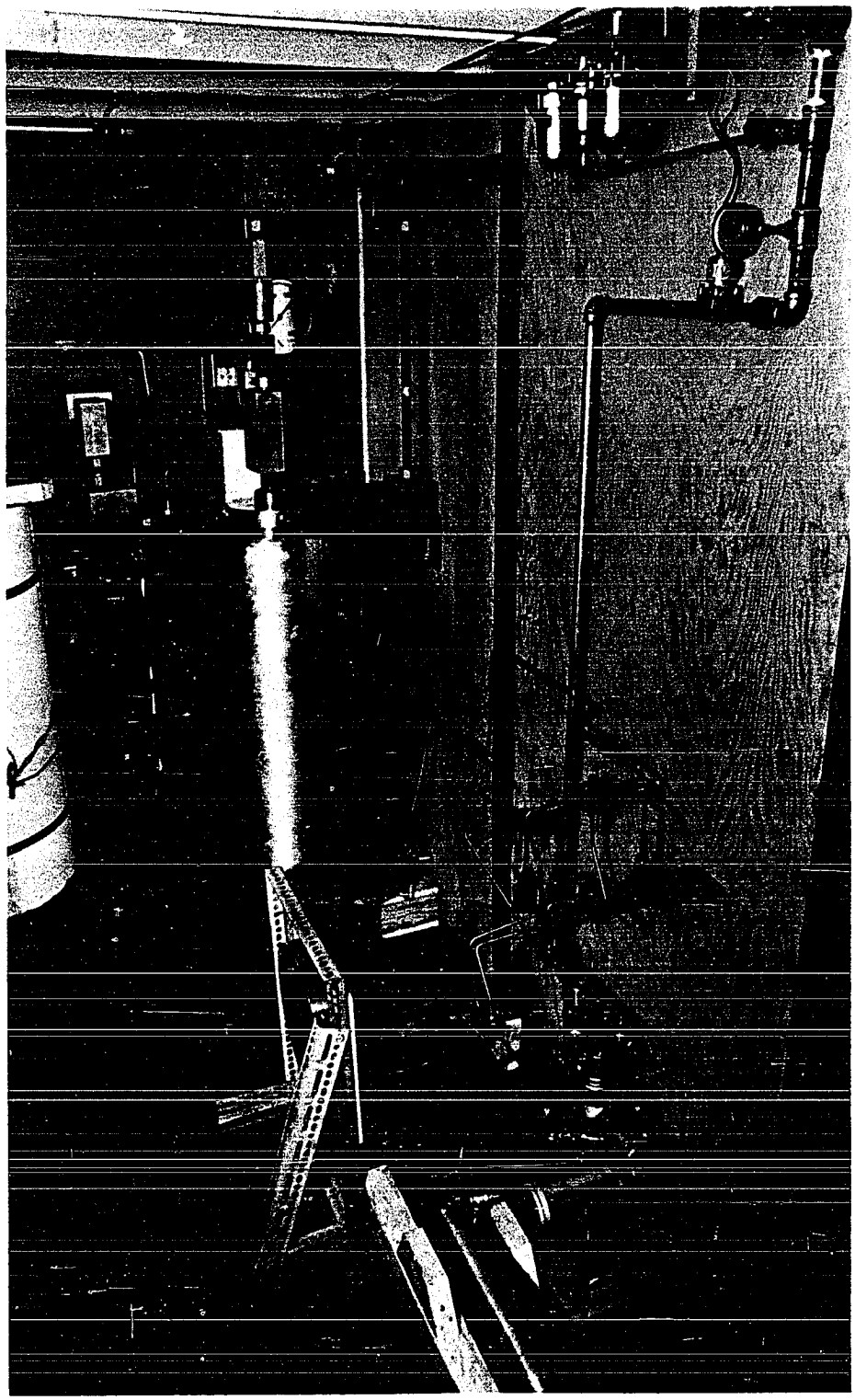


Figure 10. 200,000 psi. Equipment Inside the High Pressure Cell [from Lott (29), reproduced by permission].

Packing for the high pressure piston was made of a special, dense-grain cowhide. The internal diameter of the high pressure cylinder was one inch with outside diameters of the high and low pressure cylinders being five inches. The low pressure cylinder was fitted with a 3/8 in. cone connection, and the high pressure end closure had a seat for a 200,000 psi. double-ended cone connection. The middle cavity of the low pressure cylinder was filled with hydraulic oil and connected to a long, thin 1000 ml. cylinder which in turn was vented to the atmosphere. The cylinder was used to indicate the position of the pistons. When empty of oil the pistons were bottomed at the low pressure end. Plexol 201, used in P3, was also used in I1 and CC2. I1 was tested and rated at 200,000 psi.

The tubing used in the 200,000 psi. part of the system was of duplex construction and was obtained from Harwood Engineering Company. It was 1/16 in. I.D. and 3/4 in. O.D. Four manually operated valves and four check valves were used in the 200,000 psi. section. These valves were designed and built by Autoclave Engineers as were most of the ells, tees, cones, and other 200,000 psi. rated fittings. However, some of the fittings used were obtained from Harwood Engineering.

Reaction Section

From CC2 the feed gas flowed to the reactor, R1, shown in Figure 11. R1 was of duplex construction and was

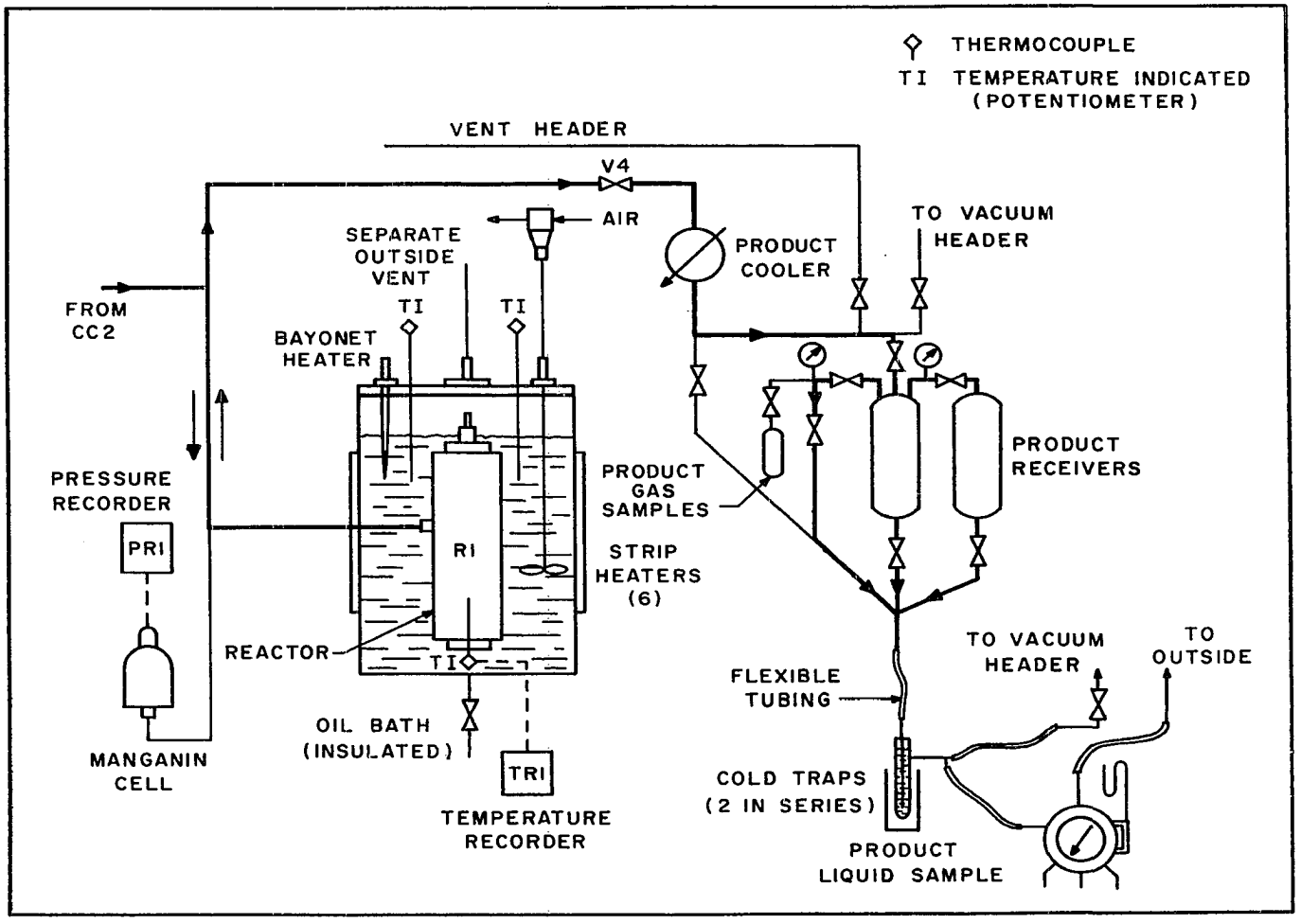


Figure 11. Flow Diagram of the Reaction and Product Collection Sections.

made of 18 percent nickel Maraging steel. It was two inches I.D., 12 in. O.D. and the outside billet was 26 5/8 in. long. The interference required for the shrink-fit of the two cylinders was 0.0376 in., which would necessitate a temperature difference of about 1700°F between the cylinders for assembly. This interference could not be obtained because the Maraging steel cannot be heated above 900°F without changing its crystal form. Therefore, the strength characteristics needed were obtained by a combination of shrink-fit and autofrettaging. The reactor was designed by Lott at the University of Oklahoma and Autoclave Engineers, Inc. It was manufactured by Autoclave Engineers. The reactor was installed vertically and is shown in Figure 12.

Bridgman seals were used in both ends of R1. It was necessary to provide entry points for a thermocouple and insulated electric wire as well as for the reactant gases. The thermocouple was installed in the bottom packing cover. It consisted of a section of 1/16 in. x 5/16 in. O.D. tubing welded together at one end and fitted with a standard cone connection at the other. The cone was fitted to a seat in the packing cover. In order to introduce electric power, an electrode was installed in the top packing cover. The electrode consisted of a 1/4 in. diameter steel shaft which had its own Bridgman type packing and was insulated from the packing holder by alumina backup rings. The other electrical lead was

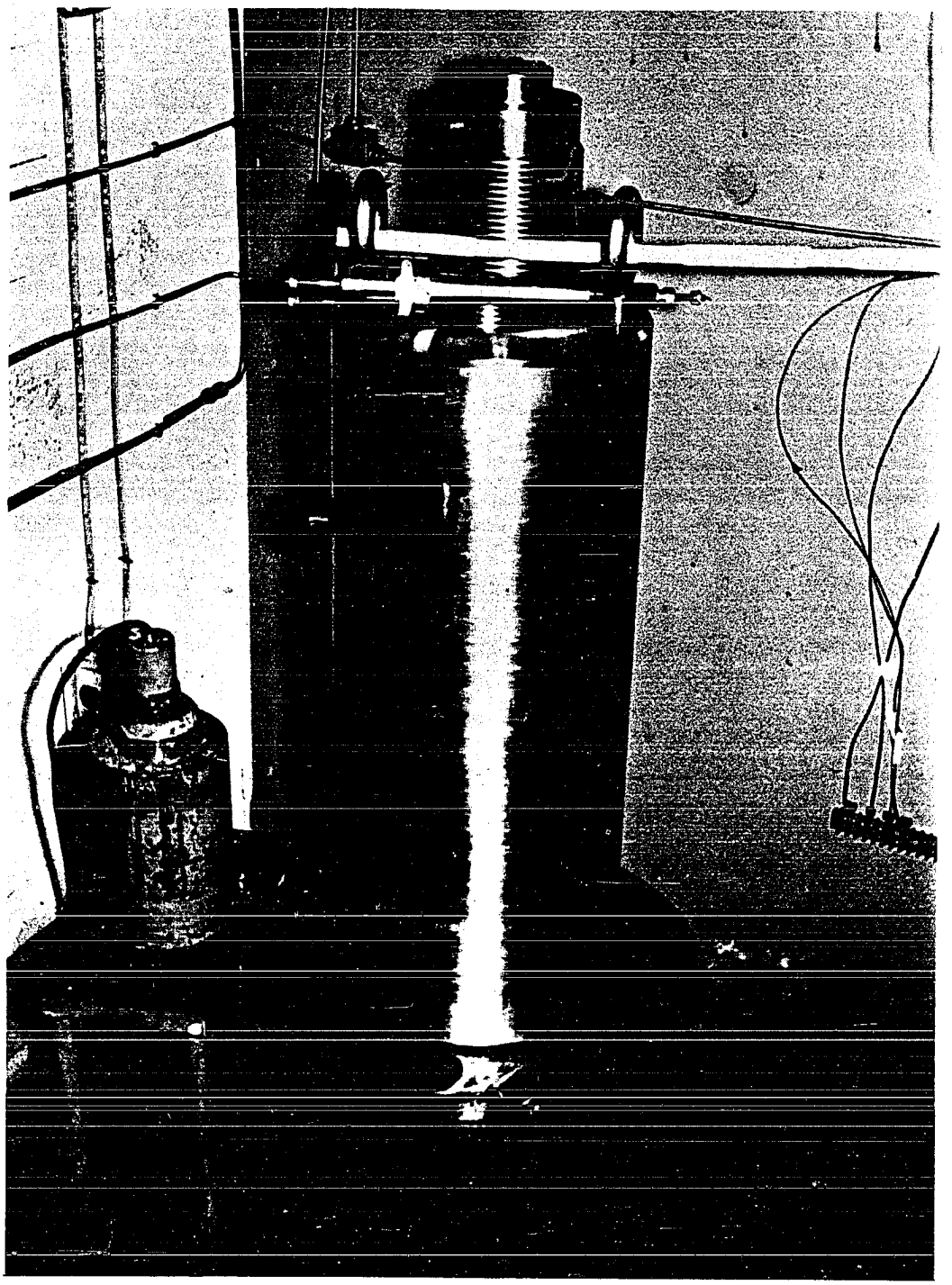


Figure 12. 200,000 psi. Reactor [from Lott (29), reproduced by permission].

connected to the packing holder which was grounded along with the reactor. The feed gases were introduced (and removed) through a 1/16 in. opening in the side of the reactor. The connection was made to the reactor, as were all the 200,000 psi. connections, by using a double ended cone.

When the top and bottom packing covers were in place, the actual reactor length was 10 inches. Part of this volume was taken up with an internal heater used to maintain a given temperature for the oxidation reaction. The heater was made from Nichrome wire wound on a core, and the core was then coated with a nonconducting cement. Two types of material were used for the heater cores and coating. One was made of high purity alumina used in both core and coating. The heating element consisted of 25.5 ft. of No. 19 Nichrome wire. In this case there was no silicon-containing material in the reactor. The second core was made of Pyrex, the 30 ft. of No. 18 Nichrome wire being inserted in porcelain insulators and then coated with Sauereisen No. 1 porcelain cement. The alumina heater is shown in Figure 13 attached to the top packing cover. The heaters were rated at 800 watts at 115 volts. Voltage to the heater was controlled by a Powerstat transformer.

Pressure was measured by a Manganin cell and recorded on a Foxboro Dynalog recorder, model 942OP. The chart paper was circular and completed one revolution in one hour. The recording was continuous. The Manganin

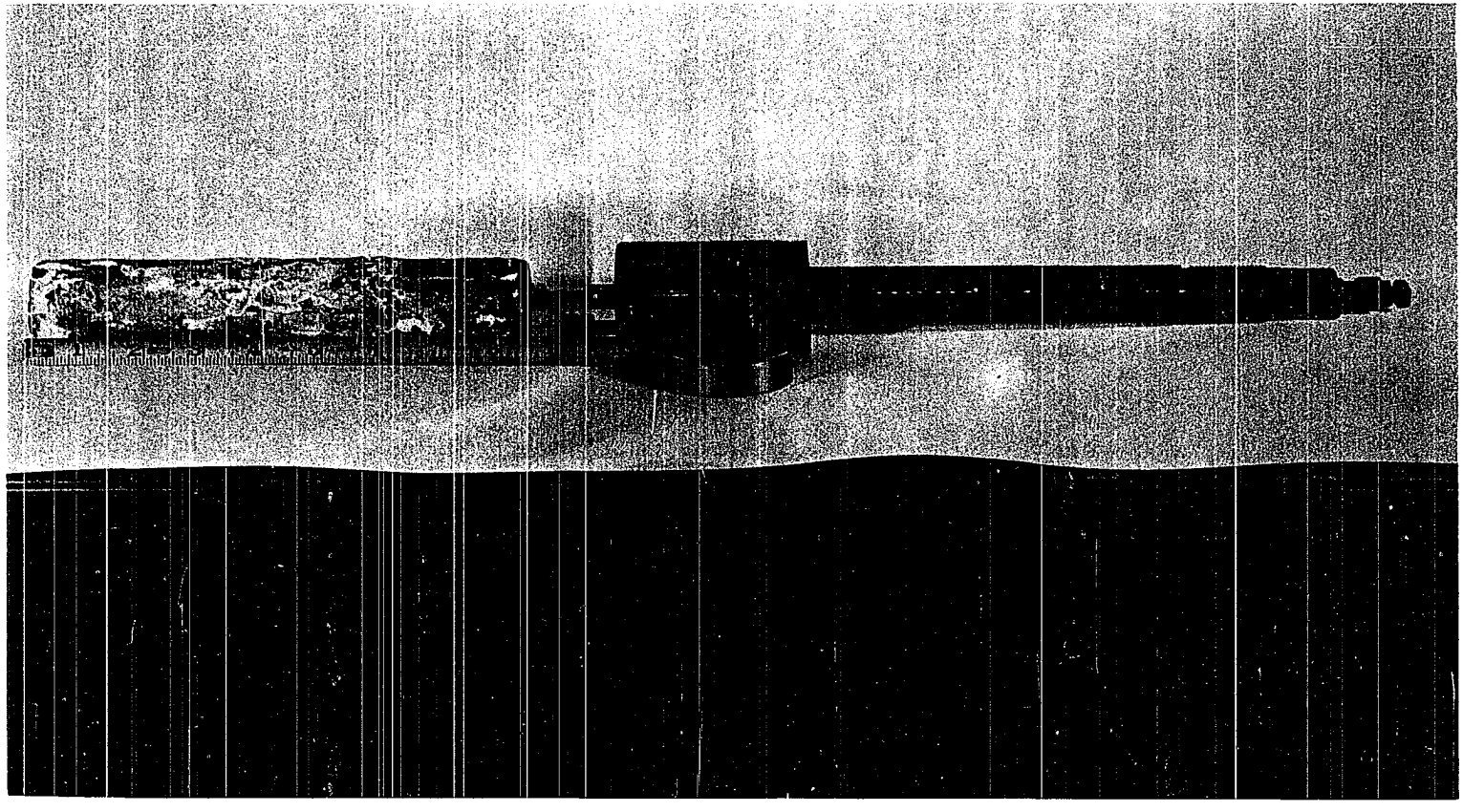


Figure 13. Internal Heater (Alumina) Attached to Top Cover.

cell was obtained from Harwood Engineering and was Model E-1608. Resistance of the internal and external coils was 120.0 ohms. The cell was rated for operation to at least 200,000 psi. The calibration used was that reported by Lott (29).

An iron-constantan thermocouple was installed in the thermowell in the bottom of R1. The output was recorded on a Bristol Dynamaster high speed recorder, Model 560, and was measured on a Rubicon Instruments potentiometer, Model 2745.

The reactor was immersed in an oil bath which contained Mobiltherm 600 heat transfer oil supplied by Mobil Oil Co. The oil bath measured 24 in. in diameter and was 36 in. long. A photograph of the oil bath is shown in Figure 14. The reactor was supported vertically on a small stand in the middle of the bath. A stuffing box was provided in the side of the bath for the reactor inlet pipe. It was equipped with a drain line and valve in the bottom. The oil bath was made of sheet steel and heated by six 1000 watt heaters equally spaced around the outside of the tank and imbedded in Thermon T3. The heaters were covered with asbestos mud, and then two inch thick Kaylo pipe insulation was installed. The heaters were connected in parallel; power from a 220 volt source was regulated by a Powerstat. An ammeter with a range of 30 amps. was installed in the circuit. The oil bath was designed for operation at a maximum oil temperature of 270^{o}C.

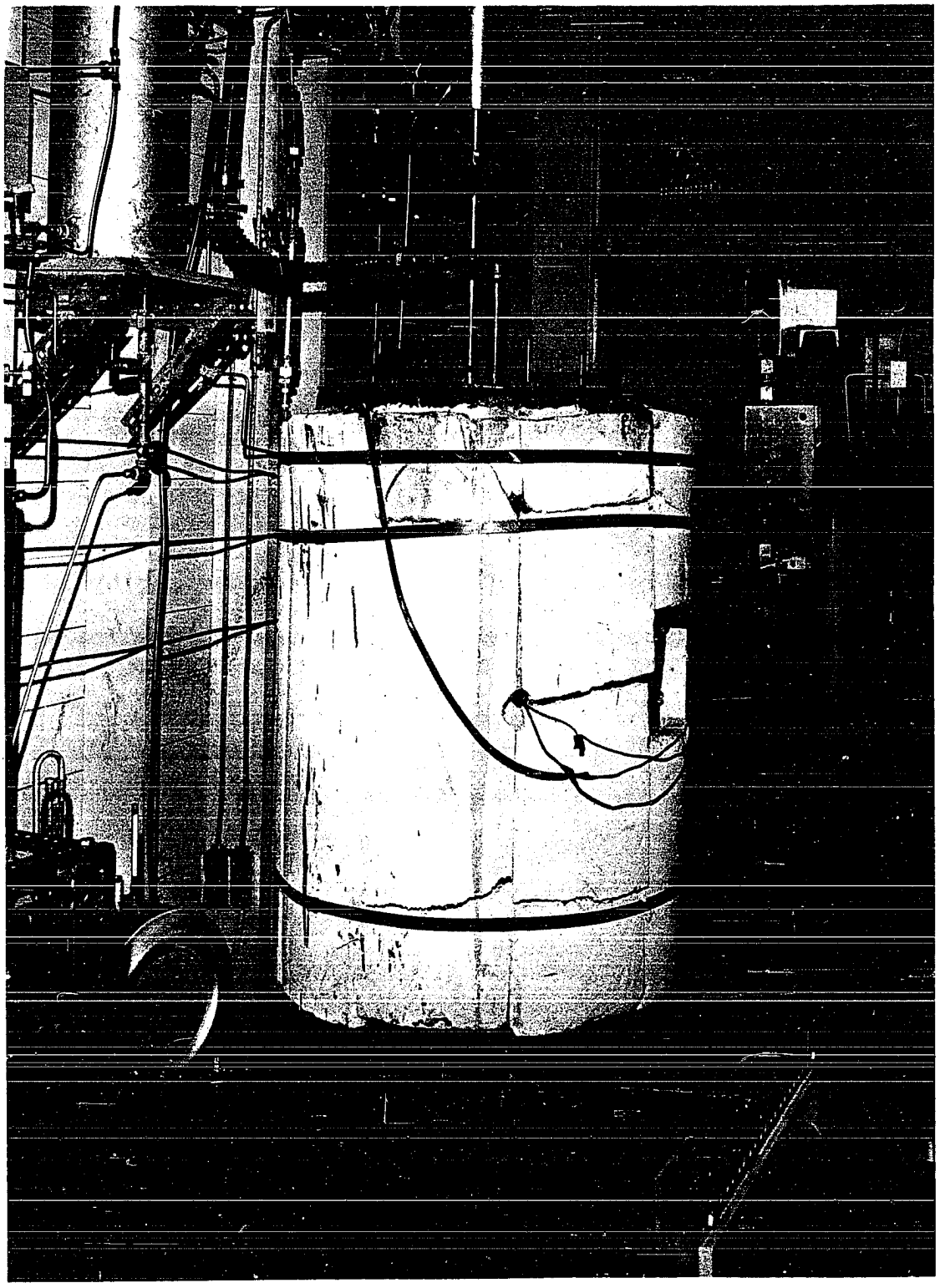


Figure 14. Oil Bath and Accessories.

The top cover of the oil bath was made of 1/4 in. steel plate, 24 in. in diameter. A gasket of 1/16 in. thick asbestos was glued to the bottom of the lid using Epoxy resin. The lid rested on the rim of the bath and was not bolted down. The top cover contained a 1 in. vent pipe, a combined seal and bearing for a Lightening air-operated mixer shaft, an opening for the reactor thermocouple, insulated electrical connections for the reactor internal heater, two thermowells and a 750 watt bayonet heater. The two thermowells contained iron-constantan couples used to measure the oil temperature. The stirrer assured that the oil was maintained at isothermal conditions. The Chromalox bayonet heater was connected to a Fenwall thermoswitch located in the wall of the oil bath. This heater was set to cut out at 215^{o}C.

Product Collection Section

From R1 the partially reacted feed gases and products were passed through a water-immersed cooling coil to the product receivers. One receiver was constructed of four inch schedule 40 pipe, 24 inches long. Pipe caps were welded on the ends, with three openings provided in the top and one in the bottom. Working pressure was designated as 500 psi. One of the top connections was the inlet to the receiver from R1, one was used as a gas sampling point and the third was used for a line to the second receiver and for a 12 in. Heise pressure gauge. The second receiver was

a 500 cu. in. stainless steel vessel previously used for oxygen. It had openings top and bottom. The bottom connections from both receivers and from a drip leg under the cooling coil were connected to two cold traps in series. The product gas was purged through the traps and all condensables were frozen out at dry ice temperature. In experiments 116-149 the product gas was then vented. For the remainder of the experiments it was passed through a wet test meter and vented. The product collection system is shown in Figure 15.

Auxiliaries

Gas samples of both feed and product gas were collected in 1CC-3AA cylinders. A vent header was installed on two sides of the barricaded cell and gas from various points in the system was vented to it to allow purging to take place safely. A vacuum line was available in the barricaded cell, tied into a Duo-seal vacuum pump made by W. M. Welch Manufacturing Co. Dry air was available at 140 psi. for operation of P1, P3 and the oil bath stirrer.

High Pressure Cell

All the high pressure equipment which operated at over 10,000 psi. was contained in a barricaded cell. Floor dimensions of the cell were seven feet by twelve feet and the ceiling was eight feet high. The walls and ceiling were made of 1/4 in. steel plates welded together.

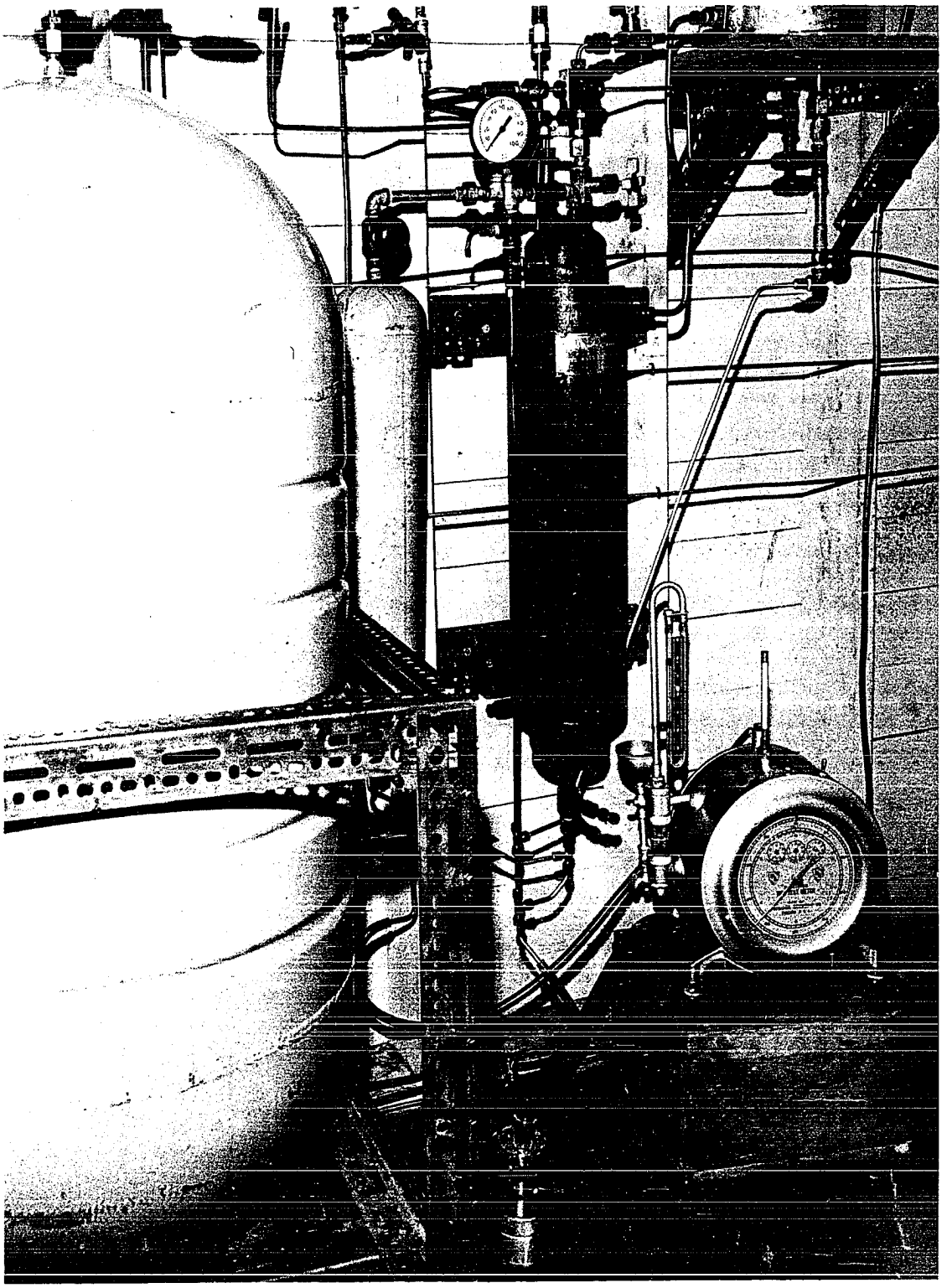


Figure 15. Liquid Product Collection Section.

The interior of the plates was backed by two inch tongue and groove wood. A Manila rope blast mat was laid on the ceiling and one was hung over the opening at one end of the cell which was used as a door. A blow-out panel six feet by eight feet was installed with small screws in the outside wall of the building. A pressure of about one psi. would allow the panel to drop away. A vent fan of high capacity was located in the bottom section of the blow out panel in order to dissipate any gas leakage. A Manila rope blast mat was hung about three feet from the blow-out panel on the outside of the building. Valves which had to be operated at pressure over 10,000 psi. were equipped with extension handles which passed through the cell walls. The 200,000 psi. valves V1, V3, V4 were fitted with extension handles with a three inch disc welded vertically to the handles. This arrangement prevented the extension handle from being blown into the working area in case the gland nut of a valve failed.

The building was equipped with fire hose and fire alarms, and two 15 lb. CO_2 extinguishers were located in the immediate vicinity of the cell.

CHAPTER VI

EXPERIMENTAL PROCEDURE

The procedure is divided into four parts, each describing a different operation required in order to prepare for and complete an experiment: Feed Preparation and Storage, Procedures Prior to Reaction, Conducting Reaction and Sample Collection. The pieces of equipment to which reference is made are shown in the flow diagrams, Figures 6, 8 and 11.

Feed Preparation and Storage

Methane and oxygen were the reactants charged to the feed mixing tank. It was assumed that the mixing tank, T1, contained a small amount of residual feed and, specifically, no air. If it did contain air, it would have been necessary to evacuate it before adding the methane. The methane was charged first to T1 in order to avoid having an explosive mixture of methane and oxygen at any stage of the operation. The explosive limits of the mixture at atmospheric pressure and temperature are approximately five to 60 volume percent methane. In this work an average methane concentration of about 92 volume

percent was used, and it was necessary to avoid getting air or oxygen into the equipment before adding methane. With the gas regulator used, a methane pressure of 90 psig. was obtained in T1. The copper tubing was then disconnected from the methane regulator, inspected and cleaned to make sure that it did not contain any organic liquid. The connection of the oxygen regulator was kept covered with a piece of clean cheese cloth to avoid accidental contamination. After connecting the tubing, oxygen was added to T1 to the pressure calculated to give about eight volume percent oxygen in the mixture. The resulting pressure was usually about 100 psig.

Water was then pumped into T1 using the water pump, P1, until the pressure was 300 psig. At this point feed from T1 was transferred batchwise to the feed storage tank by the use of the volumetric displacement pumping system, P2. After the gas side was valved in, the valve to the oil pump was opened, and oil pumped into the bottom of the cylinder until the pressure was 5,500-6,000 psi. The valve to the pump discharge side was closed, and the valve leading to T2 was opened. After the gas had depressured to T2, the valve was closed. Another valve was opened to allow the oil to drain back to the reservoir. The gas cylinder, when empty of oil, was filled to about 300 psi. with gas, and the procedure was repeated. There are two parallel units to P2, so that while one cylinder was being filled with oil, the other was being drained. Since P2 was a positive

displacement pump, even though it had a relief valve, it was necessary to avoid turning it on before the discharge valve was opened. When the feed supply in T1 had been transferred to T2, the water was drained from T1, and it was recharged with methane and oxygen. It was necessary to recharge T1 three times in order to achieve a pressure of 2,000 psi. in T2. The pressure in T2 would vary, of course, depending on the residual feed left in it before transfer from T1 started. When the pressure in T2 was about 2,000 psi., water was pumped into the bottom via P1, and the pressure was increased to 5,500 psi., which was the feed storage pressure. Enough feed was now available in T2 for about 12 experiments, depending on the pressure of reaction.

Prior to Reaction

About fifteen hours before an experiment was to be run, usually the night before, the main heaters around the oil bath and the bayonet heater were turned on. The Powerstat to the main heaters was adjusted to give an oil temperature in the range of 215-240^{o}C. In the morning the Powerstat was readjusted to bring the bath to the desired temperature while the system was brought to the desired pressure level. The receivers were then evacuated for at least 15 minutes. The pressure recorder, PR1, was zeroed. A check was made to make sure that the reactor discharge valve, V4, was closed, and that the valve from

R1 to the receivers was open. At this point, since it is assumed that a reaction had been carried out previously, the high pressure compression cylinder, CC2, contained feed gas at a pressure of 4,000-7,000 psi. The valve between CC2 and R1 was cracked to allow the reactor to fill slowly with gas. Before proceeding further, a check was made to see that the valves leading to and from the feed gas recovery tank, T3, were closed. The pressure gauge on the receivers was then checked to make sure that V4 was not leaking gas through the seat and stem. All valves from T2 to CC2, except the one ahead of CC1, were opened. Then the valve upstream of CC1 was cracked in order to allow the vessels downstream to fill with feed gas to a pressure of about 5,300 psi. The pressure in T2 was kept at from 5,000-5,500 psi., by running P1 periodically.

The valve ahead of CC1 was closed and valves were lined up to allow oil from P3 to flow to the bottom of CC1. As gas was pressured out of CC1 the pressure in CC2 and R1 was raised incrementally. When CC1 was full of oil, the pump was stopped, and the oil was drained back to the reservoir. The check valves downstream of CC1 kept it from refilling with gas as the oil drained out. CC1 was refilled with feed gas from T2 to about 5,300 psi., and after refilling, there would be enough gas in CC1 to take CC2 and R1 to at least 13,800 psi. This pressure was required before internal reactor heating was applied in order to conduct an experiment at 15,000 psi. P3 was

stopped as R1 approached 13,800 psi. V1 and V3 were closed, the oil was drained out of CC1 and the valve downstream of CC1 was closed. The valves between T2 and CC1 were closed. The reactor should then have been at the right temperature and pressure to begin a run at 15,000 psi.

If operation was planned at a pressure greater than 20,000 psi., the process of compression was repeated with CC1 until CC2 and R1 were at a pressure of 20,000 psi. V1 was closed, CC1 emptied of oil, and the valves in the intermediate part of the system were closed as before. The valve leading to T3 was opened. Oil flow from P3 was then diverted to the low pressure cylinder of the intensifier, I1. The pressure increase in R1 was slow, because of the 10:1 area ratio between the low pressure and high pressure pistons of the intensifier. Pumping with P3 was continued until the piston position indicator of the intensifier showed that the pistons were near the high pressure end. The pistons were then reversed by diverting the oil from the low pressure side to the high pressure side of I1. Once the pistons were reversed, oil was fed once more to the low pressure end, and this process was repeated until R1 was at about 46,000 psi. for a run at 50,000 psi., or at about 97,500 psi. if the final pressure of operation was at 100,000 psi. V3 was closed, the pistons in I1 were reversed, and the oil was drained from CC2 via V2. The reactor would then be at the desired temperature and pressure preparatory to initiating reaction.

The oil temperature was maintained 40-50^{o}C lower than the planned temperature of R1 for the experiment.

Conducting the Reaction

The reference temperature of the Rubicon potentiometer was checked and the chart drive of the reactor temperature recorder, TR1, was turned on. The internal heater in R1 was turned up to about 6.7 amps. As the R1 temperature increased, it was followed on TR1 and on the potentiometer. After six minutes, R1 was usually up to the experimental temperature level. Therefore, six minutes from the time the heater was turned on was designated as the starting time of the experiment. Voltage to the internal heater was decreased periodically to keep the temperature at the desired level. The pressure was recorded on PR1. Every five minutes R1 temperature was measured with the potentiometer and recorded. If the planned temperature of operation was too high and the heat of reaction could not be dissipated fast enough, a runaway or adiabatic reaction occurred. In this case, when the pressure returned to the original level for the isothermal reaction, the internal heater was usually turned off, and the contents of the reactor were released to the receivers. If the reaction remained isothermal, the internal heater was turned off after a predetermined time and the reactor was depressured to the product receivers. After pressure had equalized in R1 and the receivers, the pressure and temperature were taken.

Sample Collection

The receivers were valved off from R1. The inlet side of the cold trap was hooked up to the bottom connection from the receivers. The outlet side of the cold traps was connected to the vent. The gas and liquid left in R1 were passed slowly through the cold traps and vented. The flow rate was controlled by a needle valve. After R1 pressure was down to atmospheric, the outlet of the cold traps was connected to the vacuum header, and a vacuum was pulled on R1 for about 15 minutes. R1 was then blocked in temporarily, and the outlet of the cold traps was reconnected to the vent. A gas sample bomb was evacuated and connected to the gas sample point at the receivers. After purging the bomb twice with product gas, which was released through the cold traps, a gas sample was taken with 30 psig. in the bomb. Gas flow was then adjusted from the receivers through the cold traps. The flow rate was very slow, and required two hours time for the receivers to depressure to atmospheric for a 50,000 psi. experiment.

In experiments 150-176 the wet test meter was connected between the outlet side of the cold traps and the vent. After the receivers reached atmospheric pressure, the outlet from the cold traps was connected to the vacuum header. A vacuum was pulled on the receivers for about 30 minutes. The valves at the bottom of the receivers were then closed, and the cold traps were removed from the system. The contents of the cold traps were allowed to melt and were then

transferred to a 30 ml. sample bottle which had been weighed previously. The cold traps were connected back into the system. A vacuum was pulled on R1 and the receivers for three quarters of an hour. The cold traps were emptied and the process was repeated. The total sample collected was weighed. The sample was then stored in a freezer at $0^{o}C$.

CHAPTER VII

ANALYTICAL EQUIPMENT, PROCEDURES, AND CHEMICALS USED

Samples to be analyzed consisted of feed gas and product gas contained in 500 ml. sample bombs at 30 psig., and liquid product varying in weight from 1 to 19 gms.

Analytical Equipment

The gas samples were analyzed on a vapor phase chromatograph shown in Figure 16. The basic chromatograph was the one used by Pipkin (45), modified for this work. The unit consisted of a carrier gas system, sample addition system, column, detectors, recorder and constant temperature air bath.

Instrument grade helium was used as carrier gas. The pressure was reduced from a maximum of 2,000 psi. in the cylinder to a pressure of about 20 psi. by using a standard helium regulator. Flow to the chromatograph was then controlled at the desired rate by using a needle valve. Gas flow through the column was measured by means of a soap bubble device which consisted of a reservoir for liquid soap connected to the bottom of a burette. The gas entered at the bottom, forming a soap bubble

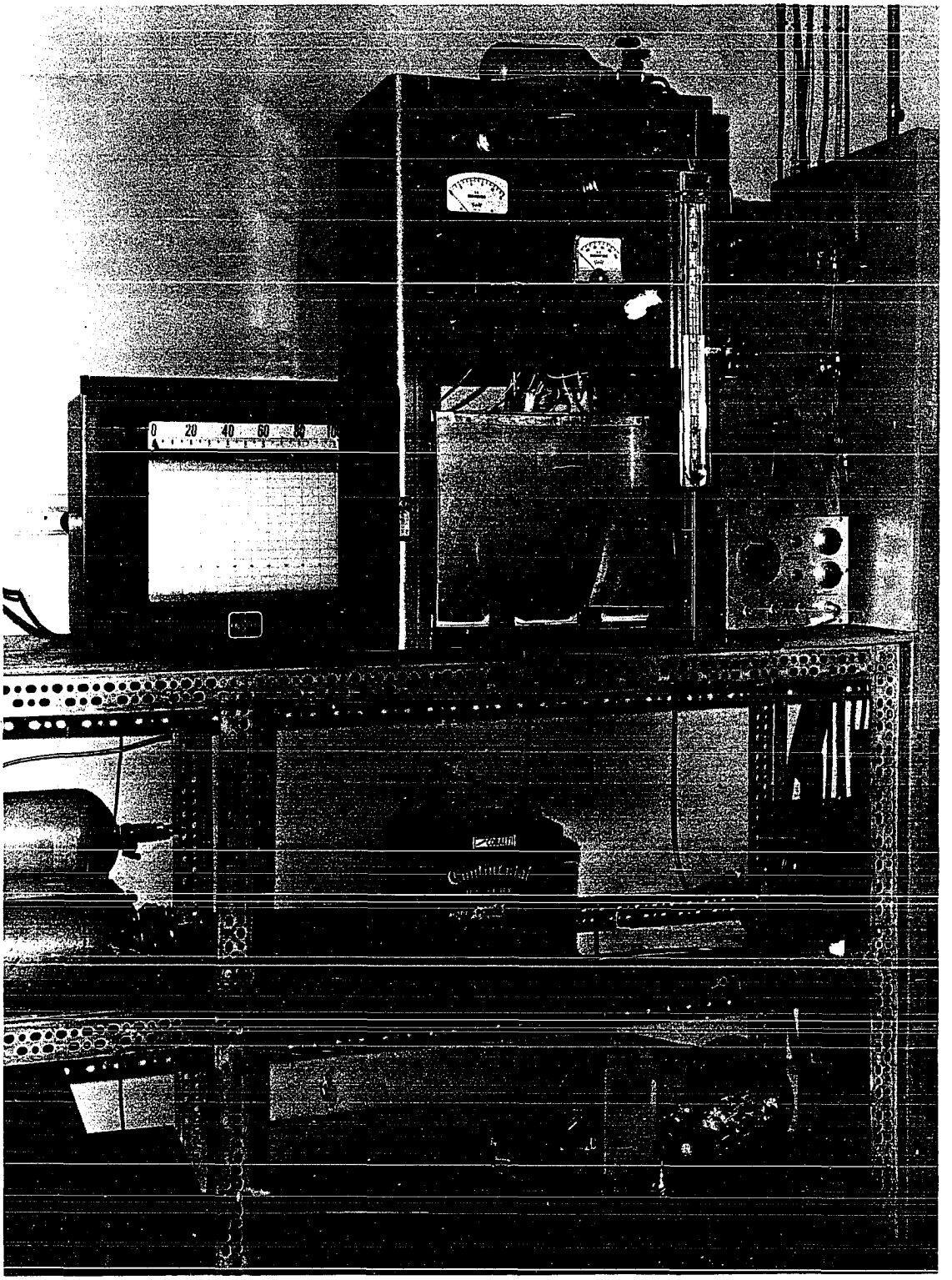


Figure 16. Vapor Phase Chromatograph.

which traversed the length of the burette. The speed of the bubble was determined and the volumetric flow rate adjusted accordingly.

The sample addition system contained two 3-way valves connected in the following manner: The top valve was connected to the sample bomb, the column inlet and the top of the sample tube. The bottom valve was connected to the helium carrier outlet line from the reference side of the detector, to a vacuum source, and to the bottom of the sample tube. The sample tube was made of eight inches of 1/4 inch copper tubing.

A third 3-way valve was used to divert helium from the reference detector directly to the column or to the bottom of the sample tube.

Two columns were used alternately. One column consisted of 14 ft. of 1/4 in. copper tubing and was packed with 60-80 mesh, 5A molecular sieves. This column was used to separate hydrogen, oxygen, nitrogen, methane and carbon monoxide. The second column contained seven feet of 1/4 in. copper tubing and was packed with 180-200 mesh silica gel. It was used to separate carbon dioxide from the other gaseous components.

The detectors were a matched pair of 8,000 ohm thermistors installed in a stainless steel block. One thermistor was installed in the carrier gas channel and the other in the sample gas channel. The thermistors made up one side of a Wheatstone bridge. The source of current

was a 12 volt wet cell battery. The cell voltage output was reduced to the proper level by use of a step switch. The voltage was recorded by a Bristol Dynamaster, Model 1PH-560, with a 0-1.0 millivolt range. Chart speed was one inch per minute.

Helium flow from the cylinder passed first through a preheater made of about two feet of 1/4 in. copper tubing and then to the reference thermistor. From here the helium flowed to the column, then to the sample detector, and to the flow meter. Alternately, helium from the reference detector was diverted to the sample tube before entering the column.

The preheater, column and detectors were enclosed in an air bath. Two small fans were used to circulate the air. A Sargent Model S Thermonitor was used to control the temperature by controlling power to two, 250-300 watt heaters.

The liquid samples were analyzed by liquid partition chromatography and by wet chemical methods.

Methyl formate, acetone, methanol and water were determined on the chromatograph, which was the one described by Lott (29) modified for a liquid sample only. The helium carrier system, recorder and air bath were of the same types and design as used for the vapor phase chromatograph.

The partition column consisted of eight ft. of 1/4 in. copper tubing packed with 30 percent diglycerol on 80-100 mesh Chromosorb W.

The detectors were a matched pair of Gow-Mac tungston filaments. One filament was installed in the channel of the brass block carrying reference gas and the other in the channel carrying sample gas. The signal from this chromatograph was also recorded on a Bristol Dynamaster, Model 1PH-560.

The liquid sample was injected into the helium carrier gas by means of a 10 microliter syringe. The sample was flash vaporized in a preheater held at 20°C above the temperature of the air bath before entering the column.

Analytical Procedures

Calibration of the chromatographs is described in Appendix B.

The operating conditions used for each of the columns are shown below:

TABLE 3.

OPERATING CONDITIONS FOR CHROMATOGRAPHS

	5A Molecular Sieve	Silica Gel	Diglycerol
Helium flow, ml/min.	85	85	85
Bath temperature, °C	34	80	123
Cell current, ma.	5	5	150

The procedure for analysis of the product gas samples was as follows:

The air bath was brought up to temperature and the apparatus allowed to reach thermal equilibrium. The sample bomb was connected to the sample point. Helium gas was valved to go directly to the column at the correct rate. The sample tube and lines up to the sample bomb were evacuated. The vacuum line was valved off, and the sample bomb was opened, allowing the sample tube to fill. The sample bomb valve was closed. The top 3-way valve was turned to a neutral position (no flow). The 3-way valve at the bottom of the sample tube was opened to the helium flow from the reference detector, and then helium was diverted from the column to the bottom of the sample tube. Lastly, the top 3-way valve was turned to have the sample flow to the column. The recorder was zeroed and peak heights on the recorder were adjusted for each component by switching in the required resistance using the step switch. Three analyses were made for each sample on both the molecular sieve and silica gel columns.

Liquid samples were analyzed in the following manner:

The preheater and air bath were brought up to temperature. The helium flow was adjusted to the desired rate. The recorder was zeroed and the resistance box switched to the correct value. The sample was then added through the rubber septum into the preheater using the syringe. As each peak was recorded, the proper resistance was switched in for the next component. Triplicate analyses were run for each sample from an experiment.

The concentrations of each component were determined from each chromatogram from the relative areas under the peaks. The areas were measured using an Ott planimeter. Percentages calculated were then converted to volume percent for the gases and weight percent for the liquids, using the appropriate calibration curve.

Formaldehyde was analyzed using the method of Romijn (46, 52). It is a standard iodometric titration with starch indicator. The excess iodine was determined via titration with thiosulfate. Duplicate samples were analyzed. Since acetone interferred with the analysis, some samples had to be corrected. The relationship used for the correction is shown in Figure 50, Appendix D. A linear relationship for correction of the effect of acetone on the iodometric determination of formaldehyde was also reported by Mach and Hermann (30).

Formic acid was determined by titration with weak NaOH using phenolthalein as indicator (15).

Chemicals Used

The methane used was instrument grade purchased in size 1A cylinders from Phillips Petroleum Company. The analysis was guaranteed as follows:

water	<	10 ppm.
oxygen	<	20 ppm.
methane	>	99.0 mol. percent

A chromatogram of the high purity methane was made.

Nitrogen was the major impurity at about 0.6 mol. percent. A maximum of 0.2 mol. percent ethane was also found in this work.

Oxygen used was USP grade bottled by Air Reduction Company. It was obtained through a local supplier.

Gases used for calibration of the chromatograph were:

Carbon monoxide, CP grade, 99.5 percent min. purity, obtained from The Matheson Company.

Carbon dioxide used was Coleman grade, 99.99 vol. percent pure, obtained from The Matheson Company.

Helium was Grade A obtained through The Bureau of Mines by a local supplier.

Chemicals used for liquid chromatographic calibrations were:

Methanol, absolute, reagent, A.C.S. code 1212 Purity 99.0 percent min. from Baker and Adamson, division of Allied Chemical Co.

Formaldehyde solution: 36.2 percent formaldehyde, 12 percent methanol, remainder water. Baker analyzed reagent obtained from J. T. Baker Chemical Co.

Formic Acid, 88 percent, remainder water, supplied by Mallinkrodt Chemical Works.

Methyl Formate, practical, B.P. 31.25-32.5^{o}C., obtained from Matheson Coleman and Bell.

Acetone, reagent, A.C.S. code 1004, purity 99.5 percent min. from Baker and Adamson, division of Allied Chemical Co.

The following chemicals were used in the titrations:

Iodine Merck, U.S.P. resublimed, from Merck and Co.

Sodium Thiosulfate, crystal, certified reagent, Fisher Scientific Co.

Potassium Iodide, crystal, 99.5 percent min. purity, from Baker and Adamson, division of Allied Chemical Co.

Potassium Iodate, crystalline powder, 99.8 percent min. purity, from Baker and Adamson, division of Allied Chemical Co.

Sodium Hydroxide pellets, 97 percent min. assay, from Baker and Adamson, division of Allied Chemical Co.

CHAPTER VIII

DISCUSSION OF RESULTS

A summary of the results obtained in this work is given in Table 6, Appendix A. The data were obtained over the following ranges of reaction conditions:

Pressure, psi.	15,000, 50,000, 97,000-98,000
Temperature, ^{o}C	220-420+
Residence time, min.	0-60

The intention was to keep the oxygen concentration constant in the methane. The average of the various feed batches was 8.24 ± 0.38 mole percent. Two heater cores were used, one made of alumina and the other of Pyrex, in order to study the effect of these materials on the reaction rate and the product distribution. Residence time is defined as the time the reactor was maintained at the desired temperature and pressure of the experiment.

Material balances were made for oxygen, carbon and hydrogen. The values are shown in Table 7, Appendix A. The first material balance shows the percentages of each element recovered as determined from the weight of gas and liquid which was removed from the system. Oxygen was considered to be the key element since it is in high

concentration in the main products--water, carbon dioxide and carbon monoxide. In the first material balance oxygen recovery ranged from 90-110 percent for 85 percent of the experiments. The lowest value was 70 percent and the highest was 117 percent.

In the second material balance listed in Table 7 for each experiment the water content of the product was adjusted so that oxygen recovery for all experiments was in the range of 93-105 percent. The ratio C:H was used as a guide for this adjustment. All the hydrogen was derived from the methane feed, and the ratio C:H must remain at 3:1. No changes in the ratio were made which resulted in the values being outside the limits of 2.99-3.01. A few values initially were outside these limits. A Control Data G15 digital computer was used for all the calculations involved in preparing Tables 6 and 7.

In order to be able to plot all data on a common basis, the concentration of the reactants and products are used on a moles per mole of feed per liter of reactor, $\frac{\text{moles}}{\text{mole-ltr.}}$. The free volume of the reactor was slightly smaller with the Pyrex core than with the alumina core. These figures were 389 and 426 ml., respectively. The concentrations of the products for the various experiments are listed in Table 8.

The Effect of Temperature

(Alumina Heater Core)

Figure 17 is a plot of residual oxygen concentration and carbon monoxide, carbon dioxide and methanol concentrations at 15,000 psi., 60 min. residence time and various temperatures, using the alumina core. These data, except for the experiment at the highest temperature, were obtained under isothermal conditions. The highest temperature, 310°C, gave an isothermal reaction for eight minutes. The temperature then increased uncontrollably from 310 to 317°C. The temperature decreased almost as quickly to 309.5°C. At the time the temperature changed the pressure increased from 15,300 to 18,200 psi. and then decreased to 14,900 psi. The total elapsed time for the pressure increase and decrease was about one minute. The experiment was continued to a total time of 60 minutes. In the other experiments there was no change in temperature or pressure after the initial heatup period of six minutes. A reaction in which temperature increased less than 30°C from the desired isothermal condition is defined as a weak adiabatic reaction. A reaction in which temperature increased more than 30°C is defined as a strong adiabatic reaction.

Some residual oxygen remained even after reaction at the highest temperature for all experiments conducted under all conditions. Oxygen consumption is greater at the higher temperature, as expected, and is not linear with temperature.

The effect of temperature on carbon monoxide formation is of great interest. No carbon monoxide was detected at

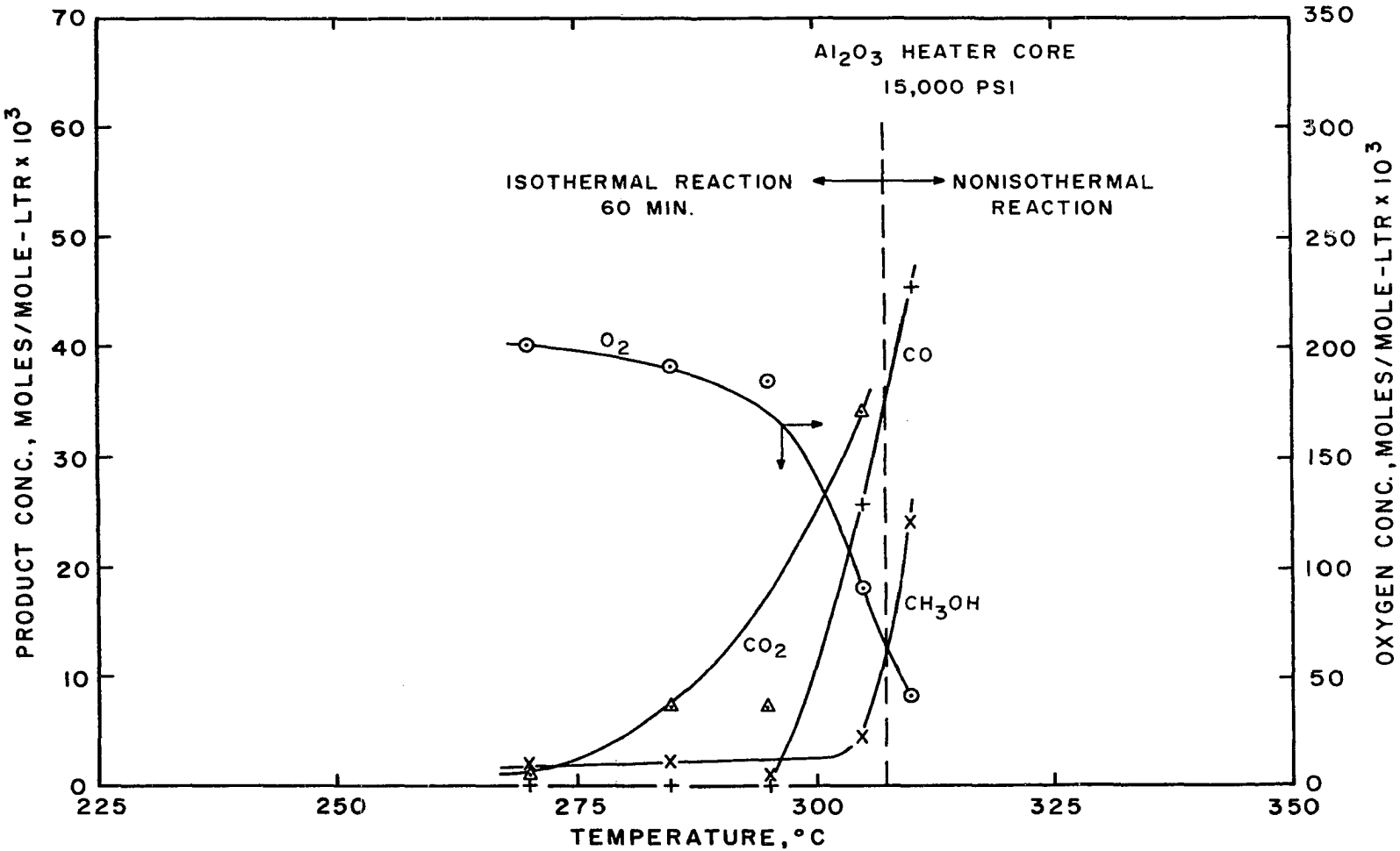


Figure 17. The Effect of Temperature on Concentrations at 15,000 psi., Alumina Core

temperatures up to and including 295°C. Above this temperature, however, the monoxide concentration increases rapidly with temperature. On the other hand carbon dioxide is formed at as low a temperature as 270°C and increases at a high rate up to 305°C. Unfortunately, the gas sample was lost from the bomb before the sample could be analyzed for carbon dioxide, and a value is not available for a temperature of 310°C.

A small amount of methanol is formed at temperatures between 270-305°C, but a significant amount is made only at 310°C.

Figure 18 contains a plot of residual oxygen, carbon monoxide, carbon dioxide and methanol in the product at 50,000 psi. and at various temperatures. The residence time is the same for the isothermal reactions as for the data shown in Figure 17, 60 minutes. At 50,000 psi. both a weak adiabatic and a strong adiabatic reaction were obtained. In each case, there is only a small and equal amount of residual oxygen. The residence times for these experiments were seven and three minutes, respectively, which was relatively short. In two isothermal runs at 295°C, the same residual oxygen concentration was also obtained, indicating the reaction was essentially completed in all four cases. At 295°C and 15,000 psi., there was very little reaction, which shows the pronounced effect of pressure on the reaction rate.

The first occurrence of carbon monoxide is between the temperatures of 280 and 285°C. As at 15,000 psi. the

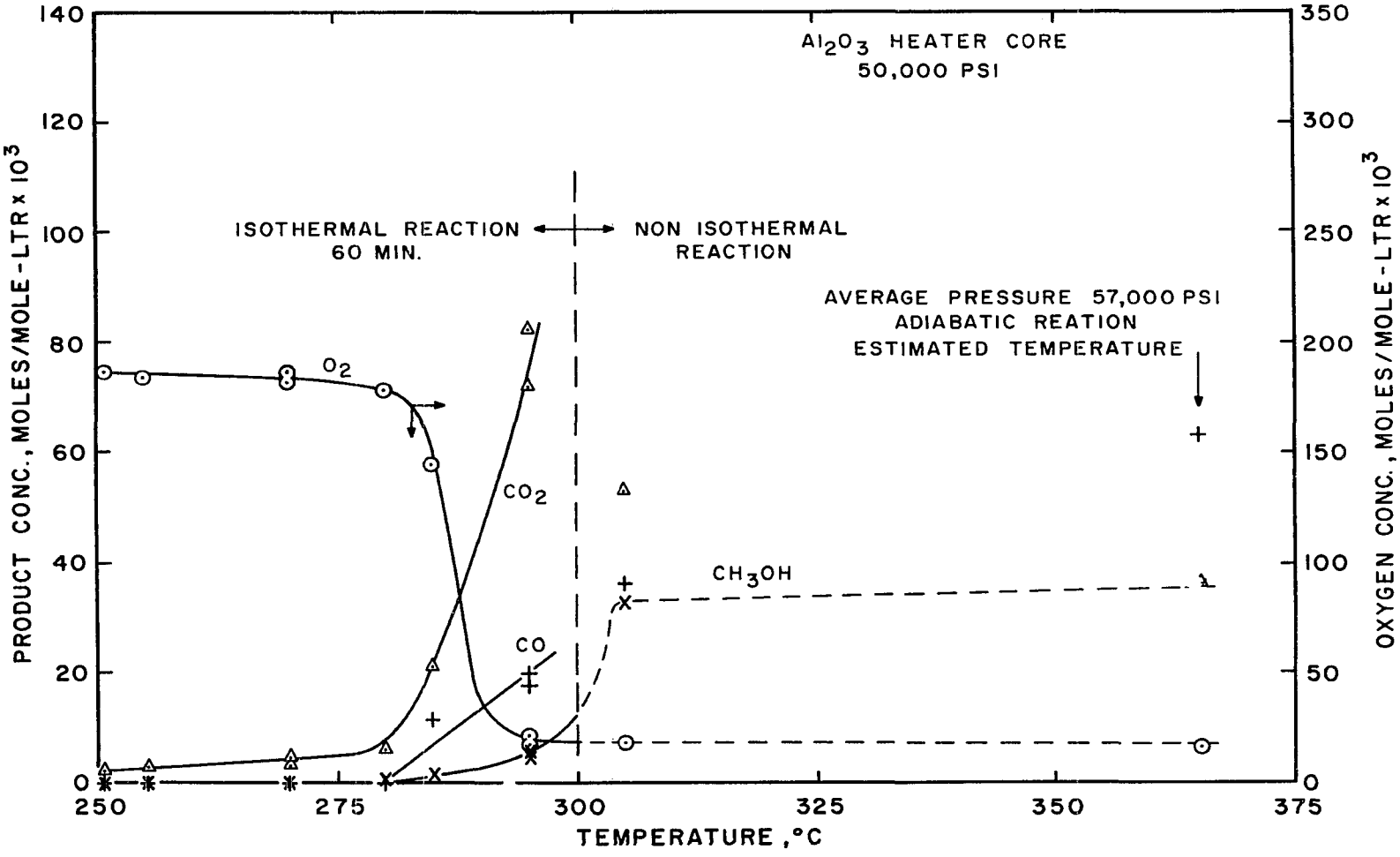


Figure 18. The Effect of Temperature on Concentrations at 50,000 psi., Alumina Core.

monoxide content increases rapidly with temperature. However, again the carbon dioxide forms at a much lower temperature, being present at 251°C. It increases slowly, but its formation accelerates rapidly above 280°C. The concentration of the dioxide remains well above the concentration of the monoxide during the course of the isothermal reactions. For the adiabatic cases, however, the carbon dioxide concentration is higher than the carbon monoxide concentration for the weak adiabatic case, but lower for the strong adiabatic reaction. The average of the sum of the carbon dioxide and carbon monoxide concentrations for the adiabatic reactions is almost equal to the average of the sum of these components for the isothermal reaction at 295°C. The residual oxygen content of all four of the experiments is almost identical, which indicates that carbon dioxide, as well as carbon monoxide is made by a chain reaction. At long residence time, as occurs with the isothermal conditions at high temperatures, part of the monoxide is converted to the dioxide. It seems highly improbable that at a low temperature such as 270°C, where no carbon monoxide is found, that all the monoxide which had formed could have been converted to the dioxide.

It is interesting to note that the methanol concentration for both the adiabatic reactions is almost identical. The concentration of methanol for the isothermal reaction even at 295°C is very small, which indicates that the methanol also is made by a chain reaction. The large difference in methanol concentration obtained between isothermal and

adiabatic reactions also tends to show that most of the oxygen was consumed during the period of the weak adiabatic reaction and little during the isothermal part of the reaction time.

The effect of reaction temperature on residual oxygen, carbon monoxide, carbon dioxide and methanol concentrations in the product is shown in Figure 19. The pressure level was 97,000 psi., and the residence time was 34 minutes. As in the previous two figures, the alumina heater core was used. Whereas there had been no problem with gas leaks below 60,000 psi., the work at 97,000 psi. was handicapped by leaks. Therefore, it was possible only to make a full set of experiments at 34 minutes, instead of at 60 minutes as was the case at the lower pressures.

The data of Figure 19 show the same general shape of curve for the consumption of oxygen as at the lower pressures. One experiment is included in which a strong adiabatic reaction was obtained at an average pressure of 93,000 psi. The results overall at 93,000-97,000 psi. parallel those obtained at 15,000 and 50,000 psi. The most important point seems to be that carbon dioxide is formed at a much lower temperature than that at which carbon monoxide is formed. Also, it is seen that whereas oxygen consumption is quite low at 295^{o}C, and 15,000 psi., it is moderately high at 50,000 and at 97,000 psi.

Figure 20 is plot of the reaction temperature and the concentrations of formaldehyde (HCHO), formic acid

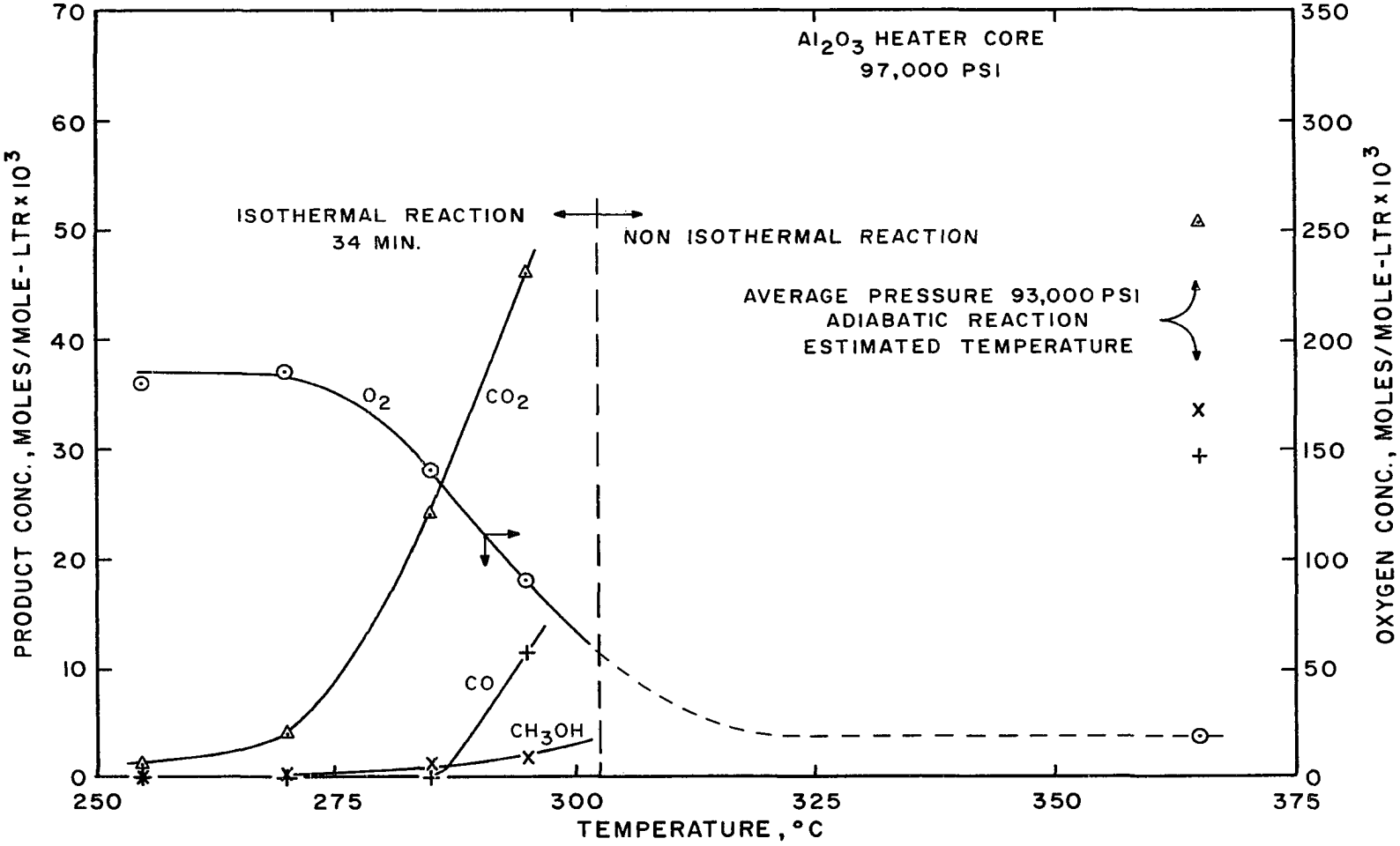


Figure 19. The Effect of Temperature on Concentrations at 97,000 psi., Alumina Core.

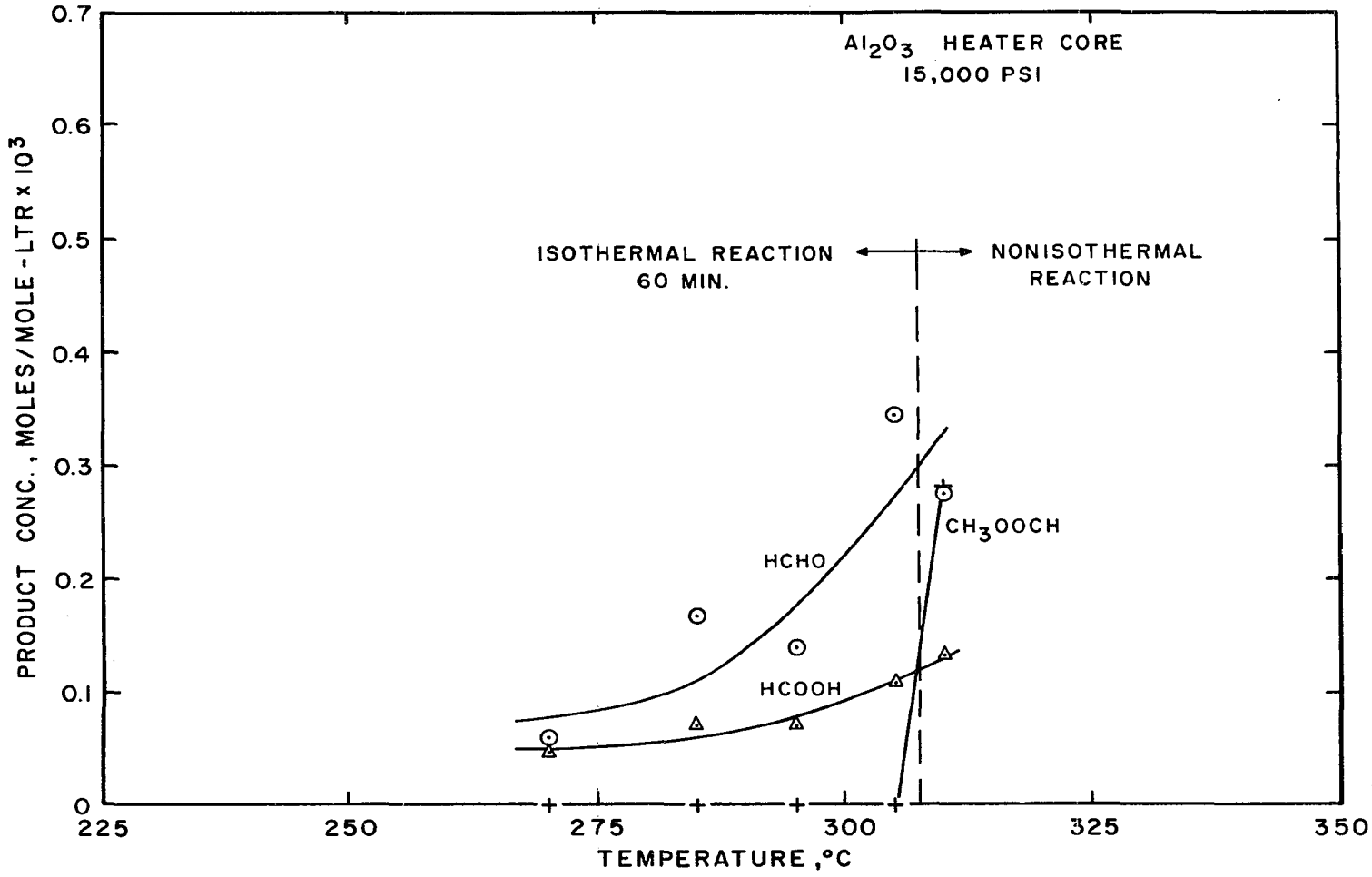


Figure 20. The Effect of Temperature on Product Formation at 15,000 psi., Alumina Core.

(HCOOH) and methyl formate (CH_3OOCH) in the product at 15,000 psi. Methyl formate is formed only at the condition of highest temperature, at which the weak adiabatic reaction apparently occurred. The concentration of formic acid increases at a slowly increasing rate as temperature increases and does not show an unusual increase under conditions of the weak adiabatic reaction. The concentration of formaldehyde increases more rapidly with temperature than does the formic acid. The data are somewhat scattered, but there is no doubt about the relationship. It is interesting to note that at the lower temperatures the concentrations of the two are almost equal.

The effect of temperature on formaldehyde, formic acid and methyl formate concentrations at 50,000 psi. is shown in Figure 21. Again the concentrations of formaldehyde and formic acid are almost the same at the lower temperatures. In this instance, however, the acid content remains at roughly the same level as the formaldehyde up to and including 295°C. In fact, one of the formic acid values is unexpectedly high. Under adiabatic conditions the formaldehyde concentration is substantially higher than the formic acid in each case. As at 15,000 psi., methyl formate does not appear at 295°C, but shows up in the adiabatic reactions.

At 97,000 psi. and a residence time of 34 minutes, the concentrations of formaldehyde and formic acid are

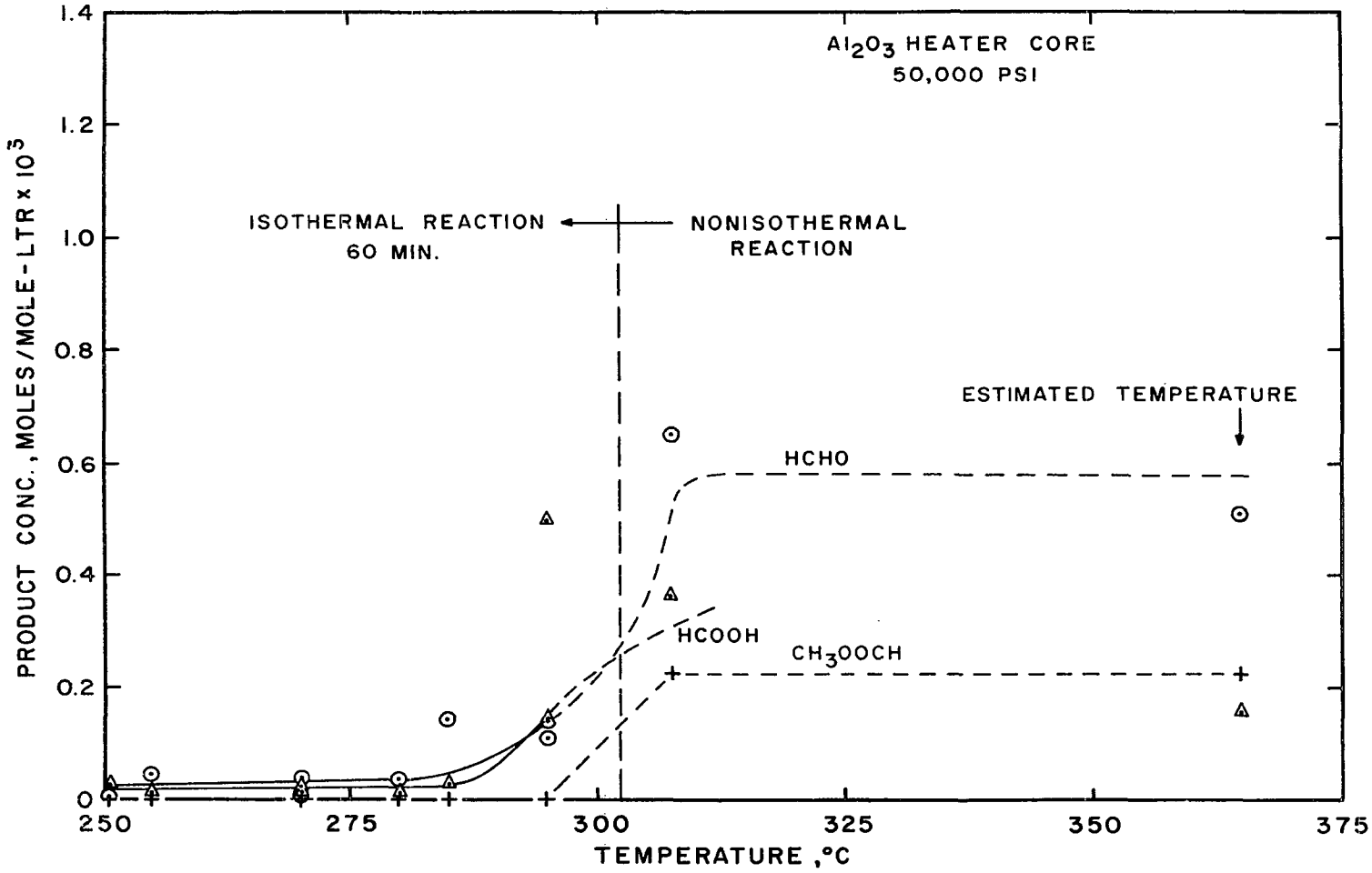


Figure 21. The Effect of Temperature on Product Formation at 50,000 psi., Alumina Core.

essentially equal at each of the temperatures which were investigated. As at the lower pressures, the aldehyde concentration is much higher when an adiabatic reaction occurs. The data are shown in Figure 22. Although the acid might be considered relatively constant with temperature, the aldehyde certainly is not. At 50,000 and 97,000 psi. the aldehyde and acid are formed at about the same concentrations as temperature increases, except when a nonisothermal reaction occurs. At 15,000 psi., however, there is a higher aldehyde concentration before temperature is increased enough to cause a weak adiabatic reaction. Methyl formate forms at a lower temperature at 97,000 psi. than it does at the lower pressure levels. However, under adiabatic conditions the methyl formate concentration is about equal at all three pressure levels.

The construction of the heater cores is described in Chapter V, EXPERIMENTAL EQUIPMENT. The alumina core was preformed with a spiralled depression, and the wire was wound tightly on it. The outside surface was then coated with alumina dust mixed with water into a paste. When dry, the powder came off at the touch. During operation some of the dust fell from the core and was blasted through the lines and valves into the product receivers. The dust proved to be very abrasive, and after about four experiments it had badly eroded the stem and seat of the reactor discharge valve. The valves were reconditioned periodically and returned to service. However, the reactor outlet hole started to erode,

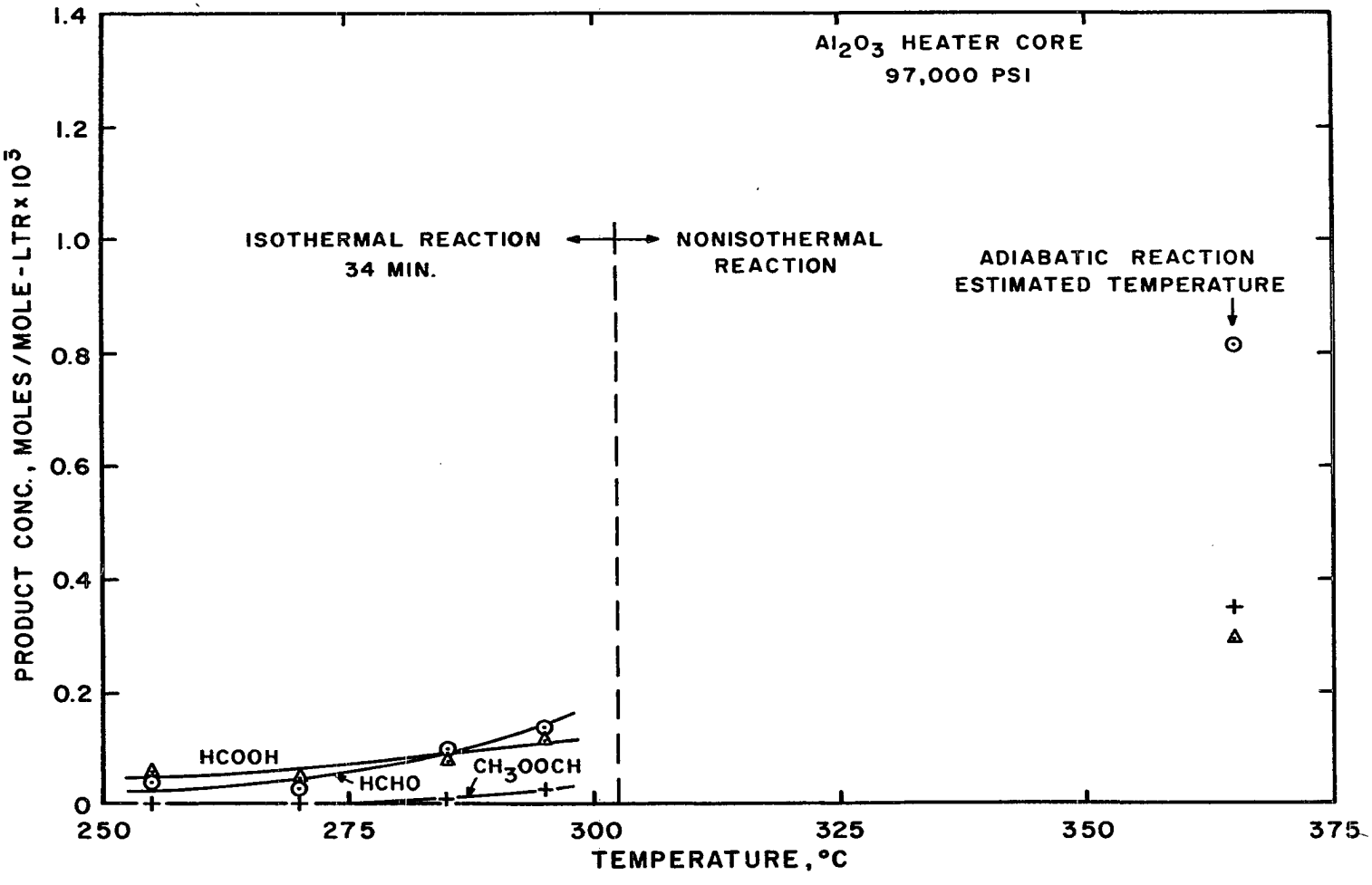


Figure 22. The Effect of Temperature on Product Formation at 97,000 psi., Alumina Core.

and use of the alumina was discontinued when this condition was discovered. The use of fine alumina is not recommended. It is now believed that the wire can be wound securely on the spiralled core, and that there is little chance of the wire shorting to the wall of the reactor.

The Effect of Temperature

(Pyrex Heater Core)

There seemed to be no change in experimental results after successive experiments using the alumina core at the same experimental conditions. One could say there appeared to be no wall effect. However, there was a pronounced change in results as successive experiments were run using the Pyrex core. Therefore, plots of the data obtained using the Pyrex core contain for reference the lines obtained from plotting the data from the alumina core. The results for the Pyrex core at 15,000 psi. are plotted in Figure 23. The consumption of oxygen and the formation of carbon dioxide and carbon monoxide are shown at various temperatures. The results at 270 and 285°C coincide with those obtained with the alumina core, but at 295°C it was not possible to maintain an isothermal reaction. A weak adiabatic reaction occurred 34 minutes after the experiment had begun. An adiabatic reaction did not occur with the alumina core until the temperature reached 310°C. The residual oxygen is down to a low level consistent with results from other nonisothermal experiments. Eleven experiments after the weak adiabatic

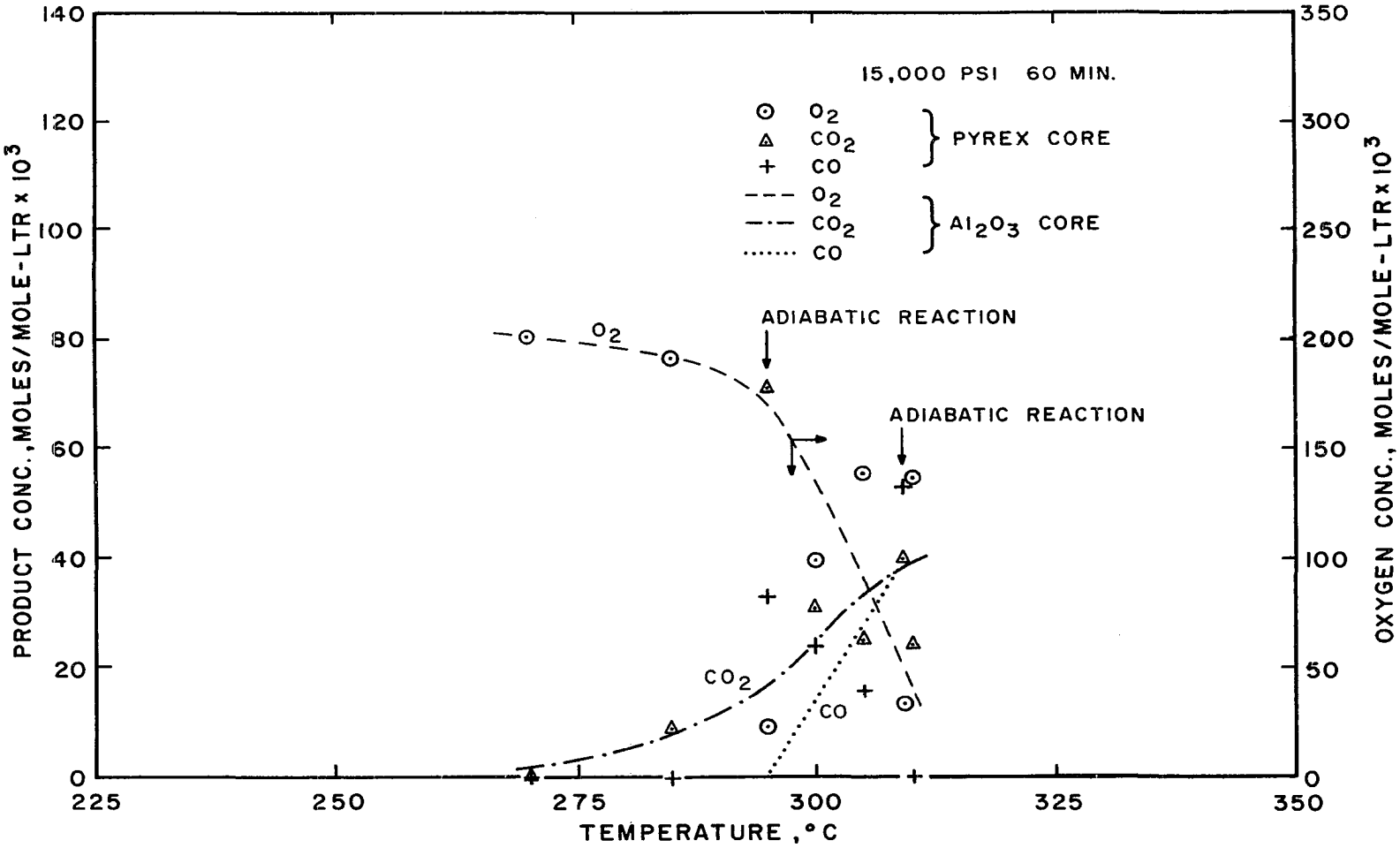


Figure 23. The Effect of Alumina and Pyrex Cores at Various Temperatures and 15,000 psi.

reaction with the Pyrex core at 295°C, a weak adiabatic reaction was obtained which initiated at about 305°C. The results are consistent with those from the weak adiabatic reaction obtained with the alumina core. The experiment shown at 300°C in Figure 23 was conducted two runs prior to the adiabatic reaction. When compared to oxygen, carbon dioxide and carbon monoxide concentrations expected for 300°C with alumina, the one conducted with the Pyrex core is a little stronger. It contains carbon monoxide and carbon dioxide, for instance, in a little more than the expected concentration, and a little less residual oxygen than expected. On the other hand the experiments made at 305 and 310°C show reduced activity. The results, then, with the Pyrex core at 15,000 psi. vary with successive experiments.

When the alumina core was removed from the reactor after the last run with it, it was discolored somewhat, rusty and black, but it was intact. The Pyrex core, however, was found to be shattered when the reactor was opened up after the last experiment. The activity obtained with the Pyrex core was very low during the last nine experiments conducted with it. The core is believed to have broken after Experiment 166, and it is believed to have caused the reduced activity at 305 and 310°C shown in Figure 23. The greatly increased surface area would be expected to reduce the reaction rate, as reported by several investigators. Also the Pyrex surface was pitted, indicating

devitrification.

The changing activity of the Pyrex core is demonstrated again in Figure 24, which shows the effect of reaction temperature on residual oxygen and gaseous product formation at 50,000 psi. A weak adiabatic reaction was obtained at 284°C soon after the core was put in. A few runs later a normal isothermal run was made at 285°C. It is interesting to note that the carbon monoxide concentrations for the weak adiabatic and isothermal runs are almost equal, but the carbon dioxide concentrations are very different. Both runs were made over a 60 minute period, and the temperature rise in the weak adiabatic case occurred ten minutes before the end of the experiment. This result, coupled with results from the alumina core, tend to lend further support to carbon dioxide being formed independently of carbon monoxide.

One of the last experiments made was at 295°C, using the Pyrex core. Figure 24 shows that the reaction rate was much less than obtained earlier at 290°C. In fact the data at 295°C are almost identical to those obtained earlier at 285°C. Therefore, it is concluded that the activity of Pyrex does not stabilize. It is unusually high when fresh and drops progressively with use. Furthermore, the mechanical strength of Pyrex is inadequate for use at high pressure. Curiously enough, the activity of the Pyrex had little apparent effect on the results of strong adiabatic reactions. The last experiment made in this investigation was a strong adiabatic reaction at 50,000 psi. One had been made 25 runs

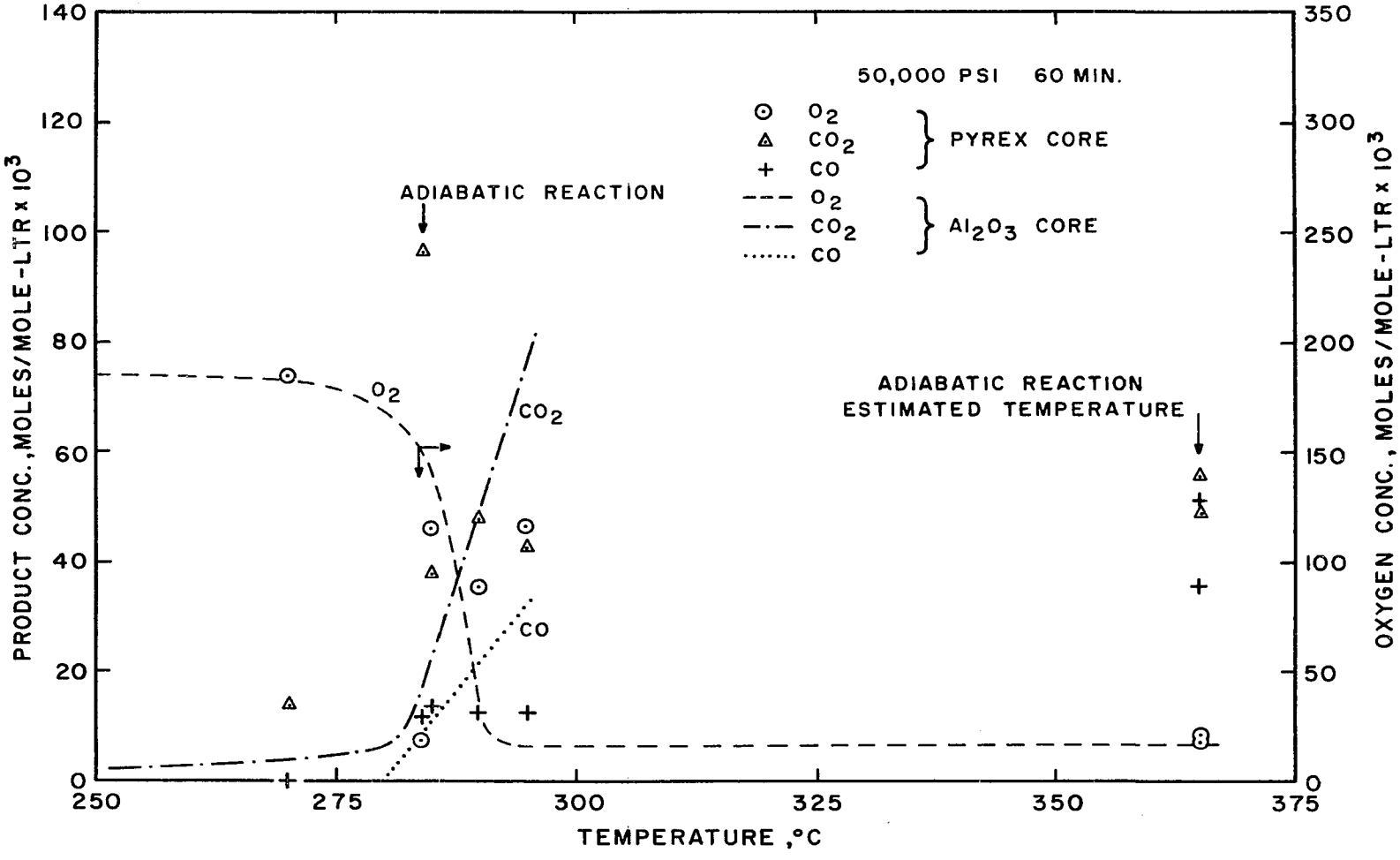


Figure 24. The Effect of Alumina and Pyrex Cores at Various Temperatures and 50,000 psi.

earlier and the results with respect to oxygen consumption and formation of carbon monoxide plus carbon dioxide were almost identical. However, the individual amounts of the monoxide and dioxide varied, which was probably caused by initiation of the adiabatic reaction at different temperatures. Apparently once the adiabatic reaction is initiated at high pressure, the surface does not have a significant effect on the reaction.

The effect of reaction temperature on the gaseous components at 98,000 psi. is shown in Figure 25. The results are similar to those obtained at 50,000 psi. in that the experiment made at 295°C near the end of the investigation shows a reduced rate of reaction. The results of the adiabatic reaction, which peaked at a pressure around 125,000 psi., show less residual oxygen than at 50,000 psi., but the same total amount of carbon monoxide plus carbon dioxide.

Figures 26, 27 and 28 are plots of the effect of temperature on the formation of organic liquids (except methanol) using the Pyrex core. The lines are those obtained using the alumina core. The results at 15,000 psi. correspond fairly well with those obtained using alumina except that concentration of formaldehyde and formic acid decreases with temperature above 300°C. The same decrease occurred with carbon monoxide and carbon dioxide and was attributed mostly to the broken heater core. At 50,000 psi., however, a higher concentration of formaldehyde and formic acid was made with the Pyrex core. The picture is complicated somewhat because concentrations of acetone of up to 2.9 wt. percent

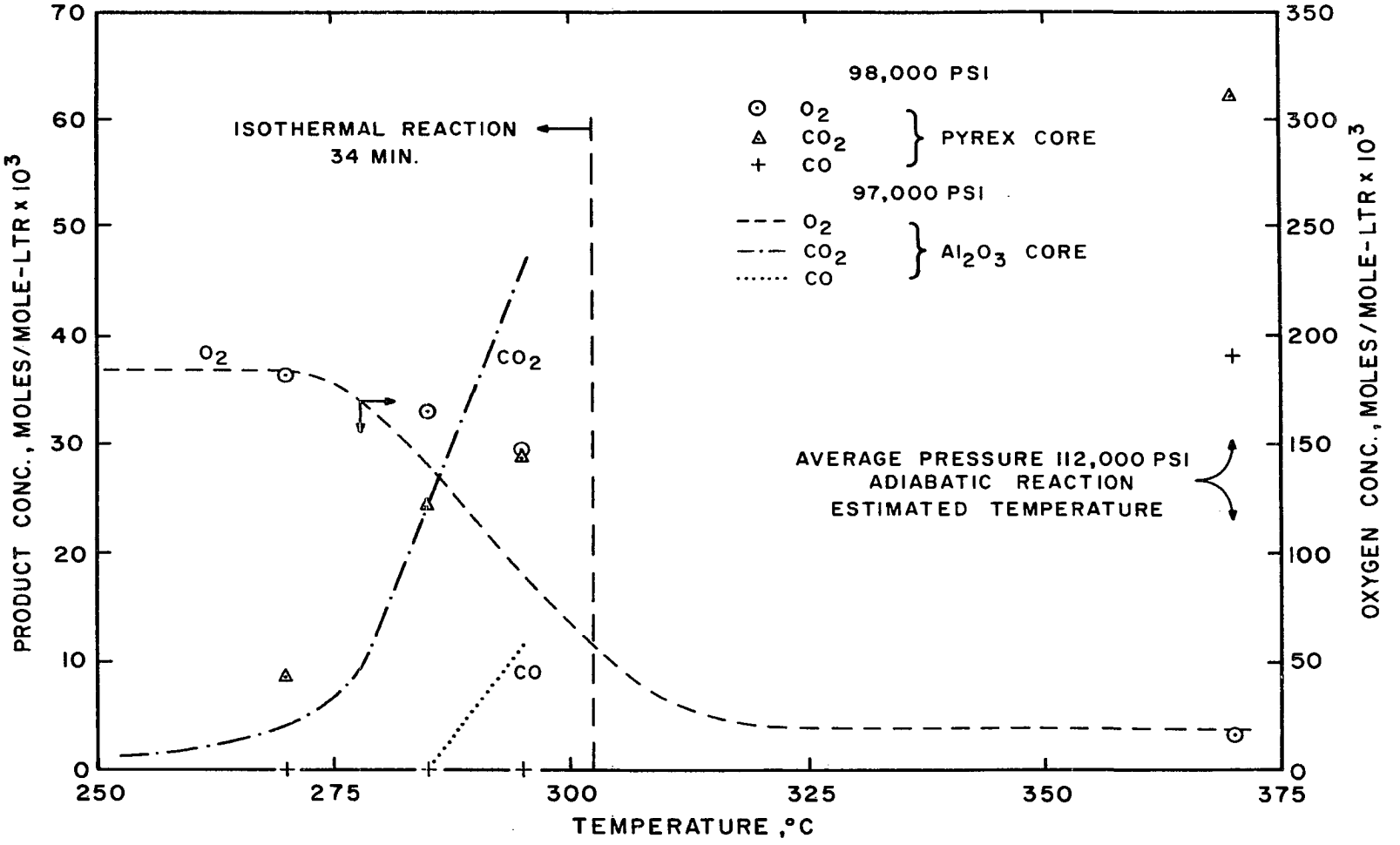


Figure 25. The Effect of Alumina and Pyrex Cores at Various Temperatures and 98,000 psi

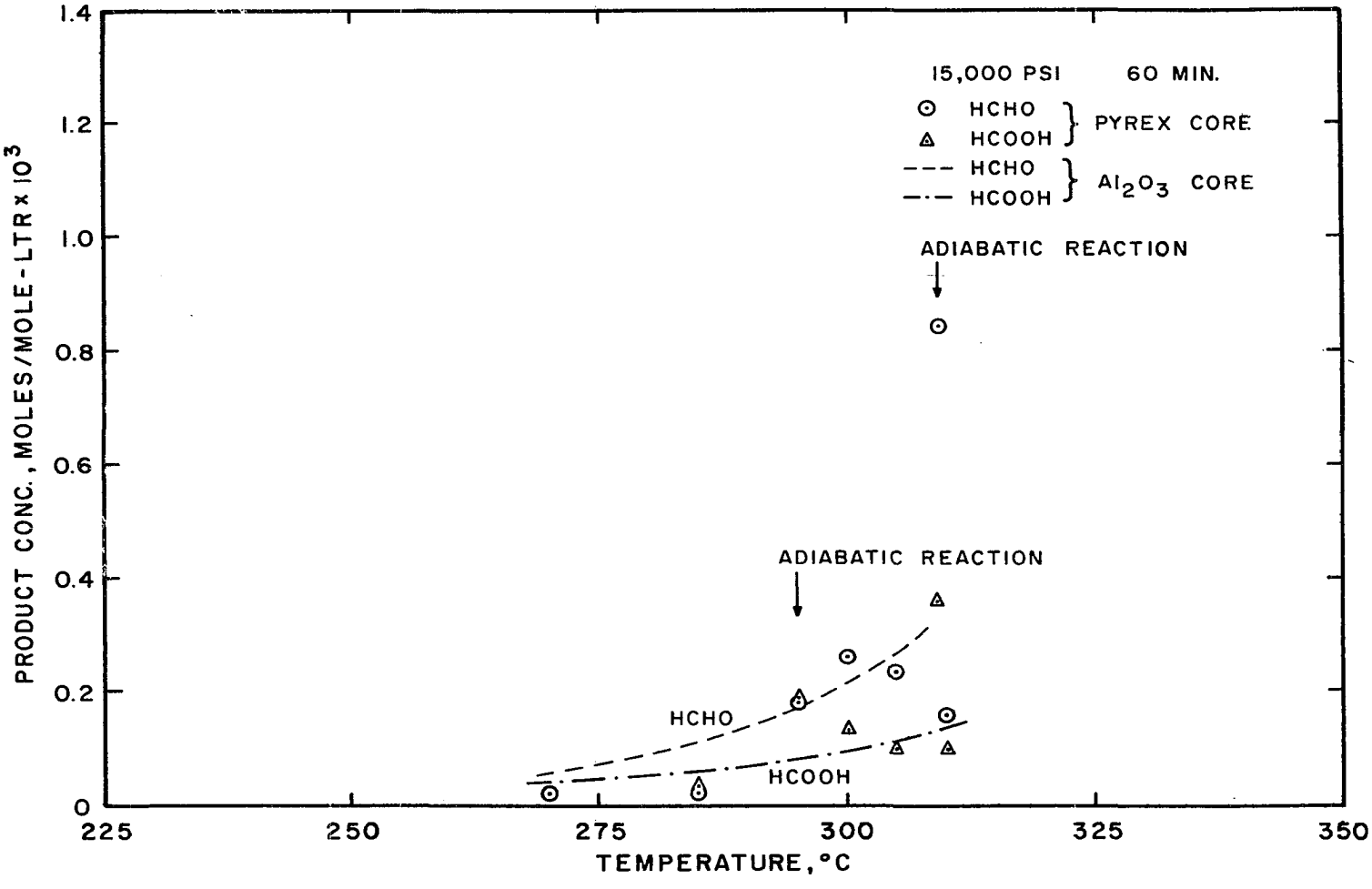


Figure 26. The Effect of Alumina and Pyrex Cores on Product Formation at 15,000 psi.

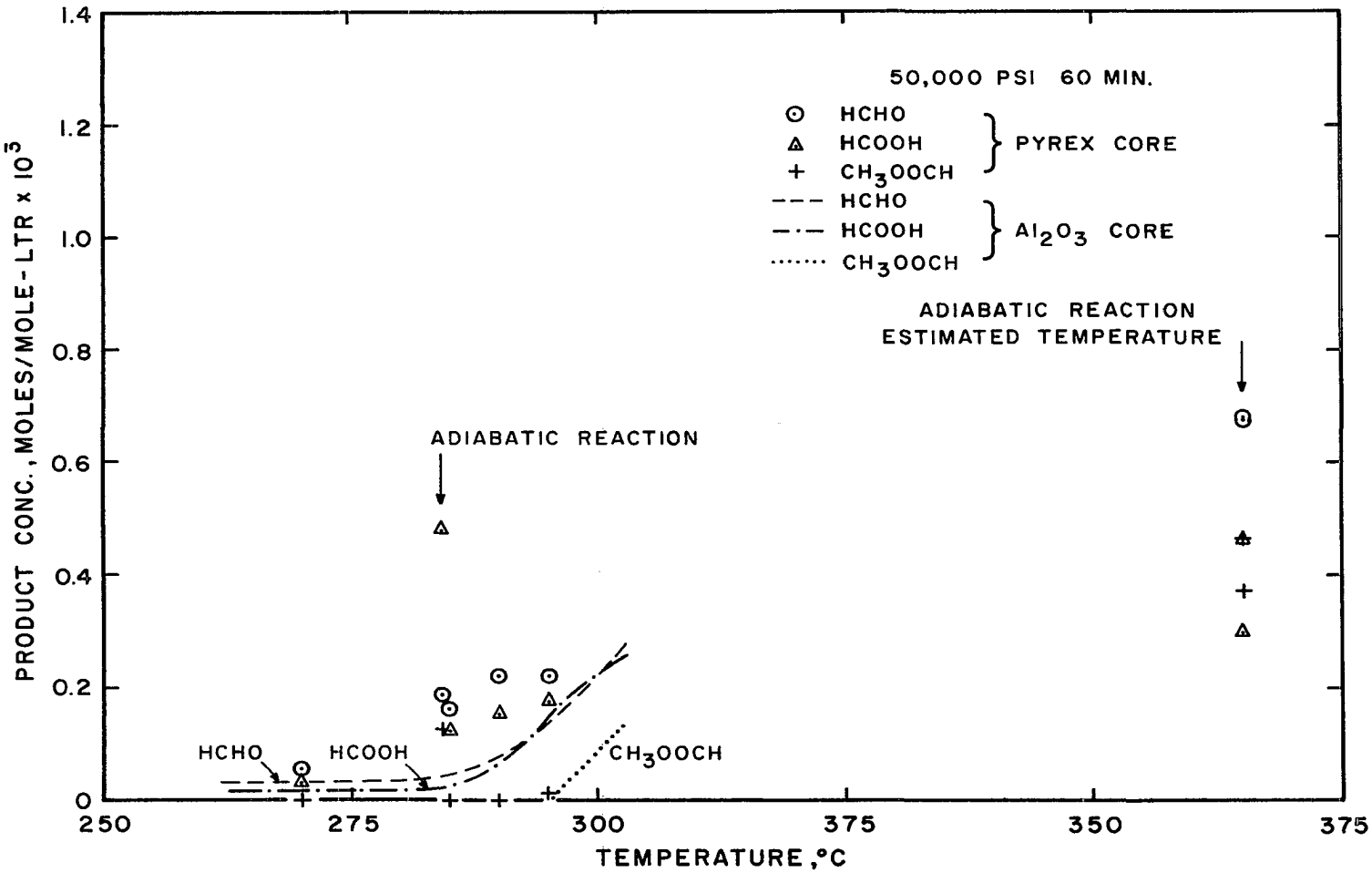


Figure 27. The Effect of Alumina and Pyrex Cores on Product Formation at 50,000 psi.

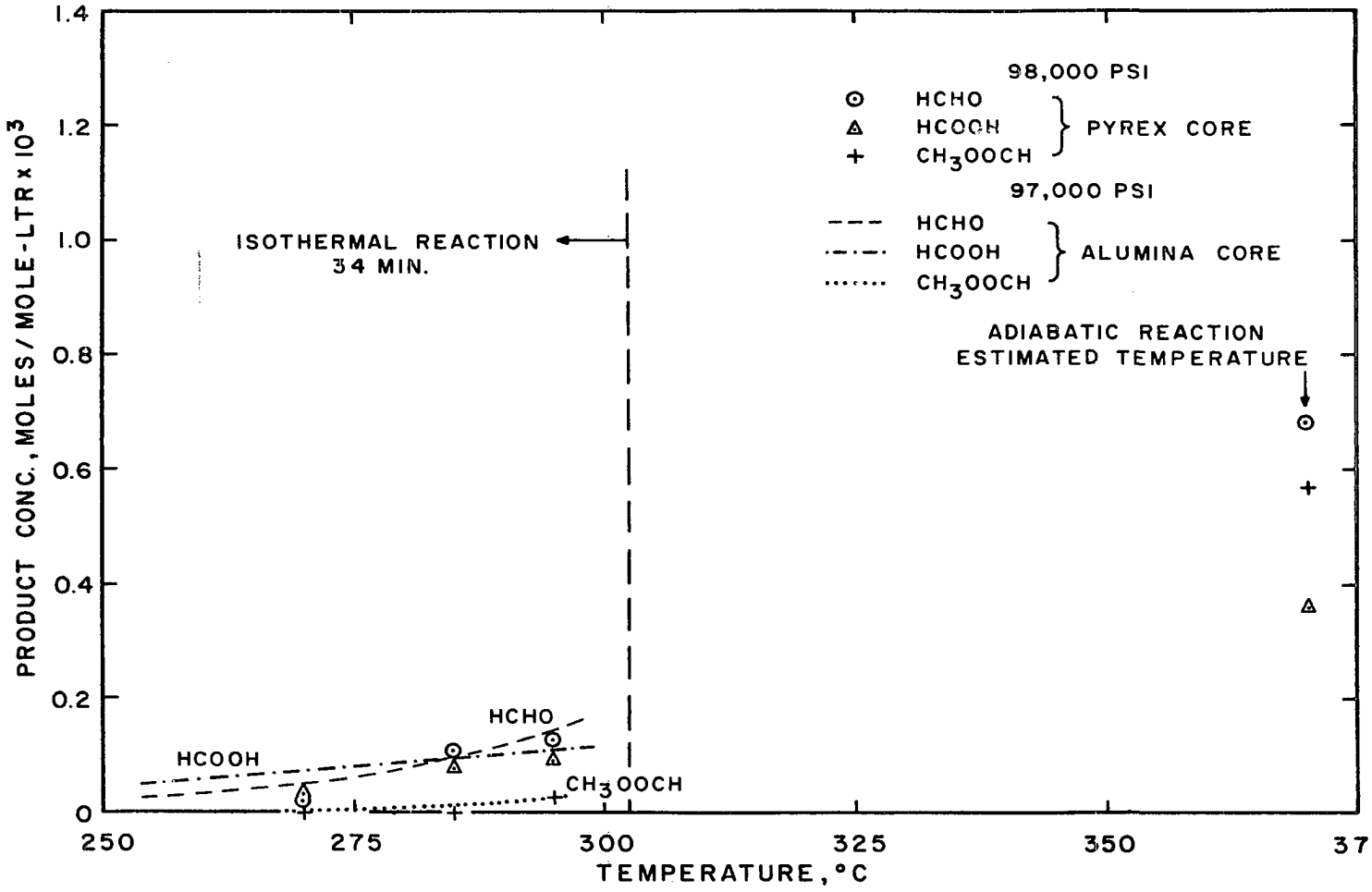


Figure 28. The Effect of Alumina and Pyrex Cores on Product Formation at 98,000 psi.

in the liquid occurred in some experiments. Those containing more than one percent acetone were not included in the plots of formaldehyde. Reference to Figure 27 shows that not only is the formaldehyde high, but the formic acid is also, and its determination is not affected by acetone. It appears that at 50,000 psi., use of Pyrex results in greater yields of aldehyde and acid than does alumina. Although there are meager data, the results at 98,000 psi. for formaldehyde, formic acid and methyl formate are almost the same as obtained with alumina.

The effect of temperature on the formation of methanol for the Pyrex core relative to the alumina core is shown in Figure 29 at the three pressure levels. The results for the isothermal cases roughly parallel those obtained for the other products using Pyrex. Increased activity was obtained at 15,000 psi., for instance, soon after the Pyrex core was installed. After the Pyrex core broke, reduced methanol formation occurred as shown by the data at 15,000 psi. and temperatures of 305 and 310°C. More methanol is made in the adiabatic cases with the Pyrex than with alumina.

The Effect of Time

(Alumina Heater Core)

Figure 30 shows the effect of residence time on the disappearance of oxygen and on the formation of carbon monoxide and carbon dioxide. The pressure level was 97,000 psi., the reaction temperature was 295°C and the data were

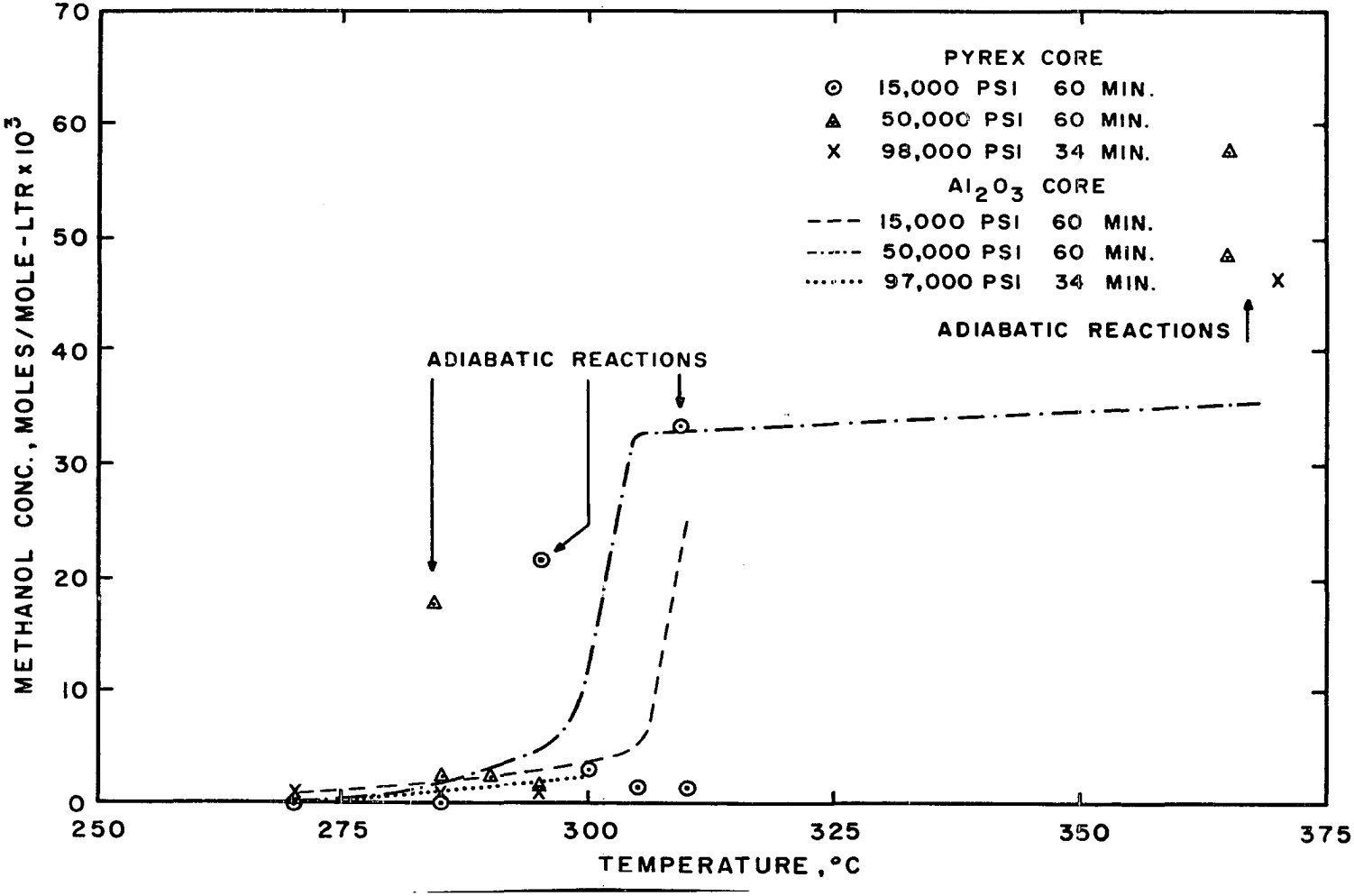


Figure 29. The Effects of Alumina and Pyrex Cores on Methanol Formation.

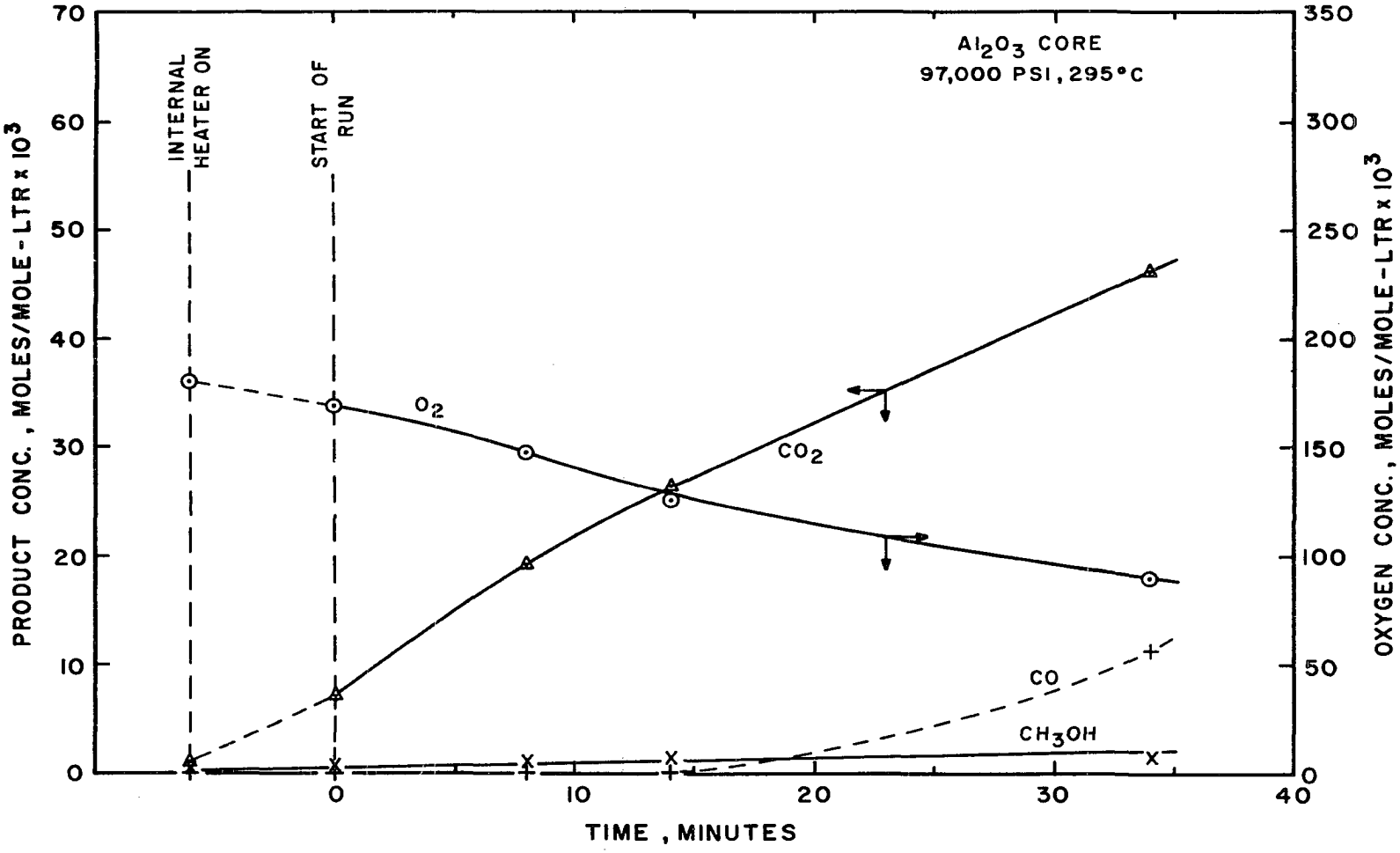


Figure 30. Concentrations at Various Residence Times at 97,000 psi., Alumina Core.

obtained using the alumina core. As stated in EXPERIMENTAL PROCEDURE, the reactants were brought to within 40-50°C of the planned temperature of operation before the internal heater was turned on. The heat-up time was six minutes. For a reaction temperature of 295°C the reactants were held at approximately 250°C for three hours while pressure was increased from atmospheric to 97,000 psi. in the reactor. Results of the experiment conducted at 255°C and 34 min. at the same pressure level are shown at minus six minutes residence time. The experiment plotted at zero residence time was one in which the temperature of the reactor was increased from 253 to 290°C in six minutes while the pressure was maintained at 98,000 psi. The results of this procedure are the same as obtained when reaction is conducted at the same pressure for 34 minutes at about 275°C. The carbon dioxide concentration is probably the most accurate indicator of the extent of reaction. By extrapolating the dioxide curve of Figure 30 to zero concentration, one finds that the heat-up period is equivalent to 3.5 min. of reaction time at the indicated temperature and pressure of 295°C and 97,000 psi., respectively. Thus it was possible to follow essentially the full course of the reaction with time. The methanol concentration in the product is very small.

The most striking feature of Figure 30 is the appearance of carbon dioxide long before there is any indication of carbon monoxide. In fact, it is only at the longest reaction time that any monoxide was found, although some formed

sometime between 14 and 34 minutes, of course. Figure 31 shows the formation of formaldehyde, formic acid, and methyl formate relative to time. The concentration of each of these products increases slowly and apparently linearly with time, and their levels remain very small.

The Effect of Time

(Pyrex Heater Core)

Figure 32 is a plot showing the effect of temperature on the amount of oxygen reacted and on the amount of CO and CO_2 formed at 50,000 psi. and 290°C. These data were obtained using the Pyrex core before the core broke. Data at 295°C would have been preferred, but a nonisothermal reaction was obtained at this temperature. The general shape of the curves is the same as obtained for the alumina core at the higher pressure. However, the rate of reaction is higher in the latter as would be expected. The data for the formation of formic acid and methyl formate with time are shown in Figure 33. Insufficient values were available for formaldehyde because of the high acetone content of some of the product samples. The data in Figure 33 are badly scattered for methyl formate and all one can say is that some methyl formate forms during the course of the reaction. Again the acid shows a slow increase with time as found with the other core.

Data at various reaction times were also obtained at 98,000 psi. and 285°C with the Pyrex core. However,

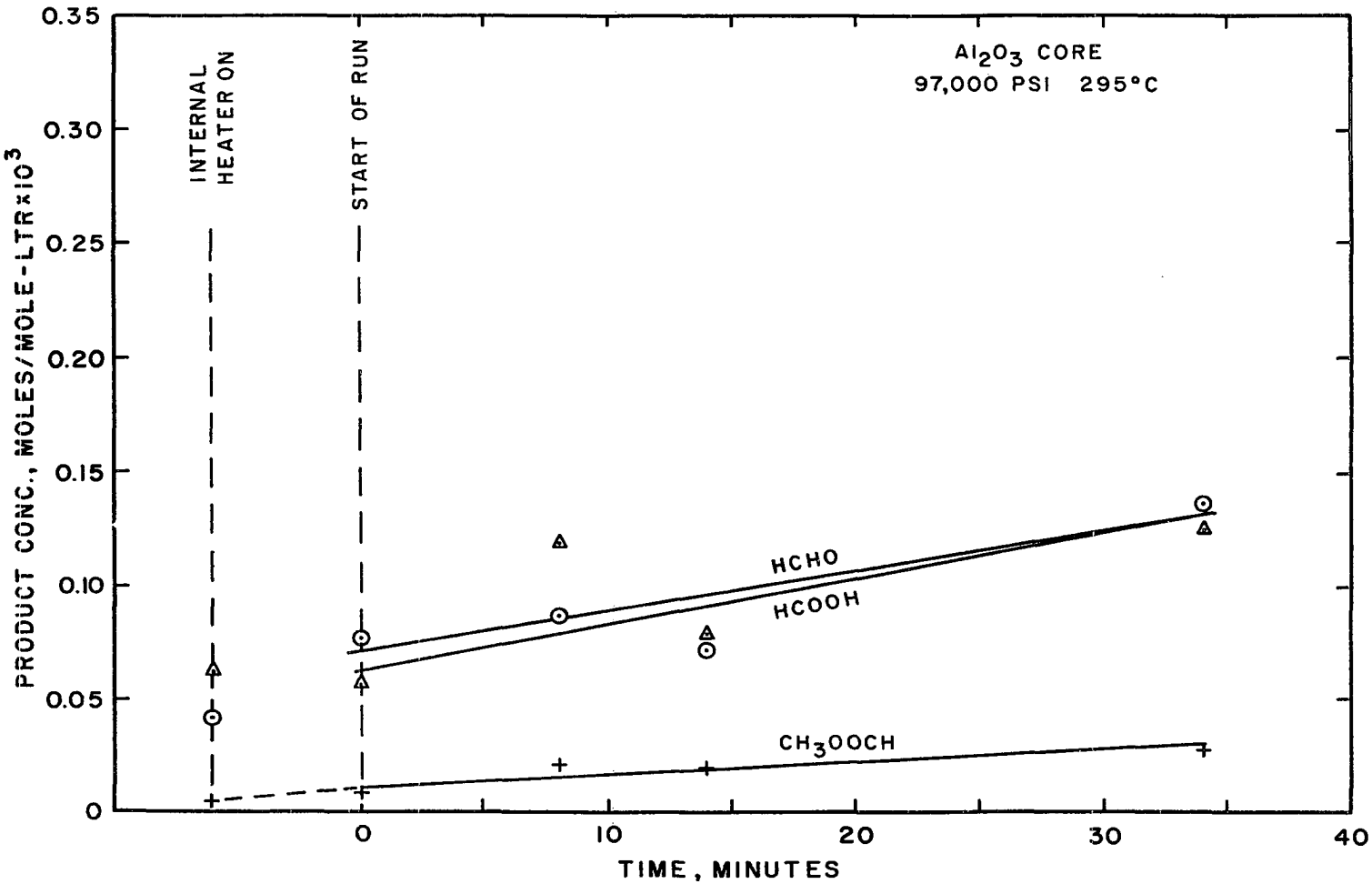


Figure 31. Formation of Products at Various Residence Times at 97,000 psi., Alumina Core

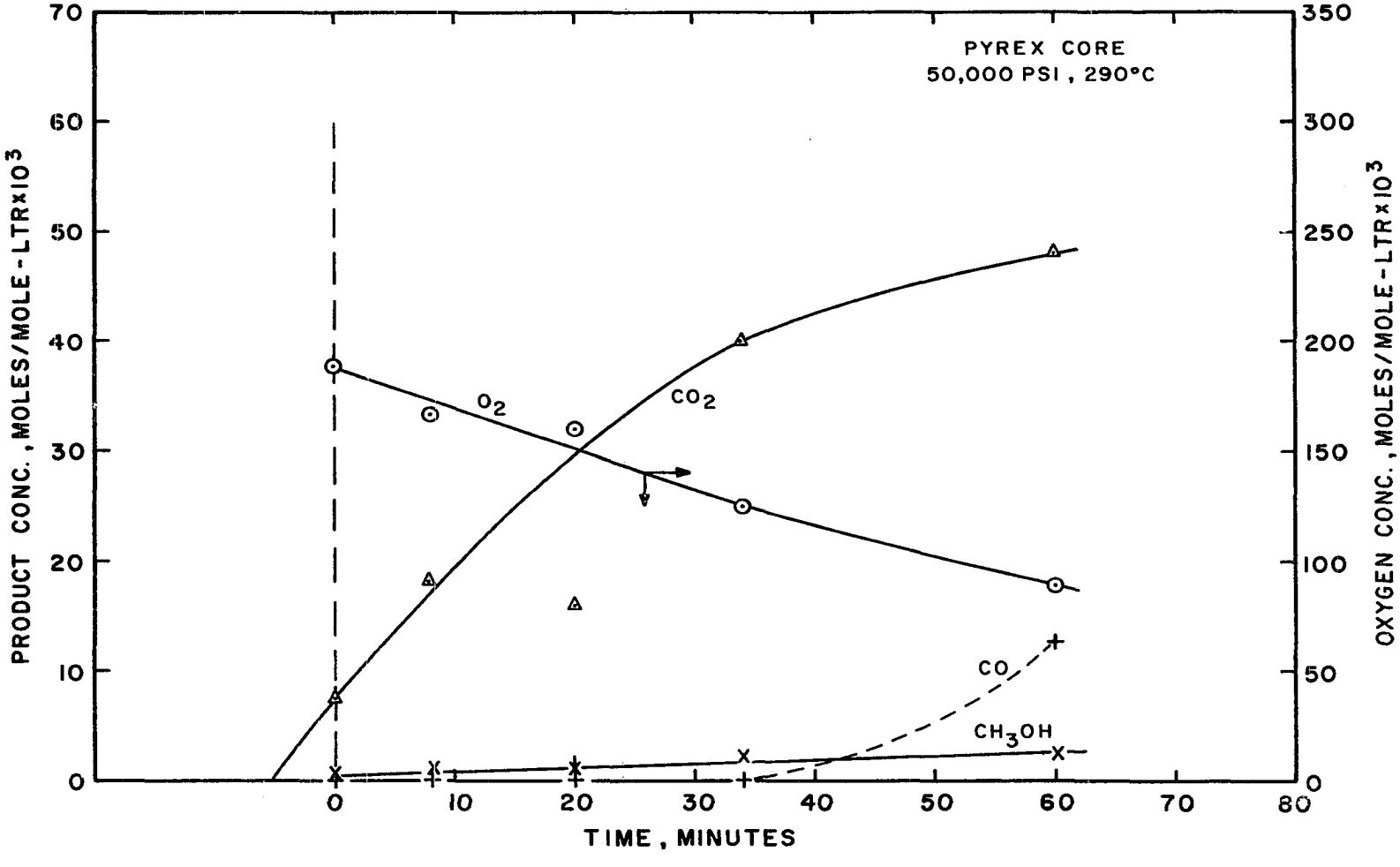


Figure 32. Concentrations at Various Residence Times at 50,000 psi., Pyrex Core.

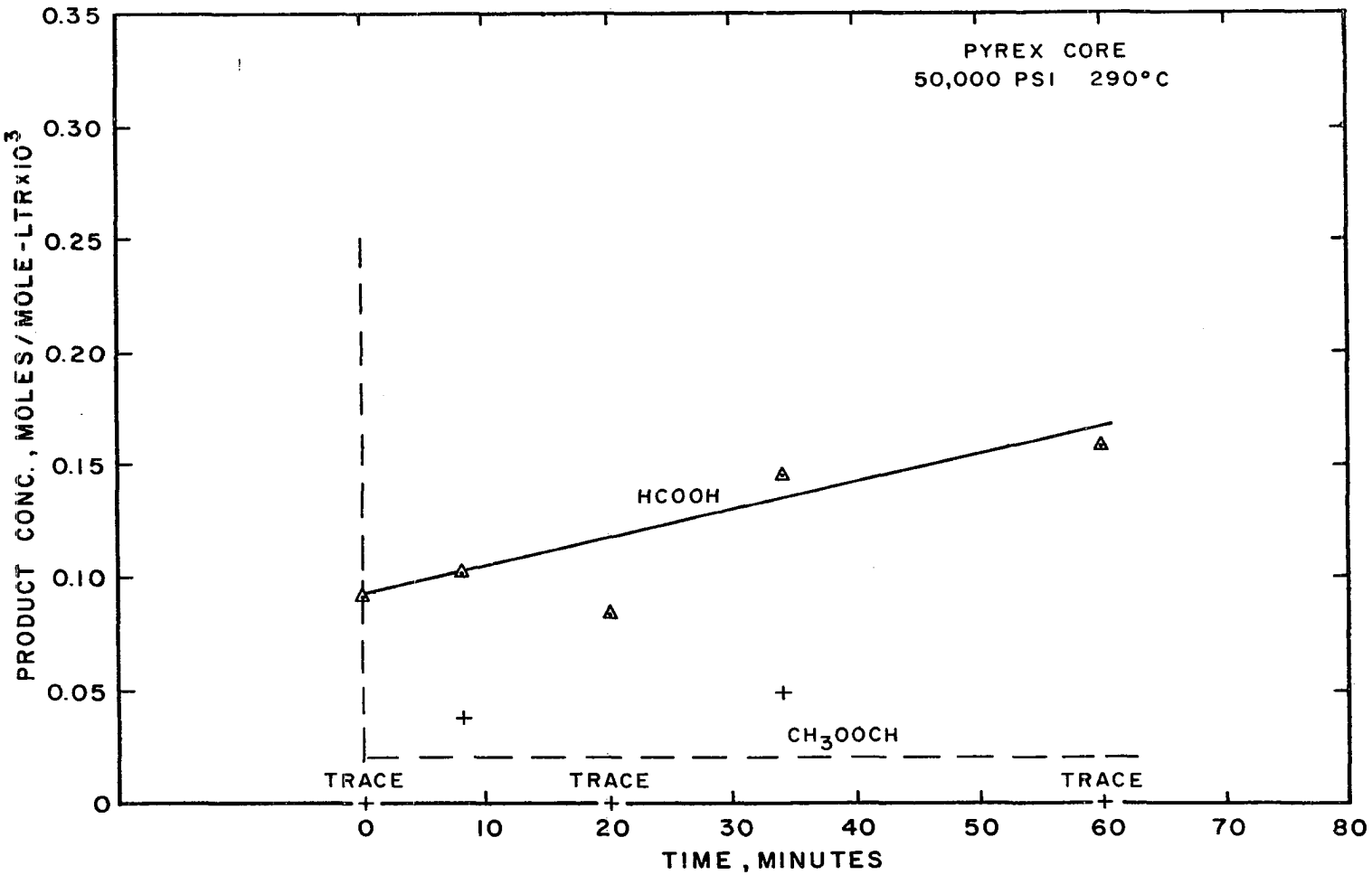


Figure 33. Formation of Formic Acid and Methyl Formate at 50,000 psi., Pyrex Core.

only three residence times were run before the large change in activity of the surface occurred. Therefore, the points for oxygen and carbon dioxide at these conditions are plotted in Figure 34 along with the lines obtained at 50,000 psi. and 290°C for comparison. Even though the pressure is much higher, the rate of reaction is lower because of the higher temperature used at 50,000 psi.

Product methanol concentrations at various pressures and temperatures for both cores are plotted in Figure 35 relative to residence time. These results tend to show that the Pyrex core was more favorable for the production of methanol. Despite the fact that the temperature is 5°C lower with the Pyrex core and at a lower pressure than with the alumina core, the methanol concentration is higher at the higher residence times.

In all cases where isothermal reactions were run the methanol concentration was very small. However, under conditions of adiabatic reaction, the alcohol formed was very high -- of the order of fifty percent of the liquid weight obtained. The formation of high concentrations of methanol only under adiabatic conditions tends to indicate that the reaction for the formation of methanol has a high energy of reaction and that it is certainly formed via a chain reaction. The mechanism proposed by Lott (29) is supported by the data obtained in this study:

$$CH_3\dot{O}O + CH_4 \longrightarrow CH_3OOH + \dot{C}H_3$$

$$CH_3OOH \longrightarrow CH_3\dot{O} + \dot{O}H$$

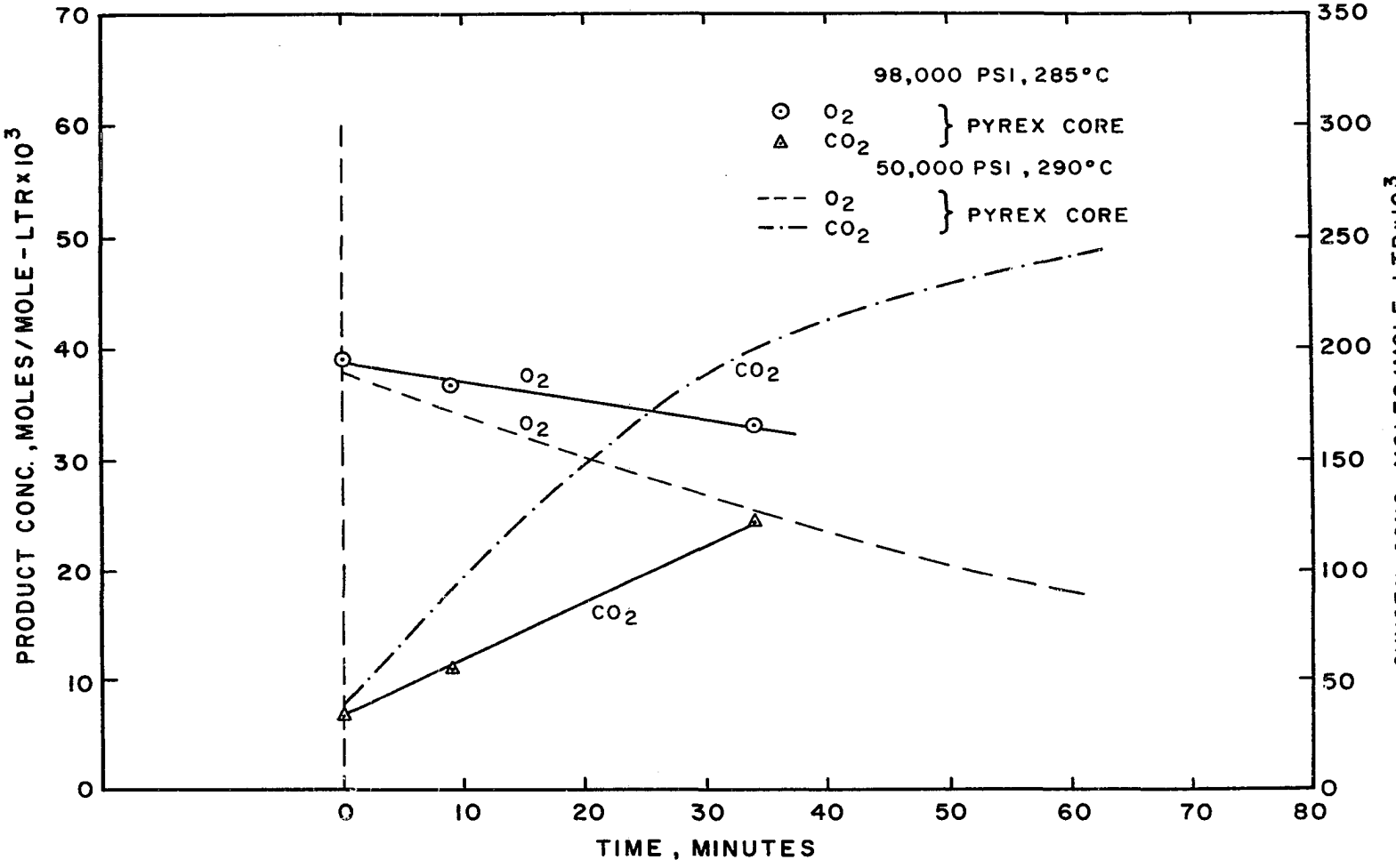


Figure 34. Concentrations at Various Residence Times, Pyrex Core.

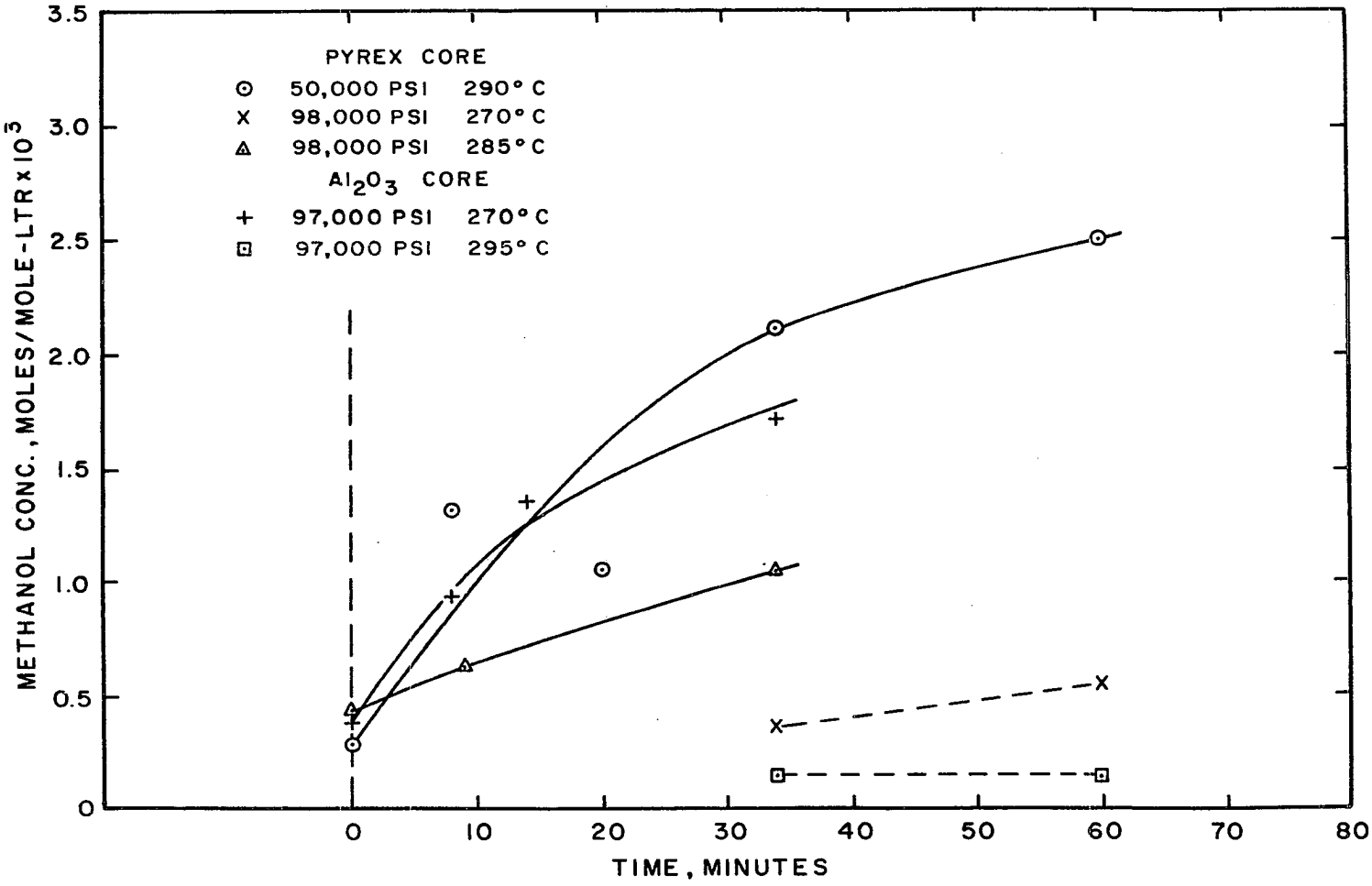


Figure 35. Methanol Formation at Various Residence Times, Temperatures and Pressures.

$$CH_3\mathring{O} + CH_4 \rightarrow CH_3OH + \mathring{C}H_3$$

For every mole of methanol made, two moles of $\mathring{C}H_3$ radicals are formed, which accelerates to a very rapid chain reaction by reaction with oxygen:

$$\mathring{C}H_3 + O_2 \rightarrow \text{intermediate radicals and products.}$$

It is believed that the high pressure allows the hydroperoxide to form. The expected high energy of activation could be in the right range for a hydroperoxide, which would have a ΔE of about -37 to -40 kcal./mole (38). The nature of the fast formation of methanol indicates that it is probably not made from a free radical specie forming another product at low pressure. The formation of methanol at high pressure may coincide with the formation of methyl formate.

Residual oxygen concentration, carbon monoxide, carbon dioxide and methanol concentrations obtained for strong adiabatic reactions using the Pyrex core are shown at three pressure levels in Figure 36. At 15,000 psi. the residual oxygen was greater than at the high pressures. The methanol concentration was lower at the lower pressure. More methanol was actually made at 50,000 psi. than at 98,000 psi. although slightly more oxygen was consumed at the higher pressure. Carbon monoxide decreases with pressure and carbon dioxide increases. It seems that above 50,000 psi., pressure does not have so pronounced an effect on the reaction as between 15,000 and 50,000 psi.

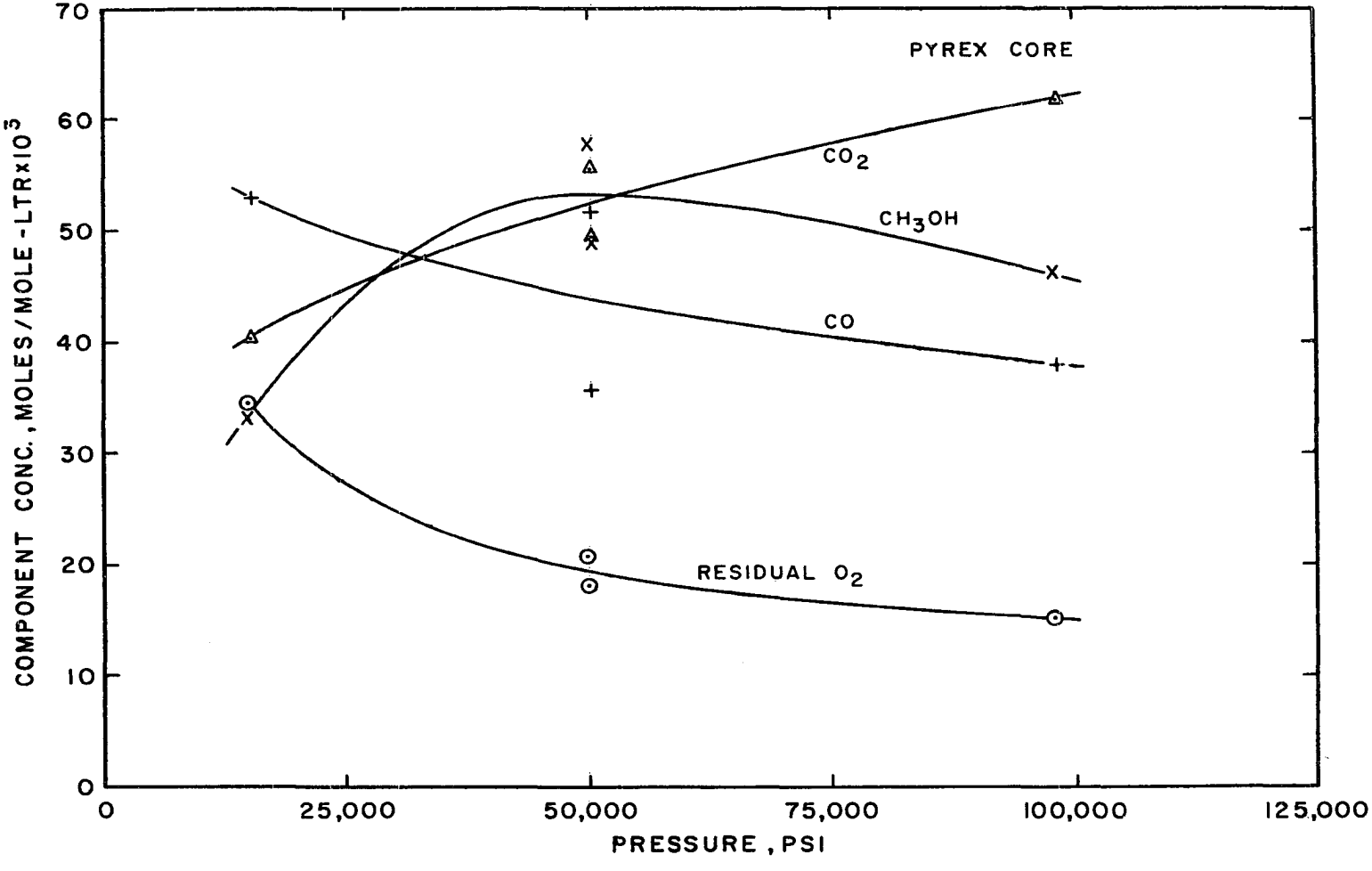


Figure 36. Concentrations Under Adiabatic Conditions, Pyrex Core.

Occurrence of Acetone

Acetone appeared in the product at short residence times and at low temperature and long residence times. The highest concentrations occurred when a small amount of petroleum naphtha was added to the synthetic hydraulic oil. Chronologically, the naphtha was added during Experiment 151, and it was gone from the system by Experiment 164, when fresh synthetic oil was added to the reservoir. High concentrations appeared after this in Experiments 165 and 166, and both these experiments were at zero residence times (defined earlier). The other possible source, other than methane, for formation of acetone was the trace of ethane, < 0.20 mole percent, which was in the instrument grade methane. Regardless of its source, acetone occurred early in the reaction and dropped in concentration during the course of the reaction.

The greatest concentration of ethane found in the feed gas before compression was 42×10^{-3} moles/mole-ltr. of feed. This ethane concentration apparently yielded a maximum of 0.04×10^{-3} moles/mole-ltr. of acetone using the alumina core and 0.06×10^{-3} moles/mole-ltr. using the Pyrex core before any naphtha was added. Several experiments after the naphtha was added, the highest concentration of acetone was 0.35×10^{-3} moles/mole-ltr. Thus, the source of increased acetone formation was the naphtha. However, usually no more than a trace of acetone was found when using the alumina core, when the feed composition was

constant for many successive experiments. It is concluded that acetone which was not formed through oxidation of naphtha was formed from ethane in the feed. Methane oxidation as a source of acetone cannot be ruled out, however.

The Reaction Rate Constant

Data obtained with the alumina heater core were used to calculate the reaction rate constant at various temperatures and three pressure levels using the integrated form of the following equation:

$$W = -\frac{d[O_2]}{dt} = k[CH_4]^m[O_2]^n$$

Previous investigators found a wide variation in the orders of the reaction with respect to methane and oxygen. The values given in Table 2 for m and n at the lowest temperatures are 2.0 and 0.5, respectively. Values of k were calculated using these exponents.

Since the methane concentration is almost constant during all of the experiments an average value $[\bar{CH_4}]$ was used. This average value allowed the equation to be integrated, with the following results,

$$k = \frac{2([O_2]_i^{\frac{1}{2}} - [O_2]^{\frac{1}{2}})}{t[\bar{CH_4}]^2}$$

where $[O_2]_i$ is the initial oxygen concentration.

Results of these calculations are shown plotted in Figure 37. Only data taken under isothermal and weak

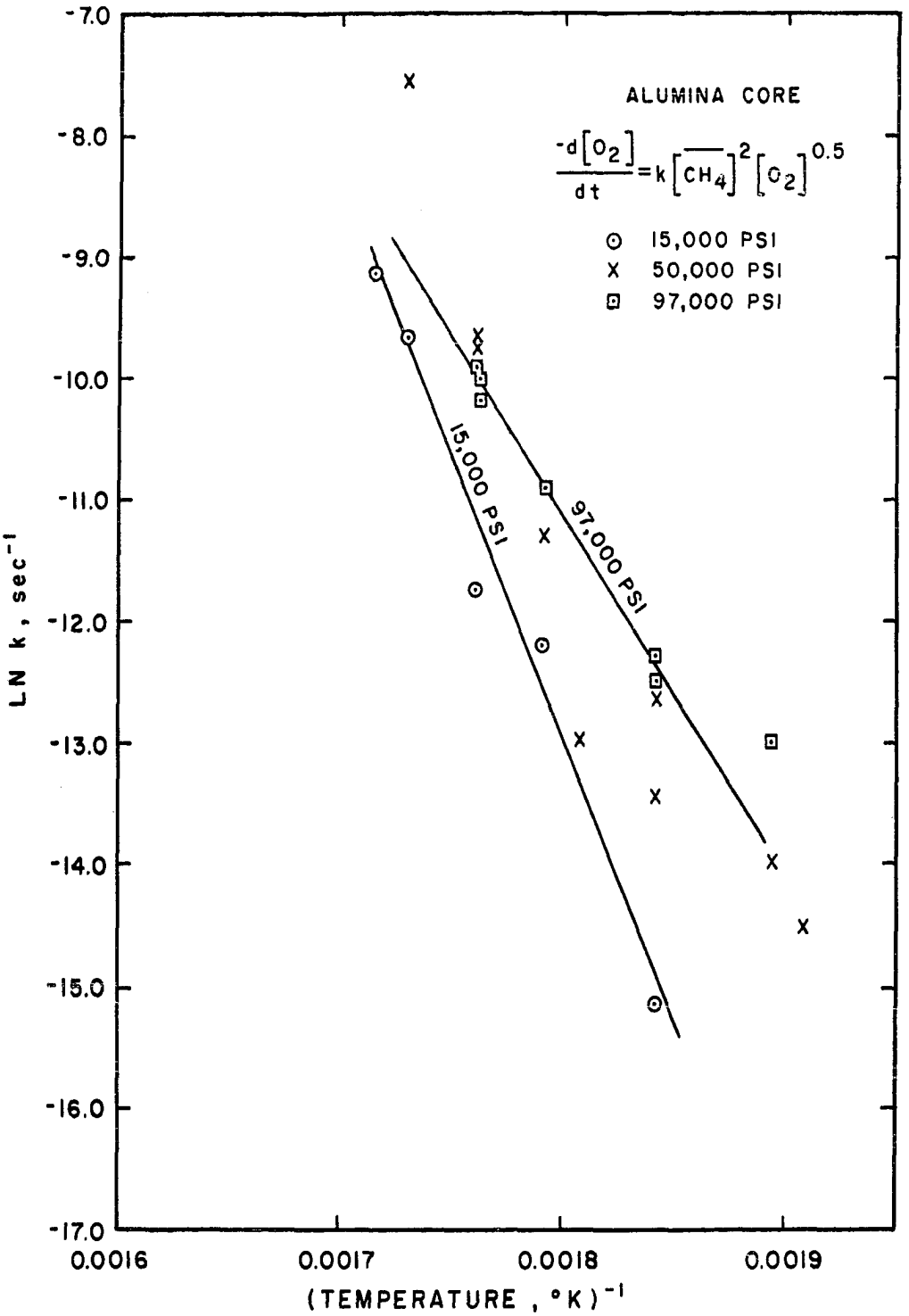


Figure 37. Correlation of the Reaction Rate Constant with Temperature for Methane, Order m = 2, and Oxygen, order n = 0.5.

adiabatic conditions were used. Experiments in which strong adiabatic reactions occurred are not included because it was necessary to estimate an average temperature due to the rapid increase in temperature from about 305 to over 420°C. The two lines drawn on Figure 37 are for 15,000 and 97,000 psi. The points for 50,000 psi fall within the lines, except at high temperature. The lines also converge, indicating the first relationship assumed is not correct.

The data were next correlated using an exponent of zero for oxygen. The results are plotted as Figure 38. Some improvement has occurred, but the points at 50,000 psi. are still in the same grouping at high temperatures as those for 97,000 psi. The line at 50,000 psi. still has curvature, and the lines for 15,000 and 97,000 still converge.

As discussed previously, Hsieu-Cheng (19) found that the oxidation of methane is zero order with respect to oxygen and methane when the partial pressure of oxygen is lower than that of methane. In a later paper (20), Hsieu-Cheng and Ruof reported that at low temperatures, 416-430°C, the rate depends only on the initial pressure of methane and oxygen, with $m = 2$ and $n = 1$.

It was felt worthwhile, in light of the paper cited, (19), and Figures 30, 32 and 34 to calculate the rate constant assuming the rate is independent of methane and oxygen concentrations. The results are shown in Figure 39. The correlation is not fully satisfactory, but it is the best obtained with the present data. Except for one point, which was obtained from a nonisothermal

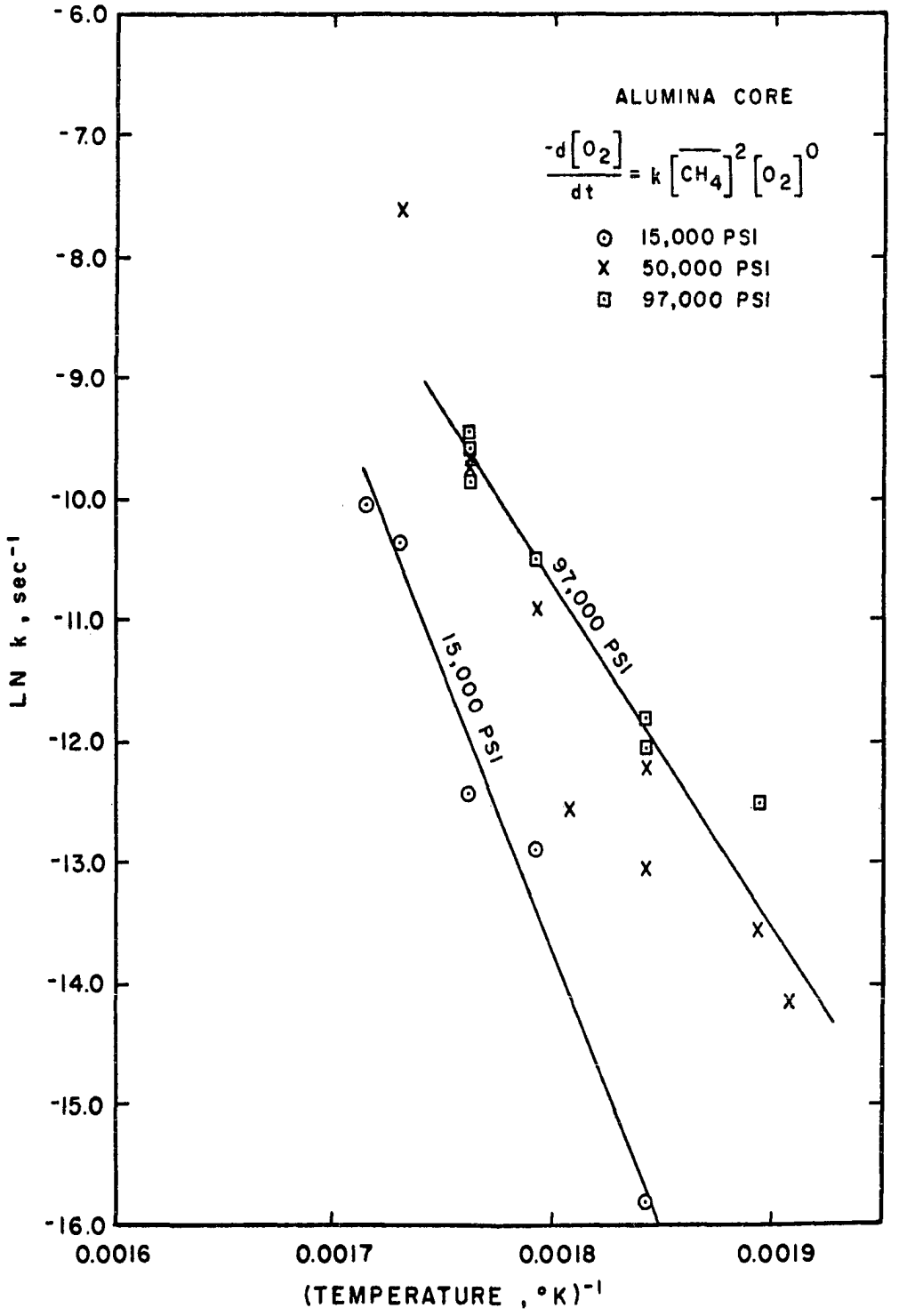


Figure 38. Correlation of the Reaction Rate Constant with Temperature for Methane, Order m = 2, Order n = 0.

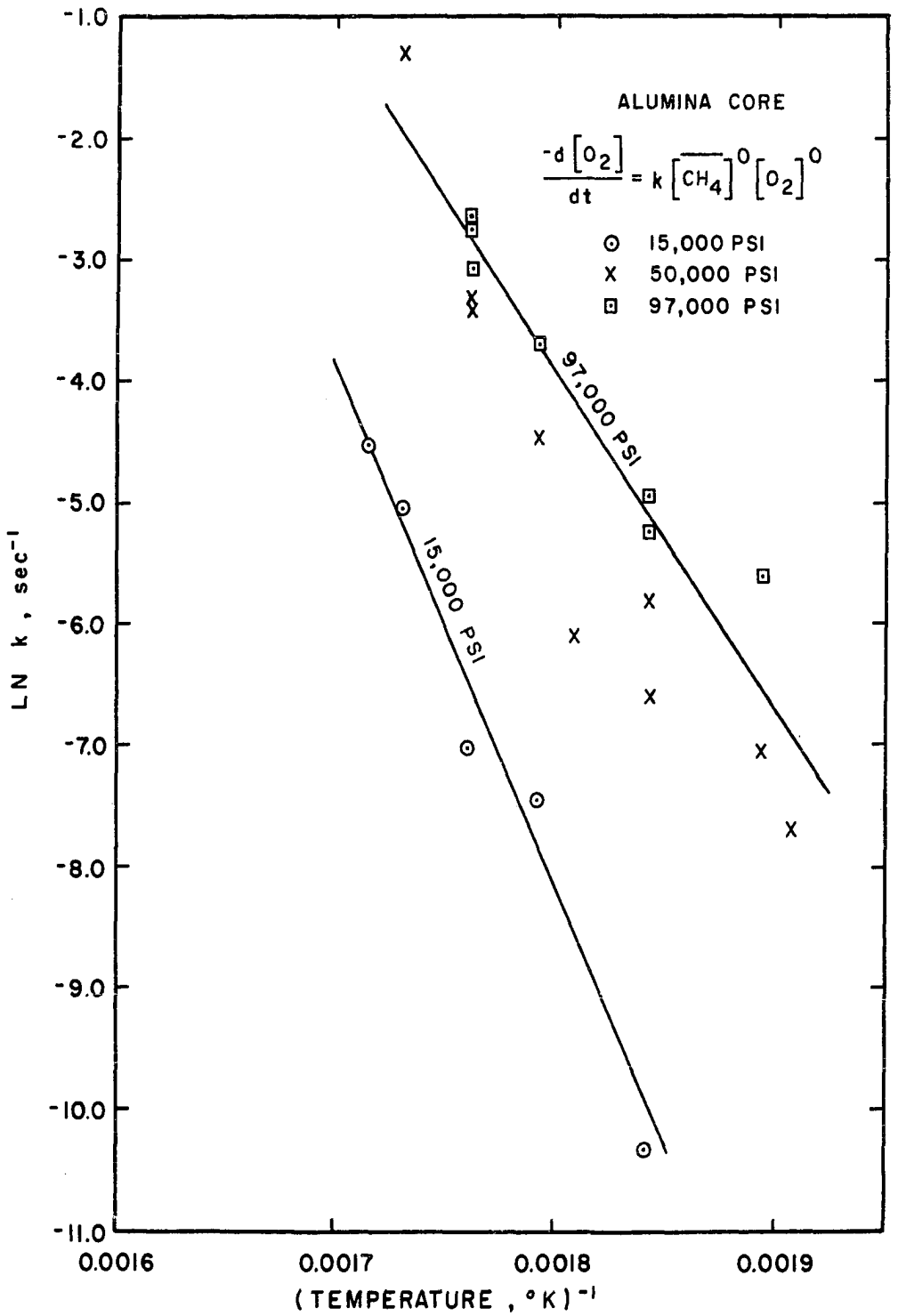


Figure 39. Correlation of the Reaction Rate Constant with Temperature for Methane, Order m = 0, and Oxygen, Order n = 0.

experiment, the points at 50,000 psi. fall within the lines drawn.

In order to obtain a common rate constant it is necessary to correct for pressure. Compressibility factors, z, and activity coefficients, γ, for methane are available up to 15,000 psi. from A.P.I. Project 44(1). Compressibility factors were calculated for 50,000 and 97,000 psi. from the present work, and these values in turn were used to calculate the activity coefficients.

The calculation started from the basic definition of Lewis fugacity,

$$\ln f - \ln f_o = \frac{1}{RT} \int_{P_o}^{P} V dP$$

where the subscript indicates the standard state of one atmosphere.

By definition $\frac{f_o}{P_o} = 1.0$. At standard state $\ln f_o = 0$

The equation was integrated by making use of the compressibility factors:

$$P = \frac{zRT}{V}$$

$$dP = \frac{RT}{V} dz - \frac{\bar{z} RT dV}{V^2}$$

$$\frac{1}{RT} \int_{P_o}^{P} V dP = \int_{z_o}^{z} dz - \int_{V_o}^{V} \frac{\bar{z} dV}{V}$$

$$\frac{1}{RT}\int_{P_o}^{P} VdP = z - z_o - \bar{z} \ln \frac{V}{V_o}$$

$$\ln f = z - z_o - \bar{z} \ln \frac{V}{V_o}$$

where

$\bar{z}$ = the average z for $P_o \rightarrow P$

The compressibility factor, z, is shown at the appropriate values of ln V in Figure 40. The values of $\bar{z}$ were determined from Figure 39 by measuring the areas under the curve with a planimeter.

The following values of z, $\bar{z}$ and γ for V_o = 45.13 ltr. were obtained for the three pressure levels and 550°K temperature.

TABLE 4

COMPRESSIBILITY FACTORS AND ACTIVITY COEFFICIENTS FOR METHANE AT 15,000, 50,000 AND 97,000 PSI.

P, psi.	z	$\bar{z}$	γ
15,000	1.573	1.043	1.487
50,000	2.645	1.146	5.560
97,000	4.240	1.230	37.2

For purposes of this calculation the gas mixture was assumed to be methane. Actual methane concentration was ~92 mole percent.

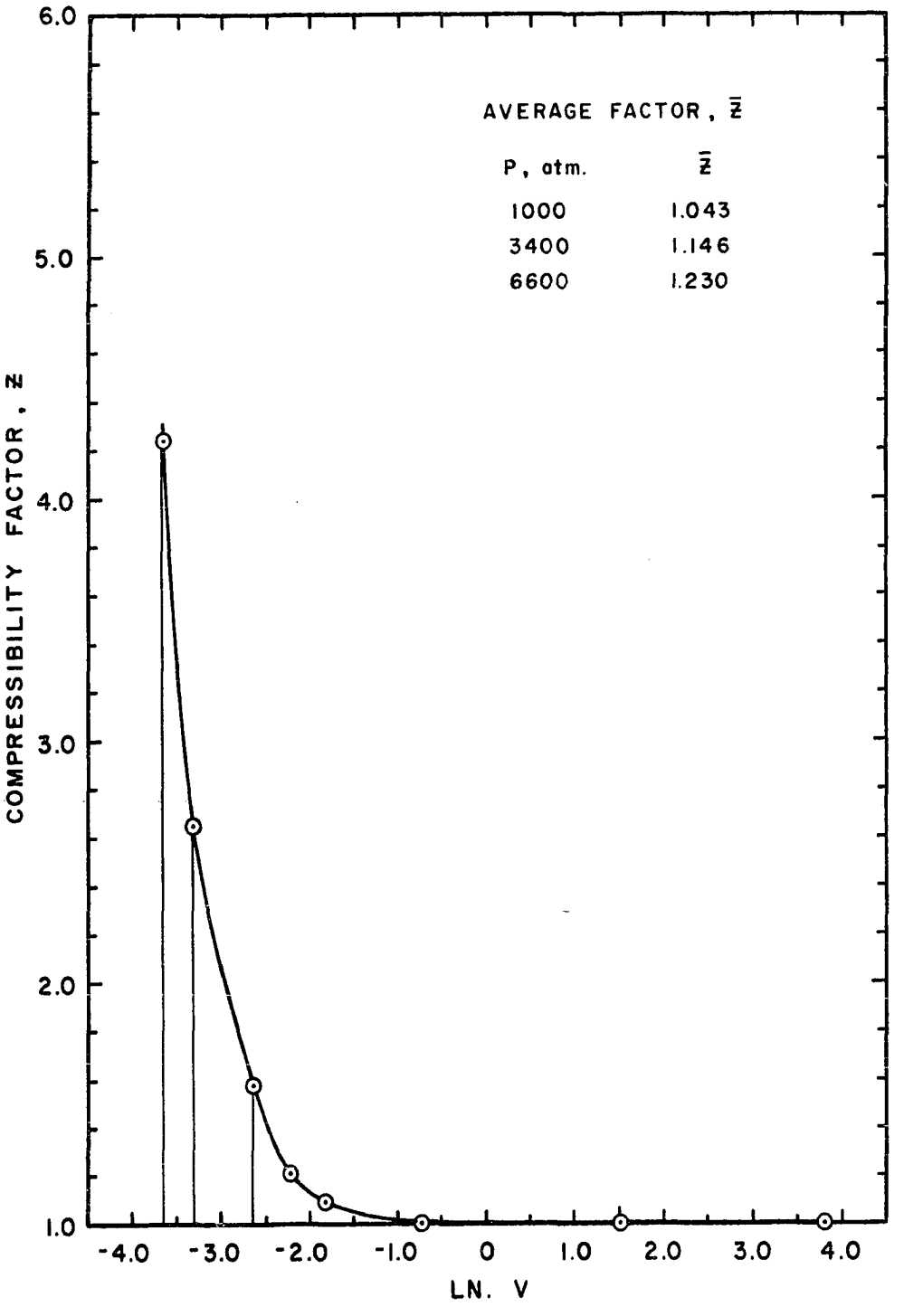


Figure 40. Correlation of the Compressibility Factor with Volume at Various Pressures.

The data plotted in Figure 39 are shown, corrected for pressure level, in Figure 41. The points at 50,000 psi. lie above those at 15,000 and 97,000 psi. Of more concern is the fact that the slope of a line for the points at 15,000 psi. is much steeper than the line shown. The best line was drawn through the data. Using a frequency factor of 10^{13} the activation energy was found to be -40.7 kcal./mole. The value of 10^{13} for the frequency factor is of the magnitude given by Shtern (48) for

$$CH_3OOH \rightarrow CH_3\mathring{O} + \mathring{O}H \qquad A = 10^{13} - 10^{15}$$

and

$$CH_3O\mathring{O} \rightarrow HCHO + \mathring{O}H \qquad A = 10^{13}$$

An inhibiting effect of methane during oxidation around 650°C was reported by Hoare and Walsh (17). It was necessary to use a negative coefficient of up to -2 for methane in the rate equation. It was found that data from the present work correlated best assuming oxygen inhibits and that m = 2 and n = -2. The integrated form of the rate equation was used as before, and the results are plotted in Figure 42. There is little difference in slopes of the lines, and the points make up three distinct lines. The correlation in Figure 43 shows the results corrected for pressure by use of the activity coefficients calculated earlier except that ln γ for 97,000 psi. was reduced from 3.61 to 3.0 in order not to overcorrect for pressure. The activation energy was calculated to be -46.2 kcal./mole using a frequency factor of 10^{13}. The data now make up one set, and only two points

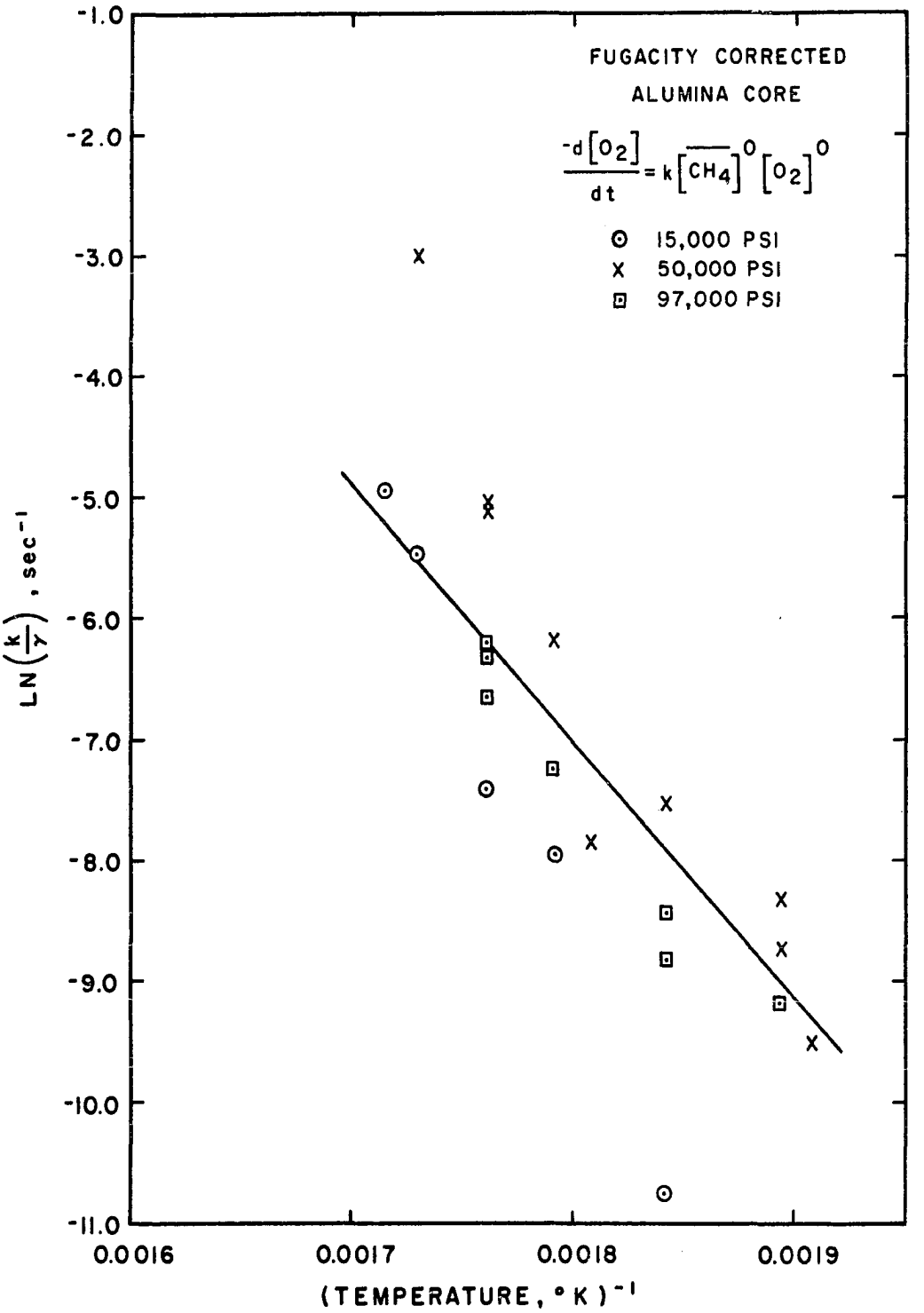


Figure 41. Correlation of the Reaction Rate Constant with Temperature Corrected for Pressure, m = 0, n = 0.

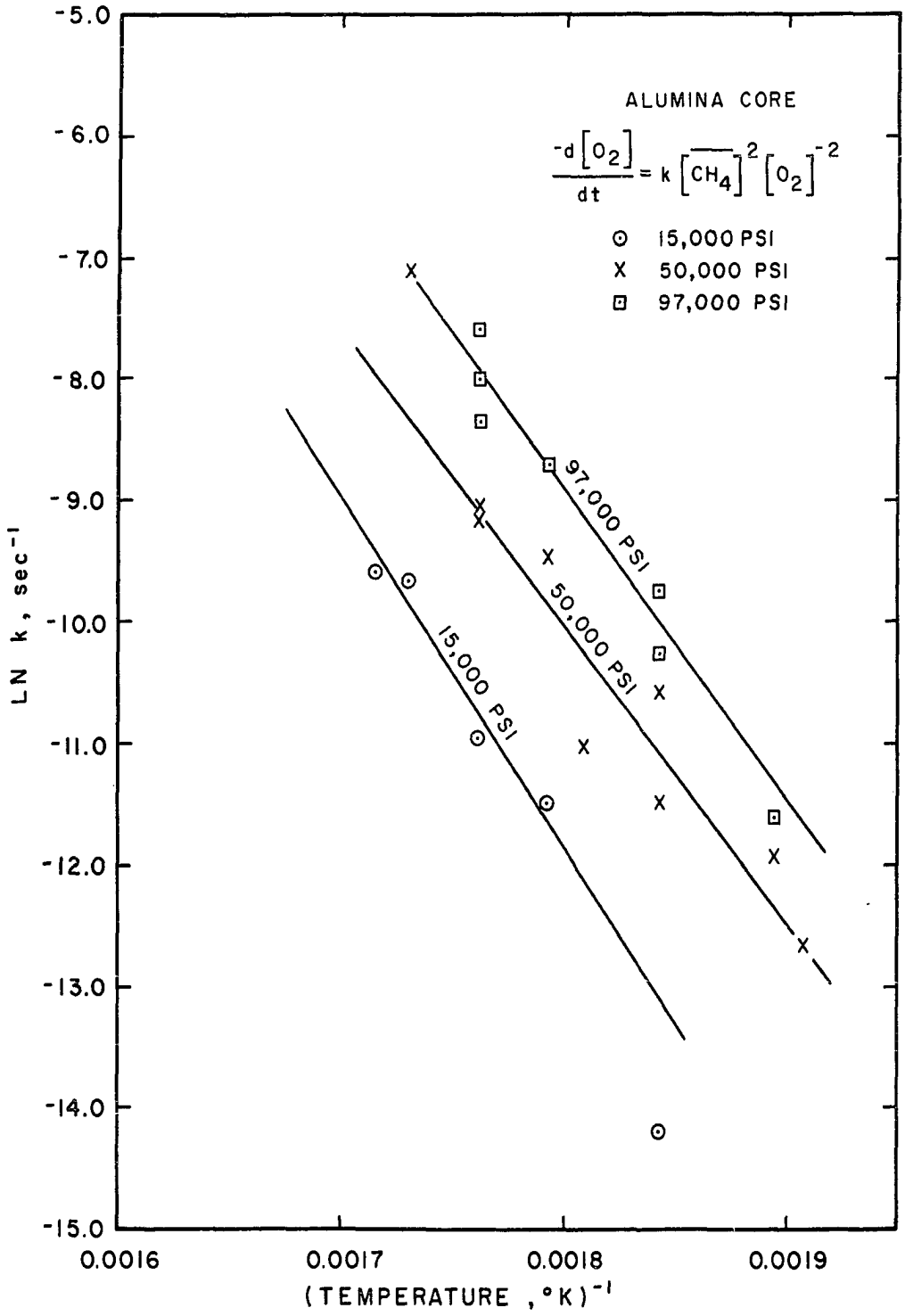


Figure 42. Correlation of the Reaction Rate Constant with Temperature for m = 2, n = -2.

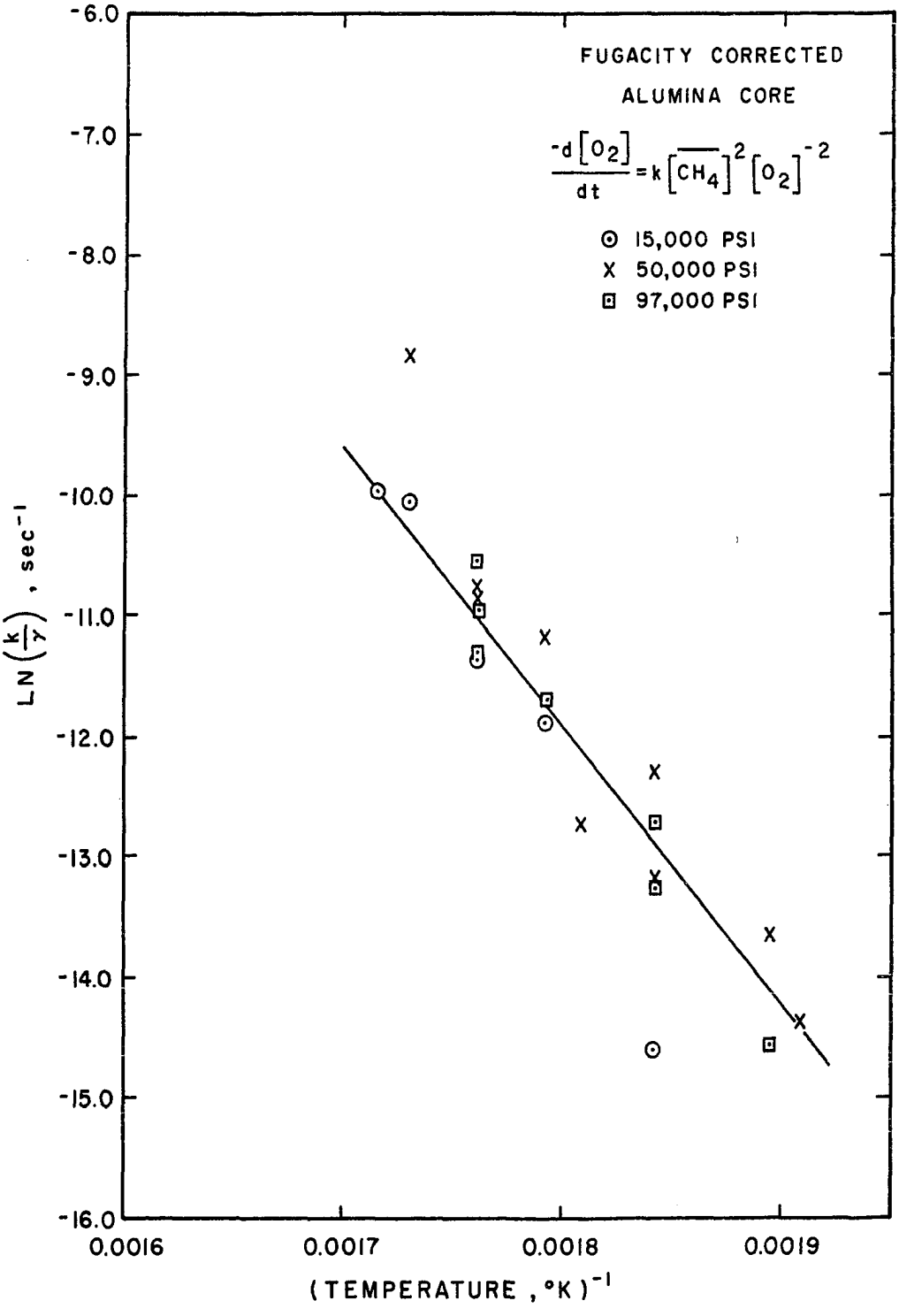


Figure 43. Correlation of the Reaction Rate Constant with Temperature Corrected for Pressure, m = 2, n = -2.

are very far off the line. Depending on the equation used, data from this work led to an activation energy of -40 to -46 kcal./mole.

It is not surprising that a single differential equation will not adequately correlate the data. There is a pronounced surface effect in the oxidation of methane, and many concurrent and consecutive reactions are believed to occur. In addition, at least two of these reactions are assumed to be chain reactions.

Proposed Mechanism

Results of this work show that the formaldehyde concentration increases with residence time, and there is no indication of a constant or decreasing composition. Therefore, formaldehyde is not believed to be a key intermediate in the partial oxidation of methane at high pressure.

In oxidations at low pressure carbon monoxide appears in higher concentration than carbon dioxide early in the reaction. At high pressure, however, the opposite is true. The initial products in high concentration are carbon dioxide and water. Those products present initially in small quantities are formaldehyde, formic acid, methanol, methyl formate and acetone. At 97,000 psi., after an induction time of > 14 minutes, carbon monoxide appears, and there is an increase in the $CO:CO_2$ ratio. Lott (29) and Newitt and Haffner (39) reported a ratio of $CO:CO_2$ of < 1.0 initially, and the ratio increased with time.

Thus, the appearance of methanol at high pressure is not the only difference between operation at low and high pressure. The early formation of carbon dioxide at a rapid rate, and the formation of formic acid and methyl formate must be explained. One concludes that the reactions which are controlling at low pressure are not those which control the mechanism at high pressure. The reactions controlling the mechanism also change with temperature. For instance a difference in product distribution was found with increasing temperature. Between 250 and 285°C, the main products are carbon dioxide and water. Between 285 and 300°C they are these products plus the monoxide. Above 305°C at pressures of 50,000 psi. and higher, when an adiabatic reaction occurs, methanol must be included as a main product. The minor products also increase in concentration with temperature, but in most cases methyl formate increases more than the others.

It is believed that a general mechanism must provide for the product distributions in each of the three temperature ranges. Transition from one range to the other must also be provided for. The following reactions are believed to predominate from 250-285°C at 50,000 psi. and above:

0. $CH_4 + O_2 \rightarrow \dot{C}H_3 + H\dot{O}_2$
1. $\dot{C}H_3 + O_2 \rightarrow \text{wall} \{\cdot OOCH_3$
2. $\text{wall} \{\cdot OOCH_3 + O_2 \rightarrow CO_2 + H_2O + \dot{O}H$
3. $\dot{O}H + CH_4 \rightarrow H_2O + \dot{C}H_3$
4. $\text{wall} \{\cdot OOCH_3 + O_2 \rightarrow HC(=O)OOH + \dot{O}H$

5. $\overset{\Omega}{HCOOH} \rightarrow \overset{\Omega}{HC\dot{O}} + \dot{O}H$

6. $\overset{\Omega}{HC\dot{O}} + CH_4 \rightarrow \overset{\Omega}{HCOH} + \dot{C}H_3$

7. wall $\{ \cdot OOCH_3 \rightarrow CH_3O\dot{O}$ (in solution)

8. $CH_3O\dot{O} \rightarrow HCHO + \dot{O}H$

where

wall $\{ \cdot OOCH_3$ is a free radical complexed at the wall.

Termination reactions occur, but all of them are given later after the other chain reactions have been listed. Between 250 and 285°C, small amounts of methanol and methyl formate are also made, but the energies of activation are too high for these reactions for much product to be made via the main chain mechanism which accounts for high concentrations of methanol.

Between 285-300°C, the reactions given previously, plus the following are most important:

9. $H\dot{O}_2 + HCHO \rightarrow H_2O_2 + HC\dot{O}$

10. $H\dot{C}O + O_2 \rightarrow CO + H\dot{O}_2$

It is at this temperature level that appreciable amounts of $CH_3O\dot{O}$ (soluble) appear and are converted to formaldehyde, which in turn is converted to carbon monoxide. This submechanism is a chain reaction, of course.

Above 300°C the reaction rate is rapid and adiabatic reactions usually occur at about 305°C. At this temperature level, methanol is now formed in large amounts, along with previous products:

11. $CH_3O\dot{O} + CH_4 \rightarrow CH_3OOH + \dot{C}H_3$

12. $CH_3OOH \rightarrow CH_3\dot{O} + \dot{O}H$

13. $CH_3\dot{O} + CH_4 \rightarrow CH_3OH + \dot{C}H_3$

Due to the relatively high energy of activation, the chain reaction forming methanol is very rapid. A large amount of heat is released, and it is not possible to conduct an isothermal reaction at this temperature level.

The termination reactions can now be included:

14. $CH_3\dot{O} + H\dot{C}O \rightarrow CH_3OOCH$

15. $CH_3 + \dot{O}H \rightarrow CH_3OH$

16. $H\dot{O}_2 \xrightarrow{wall}$ termination

17. $CH_3O\dot{O} \xrightarrow{wall}$ termination

18. $2\ H_2O_2 \xrightarrow{wall} 2H_2O + O_2$

Acetone is not included because it may not be formed through oxidation of methane. The ratio of methanol to methyl formate in the product is about 100 to one. If the chain length were 100, all the methyl formate made would come through reaction 14. Bimolecular terminations probably lead to very small amounts of compounds not identified.

Reactions at high pressure are characterized by higher rates than at low pressure or by achievement of the same rate at a lower temperature. One would expect a change in product distribution at lower temperature because many reactions are involved having different energies of activation. High pressure also favors a reduction in volume of the system, and apparently peroxides or hydroperoxides are

able to form even though the temperature is relatively high for their formation. High pressure reduces the rate of diffusion of the components. Therefore bimolecular terminations are favored over surface unimolecular reactions.

The main feature of the general mechanism is that a logical reason for the induction time encountered at high pressure and at low pressure and high temperature is advanced. As they are formed, $CH_3O\dot{O}$ radicals are complexed or trapped by any surface, with the oxygen end of the radical held nearest the surface. At high pressure, the methyl end is capable of being attacked by oxygen, forming a highly unstable oxygen-rich radical, which decomposes immediately forming carbon dioxide and water. A small fraction of the large radicals form performic acid. Except for a small equilibrium number of $CH_3O\dot{O}$ radicals which enter solution, most of the $CH_3O\dot{O}$ radicals are held at the surface until the surface is covered. It is probably necessary for the surface to be neutralized electrically by the paramagnetic nature of the free radical. Oxygen is probably concentrated at the surface for the same reason--it is paramagnetic. When the surface is saturated, the large number of $CH_3O\dot{O}$ radicals become available for formation of formaldehyde and large amounts of methanol if the temperature is high enough.

It is an interesting point, that the result of a strong adiabatic reaction at high pressure does not seem to be influenced by the surface area. A large surface area,

occurring because of a broken heater core for instance, required a high temperature to initiate a runaway reaction. The end result in peak temperature and product distribution was essentially the same as that of a reaction initiated at lower temperature, however.

At high temperature and low pressure the $CH_3O\dot{O}$ radicals held at the wall are not able to react with oxygen. Consequently, very little carbon dioxide is made early in the reaction. After the wall saturates with these radicals, they become available for formation of formaldehyde and carbon monoxide. The findings of Hoare and coworkers (3), giving the relative affinities of $\dot{O}H$ and $H\dot{O}_2$ radicals for CH_4, carbon monoxide and HCHO are significant. The $H\dot{O}_2$ radicals preferentially react with formaldehyde over carbon monoxide in a ratio of 340:1. Therefore the chain reaction needed for formation of the monoxide is very favorable (reactions 9 and 10).

At low pressure the formation of methylhydroperoxide is not favored and consequently virtually no methanol is made. The high temperatures used, of course, also work against peroxide formation. Photo-iniation at low temperature and pressure results in a small amount of methanol being made. The hydroperoxide can form and then decompose slowly at the low temperature.

The results at 15,000 psi., as might be expected, are about midway between those obtained at atmospheric pressure and those obtained above 50,000 psi. Adiabatic

reactions initiate at a higher temperature and less methanol is made.

Below 285°C, where the main products are carbon dioxide and water, the proposed mechanism provides a $H_2O:CO_2$ ratio of slightly over 2.0. The average value of this ratio estimated from the data is 3.1. Between 285 and 300°C the main products are water, carbon dioxide and carbon monoxide. The formation of the monoxide leads to one mole of water through the $\dot{O}H$ radical formed with formaldehyde. If all the hydrogen peroxide is converted at the wall to water, then the overall ratio of $H_2O:(CO_2 + CO + CH_3OH)$ would be 2.0. The average of experiments carried out in this temperature range was 1.98.

When runaway reactions occurred, the average ratio of water to $(CO_2 + CO + CH_3OH)$ was 1.26. The drop in ratio from 1.98 to 1.26 as temperature increases reflects the large amount of methanol formed under adiabatic conditions. Only one mole of water is made for each mole of methanol according to the mechanism.

An effect of pressure on the ratio of water to $(CO_2 + CO + CH_3OH)$ was found. The values are shown in the following table:

TABLE 5

THE EFFECT OF TEMPERATURE AND PRESSURE ON THE RATIO $\frac{H_2O}{CO_2 + CO + CH_3OH}$

Pressure Psi.	Temperatures, °C		
	250-280	285-300	over 300
15,000	--	2.2	1.4
50,000	3.4	1.98	1.22
97-98,000	2.8	1.88	1.17

The effect of pressure on the ratio is less pronounced than the effect of temperature. At high pressure more methanol is made than at low pressure, and therefore less water is made at the high pressure. This result accounts at least in part for the lower ratio. In the temperature range 250-280°C very little reaction occurs, and consequently, there is not much liquid or gas product to measure. The values at the higher temperatures are therefore more accurate.

The data of Figure 1 show that the ratio $H_2O:CO_2 + CO$ is about 1.9 at 235 mm. Hg. pressure, 472°C temperature, and residence time of 16 minutes. At 30 minutes the ratio is 2.0, which is expected from the stoichiometric reaction for the formation of water and carbon dioxide. Thus, results at low pressure correspond to results at high pressure in the temperature range 285-300°C where little methanol or other organic oxygenated compounds are

made. Unfortunately, Newitt and Haffner partly filled the product receiver with water before an experiment, and no data on water are presented with which to make a comparison.

The mechanism proposed appears to provide for the findings at all pressures investigated, and over the temperature range 250 to at least 500^{o}C.

CHAPTER IX

CONCLUSIONS

1. Alumina has little or no surface effect during the partial oxidation of methane at high pressure. Surface effect is defined as a change in the oxygen consumed and the product distribution obtained from a given set of experimental conditions in successive experiments.

2. The use of alumina powder or cement should not be used in a reactor at high pressure. Hard, fused alumina is satisfactory.

3. Pyrex is not a satisfactory material for use in high pressure reactors during the partial oxidation of methane. There is some surface effect, visible devitrification of the Pyrex, and it is mechanically weak.

4. It was theorized that carbon dioxide is made at high pressure by the following chain process during the partial oxidation of methane:

$$\dot{C}H_3 + O_2 \rightarrow \text{wall}\{\cdot OOCH_3$$

$$\text{Wall}\{\cdot OOCH_3 + O_2 \rightarrow CO_2 + H_2O + \dot{O}H$$

$$\dot{O}H + CH_4 \rightarrow H_2O + \dot{C}H_3$$

5. An induction time occurs for the formation of carbon monoxide, but not for the other products.

6. The data confirm the proposed chain mechanism of Lott for the formation of methanol.

7. Below 285°C and at pressure of 50,000 psi. or higher, the products of the reaction are carbon dioxide, water, methanol, formaldehyde, formic acid and methyl formate.

8. Above 285°C and at 50,000 psi. or higher pressure, carbon monoxide is also a product of the oxidation. Carbon monoxide appears above 295°C at 15,000 psi.

9. As pressure increases above 15,000 psi., the temperature required for strong adiabatic reaction decreases. It is about 312°C at 15,000 psi. and 305°C at 50,000-97,000 psi. for constant surface effect.

10. The effect of pressure on the reaction rate and product distribution is less between 50,000 and 100,000 psi. than between 15,000 and 50,000 psi. (The highest concentration of methanol on a mole per mole of feed per ltr. basis was made during a strong adiabatic reaction at initial pressure of 50,000 psi.).

11. In the differential equation,

$$-\frac{d[O_2]}{dt} = k[C\bar{H}_4]^m [O_2]^n$$

with m = 2, the coefficient n must be -2 in the pressure range 15,000-97,000 psi. to correlate the data.

12. The overall energy of activation for the oxidation of methane at high pressure is 40-46 kcal./mole using a frequency factor of 10^{13}.

NOMENCLATURE

a_i = kinetic coefficient, $k_i[X_j]$

A_i = frequency factor (Arrhenius equation)

d = diameter

E = energy of activation

f = fugacity

g_1 = rate constant of termination of active centers

k = overall reaction rate constant

k_i = reaction rate constant

m = order of reaction with respect to methane

M = any third body in a reaction

M_t = concentration of all molecules

n = order of reaction with respect to oxygen

n_o = number of active centers at any time

P = total pressure

P_o = standard pressure, one atm.

P_i = product of reaction

R = universal gas constant

S = state of activation of surface

t = time

T = temperature

V = reactor volume

V_o = standard volume, one atm.

w = overall rate of reaction

w_o = rate of initiation of active centers

w_i = rate of free radical reaction, $i \neq o$

X = intermediate (unspecified)

X_i = reactant in reaction

Y_i = free radical in reaction

z = compressibility factor

z_o = compressibility factor at standard state

$[\ ]$ = concentration

$[\ ]_i$ = initial concentration

$\bar{z}$ = bar denotes average

Greek

ν = chain length

Δ = difference

τ = induction time

γ = activity coefficient

LITERATURE CITED

1. American Petroleum Institute, Research Project 44, "Data on Hydrocarbons and Related Compounds," Carnegie Institute of Technology, Pittsburgh (1957).

2. Avramenko, L. I., Kolesnikova, R. V. and Kuznetsova, N. L., Izv. Akad. Nauk SSSR, Otd. Khim. Nauk 1963, 620.

3. Blundell, R. V., Cook, W. G. A., Hoare, D. E. and Milne, G. S., Symp. Combust. 10th, Univ. Cambridge 1964, 445.

4. Bone, W. A. and Allum, R. E., Proc. Roy. Soc. A134, 578 (1932).

5. Bone, W. A. and Gardner, J. B., Proc. Roy. Soc. A154, 297 (1936).

6. Chamberlain, G. H. N., Hoare, D. E. and Walsh, A. D., Disc. Faraday Soc. 14, 89 (1953).

7. Chamberlain, G. H. N. and Walsh, A. D., Proc. Roy. Soc. A215, 175 (1952).

8. Cheaney, D. E. and Walsh, A. D., Fuel 35, 258 (1956).

9. Enikolopyan, N. S., Zhur. Fig. Khim. 33, 642 (1959).

10. Fisher, I. P. and Tipper, C. F. H., Trans. Faraday Soc. 59, 1163 (1963).

11. _____, Trans. Faraday Soc. 59, 1174 (1963).

12. Fort, R. and Hinshelwood, C. N., Proc. Roy. Soc. A129, 284 (1930).

13. Gudkov, S. F., Tr. Vses. Nauchu. - Issled. Inst. Prorodu. Gazov. 1961, 118.

14. _____, Tr. Vses. Nauchu. - Issled. Inst. Prorodu. Gazov. 1961, 125.

15. Hamilton, L. F. and Simpson, S. G., "Quantitative Chemical Analysis," 10th edition, The MacMillan Company, New York (1952).

16. Hoare, D. E., Trans. Far. Soc. 49, 638 (1953).

17. Hoare, D. E. and Walsh, A. D., Fifth Symposium on Combustion, New York (1955).

18. Hoare, D. E. and Walsh, A. D., Proc. Roy. Soc. A215, 454 (1952).

19. Hsieu-Cheng, Yao, Am. Chem. Soc. Fuel Chem., Preprints 1962, 115.

20. Hsieu-Cheng, Yao and Ruof, C. H., Combustion Flame 8, 179 (1964).

21. Karmilova, L. V., Enikolopyan, N. S. and Nalbandyan, A. B., Zhur. Fiz. Khim. 34, 550, 990 (1960).

22. _____, Zhur. Fiz. Khim. 35, 1046 (1961).

23. _____, Zhur. Fiz. Khim. 35, 1458 (1961).

24. Kleimenov, N. A. and Nalbandyan, A. B., Doklady Akad. Nauk SSSR 124, 119 (1959).

25. Kleimenov, N. A. and Nalbandyan, A. B., Rev. Chim. (Bucharest) 11, 391 (1960).

26. Knox, J. H., Combust. Flame 9, 297 (1965).

27. Kompaneets, A. S. and Moshkina, R. I., Kinetika i Kataliz 6, 1098 (1965).

28. Lewis, B. and von Elbe, G., "Combustion, Flames and Explosions of Gases," 2nd edition, Academic Press, New York (1961).

29. Lott, J. L., Ph.D. Dissertation, University of Oklahoma (1965).

30. Mach, F. and Hermann, R. F., Anal. Chem. 63, 417 (1923).

31. Mantashyan, A. A. and Nalbandyan, A. B., Izv. Akad. Nauk Arm. SSR, Khim. Nauki 15, 3 (1962).

32. Markevich, A. M., Moshkina, R. I. and Filippova, L. F., Izvest. Akad. Nauk SSSR, Otdel. Khun Nauk 1958, 502.

33. Mari, R., Letort, M. and Dzierzynski, M., Compt. Rend. 252, 3241 (1961).

34. Mari, R. Letort, M., Niclause, M. and Dzierzynski, M., Bull. Soc. Lorraine Sci. 1, 29 (1961).

35. Meerssche, M. van, Ann. Mines Belg. 48, 643 (1949).

36. Michael, J. V. and Glass, G. P., Am. Chem. Soc., Div. Fuel Chem. Preprints 8, 195 (1964).

37. Minkoff, G. J. and Salooja, F. C., Fuel 32, 516 (1953).

38. Minkoff, G. J. and Tipper, C. F. H., "Chemistry of Combustion Reactions," Butterworths, London (1962).

39. Newitt, D. M. and Haffner, A. E., Proc. Roy. Soc. A134 591 (1932).

40. Newitt, D. M. and Szego, P., Proc. Roy. Soc. A147, 555 (1934).

41. Norrish, R. G. W., "Cinétique et mécanisme des réactions d'inflammation et de combustion en phase gazeuse," Centre Nat'l. Recherche Sci., Paris (1948).

42. Norrish, R. G. W. and Foord, S. G., Proc. Roy. Soc. A157, 503 (1936).

43. Norrish, R. G. W. and Reagh, J. D., Proc. Roy. Soc. A176, 496 (1940).

44. Norrish, R. G. W. and Wallace, J., Proc. Roy. Soc. A145, 307 (1934).

45. Pipkin, O. A., Ph.D. Dissertation, University of Oklahoma (1964).

46. Romijn, Z. Anal. Chem. 36, 18 (1897); 39, 60 (1900).

47. Schneider, I. A., Acad. Rep. Populare Romine, Studii Cercetari Chim. 11, 325 (1963).

48. Schtern, V. Ya., "The Gas Phase Oxidation of Hydrocarbons," The MacMillan Company, New York (1964) (translated M. F. Mullins).

49. Semenov, N. N., "Chain Reaction" English edition, Oxford University Press (1935).

50. Semenov, N. N., "Some Problems in Chemical Kinetics and Reactivity," Vol. 2 Princeton University Press, Princeton, New Jersey, (1959). (Translated by M. Boudart.)

51. Stadnik, P. M. and Gomonai, V. I., Kinetike i Kataliz 4, 348 (1963).

52. Sutton, F., "A Systematic Handbook of Volumetric Analysis," 12th edition, J. and A. Churchill Ltd., London (1935).

53. Vanpée, M., Ann. Mines Belg. 47, 1053 (1948).

APPENDIX A

SUMMARY OF EXPERIMENTAL RESULTS

TABLE 6.

EXPERIMENTAL RESULTS

ALUMINA HEATER CORE

Experiment No.	Pressure psi.	Temperature °C	Residence Time min.	Feed, gm.		Liquid Products, gm.						Gas Products, gm.			
				O_2	CH_4	HCHO	HCOOH	CH_3OH	Acetone	MF	H_2O	O_2	CO	CO_2	CH_4
132	15,400	270	60	20.01	105.5	.0064	.0054	.1584	0	0	2.877	19.96	0	.1638	104.0
126	14,600	285	60	18.63	98.2	.0143	.0094	.1909	Trace	Trace	3.890	17.65	0	.9393	97.32
130	16,000	295	60	19.54	103.0	.0127	.0099	.0496	0	0	5.434	17.85	0	.9930	102.2
128	15,000	305	60	18.54	97.69	.0297	.0141	.4416	0	Trace	6.937	8.362	2.066	4.331	94.61
131*	15,000	310	60	18.38	96.86	.0236	.0177	2.193	0	.0481	6.152	3.745	3.626	--	92.32
116	47,200	251	60	28.89	164.3	.0013	.0059	.0111	.0059	0	.9827	30.05	0	.0390	162.1
119	50,000	255	60	31.38	178.5	.0066	.0031	.0478	.0062	Trace	1.162	30.67	0	.5919	177.2
121	49,100	270	60	30.14	171.4	.0056	.0045	.0195	Trace	0	1.269	29.03	0	.8114	170.2
136	50,300	270	60	32.29	170.2	.0010	.0024	0	0	0	.9996	29.79	0	.8773	170.5
122	51,200	280	60	30.63	174.2	.0056	.0035	.0281	0	0	1.568	28.80	0	1.359	173.02
129	50,400	285	60	32.24	169.9	.0215	.0086	.2393	Trace	Trace	5.866	22.86	1.589	4.766	166.6
127	48,900	295	60	31.41	165.5	.0202	.0329	.6810	Trace	Trace	6.750	3.183	2.725	15.44	158.6
137	49,200	295	60	31.74	167.2	.0168	.1132	.7806	0	Trace	9.567	2.628	2.387	17.88	159.5
125*	49,000	303	3	31.44	165.7	.0749	.0357	5.523	.0115	.0669	5.818	2.439	8.563	7.637	156.8
142*	49,000	304	7	29.10	166.8	.0946	.0830	5.061	Trace	.0664	11.29	2.642	4.928	11.37	157.0
120	95,400	255	34	37.53	213.5	.0076	.0177	.0476	.0091	.0014	1.358	35.84	0	.7081	213.4
123	95,700	270	34	39.76	209.6	.0058	.0142	.0277	.0042	Trace	1.332	36.31	0	1.075	209.4
140	99,700	270	60	35.57	207.2	.00225	.00176	.02642	Trace	Trace	.9480	31.163	0	3.709	206.1
124	96,100	285	34	38.73	204.2	.0183	.0234	.2316	.0046	.0046	4.304	26.84	0	6.391	204.0
143	98,400	295	0	36.92	211.6	.0142	.0161	.0753	.0037	.0033	2.069	33.41	0	1.894	210.4
145	99,200	295	8	36.33	208.2	.0157	.0331	.1810	.0034	.0075	3.175	28.58	0	5.242	206.5
141	99,100	295	14	36.17	207.32	.0129	.0215	.2622	Trace	.0070	3.610	24.10	0	6.934	206.9
133	96,500	295	34	38.89	204.9	.0246	.0348	.3308	0	.0102	7.853	17.27	1.921	12.23	199.9
144	93,000	365	6	34.58	198.2	.1416	.0787	6.215	.0098	.1219	13.11	3.378	4.768	12.91	190.0

TABLE 6. (CONTINUED)

Experiment No.	Pressure psi.	Temperature °C	Residence Time min.	Liquid Products, gm. O_2	CH_4	HCHO	HCOOH	CH_3OH	Acetone	MF	H_2O	Gas Products, gm. O_2	CO	CO_2	CH_4
				PYREX HEATER CORE											
172	15,400	270	60	17.02	98.54	.00094	0	.00051	0	0	.3606	16.82	0	0	98.14
147	15,700	285	60	16.60	95.16	.00155	.00310	.00775	0	0	.95660	15.46	0	1.018	93.91
154	14,600	295	34	16.04	90.36	.01059	.00822	.07459	Trace	0	2.069	12.09	.9525	2.005	89.19
148*	15,500	295	60	16.03	91.87	.01369	.02129	1.665	Trace	.00760	5.896	1.706	2.256	7.652	87.02
157	15,000	300	60	16.10	90.70	.01904	.01523	.2264	Trace	0	3.970	7.602	1.600	3.275	88.55
169	15,000	305	60	15.79	91.43	.01596	.01190	.1074	Trace	Trace	2.767	10.75	1.084	2.757	89.64
159*	15,200	309	1.5	16.44	92.62	.06240	.04101	2.639	.01613	.00080	6.145	2.726	3.649	4.384	86.85
173	15,200	310	60	16.10	93.21	.01221	.01143	.09742	0	0	2.477	10.81	0	2.680	92.64
160	49,500	270	60	28.25	156.4	.00728	.00743	.04799	.02755	Trace	1.442	24.61	0	2.573	155.8
149*	49,500	284	60	27.53	151.8	.02349	.09257	2.377	Trace	.00318	11.29	2.361	1.340	17.77	149.9
155	49,400	285	60	27.83	156.8	.02013	.02339	.2938	.01197	Trace	5.089	15.42	1.570	7.173	153.7
166	48,000	290	0	28.57	158.2	--	.01766	.03702	.02293	Trace	1.339	25.33	0	1.385	158.4
152*	50,200	290	1.1	28.25	159.2	.08638	.05759	6.606	.02541	.09655	10.06	2.798	6.118	9.177	149.4
161	49,500	290	8	28.13	155.7	--	.01962	.1754	.08443	.00922	2.670	22.09	0	3.339	155.2
158	49,600	290	20	27.61	155.6	.01709	.01612	.1402	.02321	Trace	3.023	21.06	0	2.955	155.2
162	50,000	290	34	28.56	158.1	--	.02807	.2859	.05198	.00125	4.800	16.63	0	.7501	155.1
156	49,200	290	60	29.35	165.4	.02897	.03210	.3523	.01644	Trace	7.395	12.48	1.555	9.324	152.3
168	49,800	295	60	27.60	159.8	.02789	.03501	.2225	.00593	.00297	5.639	15.81	1.445	7.976	155.9
176	49,200	322	2	27.93	161.7	.08715	.09228	7.929	.02392	.1196	8.837	2.484	4.271	10.53	151.1
151	97,000	270	34	34.08	192.0	.00364	.00692	.05972	.00398	Trace	1.656	29.64	0	1.906	193.0
150	97,700	270	60	33.79	193.7	.00554	.00831	.09138	.00277	Trace	2.661	28.34	0	4.446	192.4
153	97,000	280	8	34.49	194.3	.00776	.00961	.06323	.01686	Trace	1.585	30.35	0	2.736	194.3
146*	112,000	281	7.8	34.55	198.1	.1075	.08714	7.787	.01854	.01817	10.36	2.544	5.596	14.37	187.3
165	98,800	285	0	36.31	201.0	--	.02310	.07512	.05258	Trace	1.718	33.41	0	1.570	200.0
163	97,700	285	9	35.51	196.6	.01899	.01728	.1049	.02118	.00267	2.269	30.62	0	2.529	196.0
175	99,300	285	20	34.60	200.3	.0110	.0104	.0471	.0128	.0007	1.367	32.55	0	2.142	198.1
164	99,700	285	34	36.13	200.0	.0168	.0194	.1775	.0097	.0041	3.509	28.22	0	5.705	197.9
174	97,800	295	0	34.41	199.2	.0079	.0076	.0328	.0043	Trace	1.260	30.75	0	2.202	199.3
171	99,000	295	9	34.68	200.8	.0147	.0162	.0603	.0058	Trace	2.523	29.29	0	3.874	199.1
170	98,100	295	34	34.38	199.0	.0203	.0224	.1726	.0063	.0359	4.256	24.95	0	6.611	196.7

*Nonisothermal Reaction

TABLE 7.

MATERIAL BALANCES

Run No.	Uncorrected for Water			Corrected for Water			C/H
	O	C	H	O	C	H	
132	111.8	97.18	98.33	104.7	98.71	99.03	2.990
126	114.3	96.95	98.34	102.9	99.41	99.47	3.000
130	116.9	96.50	98.43	101.7	99.61	99.88	2.992
128	103.8	99.23	99.56	100.7	99.91	99.87	3.001
116	103.0	99.85	99.97	103.0	99.85	99.97	2.996
119	102.5	99.43	99.60	102.5	99.43	99.60	2.995
121	102.1	99.48	99.61	102.1	99.48	99.61	2.996
136	97.00	100.4	100.5	97.00	100.4	100.5	2.997
122	101.9	99.58	99.71	101.9	99.58	99.71	2.996
129	101.1	99.67	99.52	101.1	99.67	99.52	3.004
127	74.38	105.0	102.3	96.47	100.2	100.1	3.000
137	84.39	103.5	101.2	98.69	100.4	99.75	3.019
125*	70.06	106.3	103.1	94.83	100.9	100.6	3.010
142*	92.24	101.4	100.1	100.0	99.83	99.40	3,013
120	99.47	100.1	100.3	99.47	100.1	100.3	2.994
123	96.74	100.5	100.7	98.59	100.1	100.5	2.990
140	97.78	100.4	99.9	98.83	100.2	99.81	3.010
124	91.92	101.6	101.4	93.84	101.2	101.2	3.007
143	99.39	99.8	99.88	99.39	99.80	99.88	3.000
145	97.29	100.1	99.88	97.29	100.1	99.88	3.001
141	90.44	101.7	101.3	93.58	101.1	101.0	3.004
133	90.05	102.0	101.0	97.74	100.3	100.2	3.004
144*	88.80	102.1	101.3	93.18	101.2	100.9	3.011
172	98.82	99.61	99.62	100.7	99.61	99.78	2.995
147	102.8	99.08	99.15	102.8	99.08	99.15	2.998
154	99.65	100.2	99.78	99.65	100.2	99.78	3.012
148*	92.73	101.5	99.88	99.78	100.1	99.23	3.026
157	91.73	101.5	101.1	98.74	100.1	100.5	2.989
169	100.7	99.89	99.47	100.67	99.89	99.47	3.013
159*	92.41	101.5	100.4	99.33	100.2	99.79	3.011
173	93.54	100.9	101.0	95.51	100.5	100.8	2.991

TABLE 7. (CONTINUED)

Run No.	Uncorrected for Water O	C	H	Corrected for Water O	C	H	C?H
160							
149*	99.38	100.3	98.91	99.38	100.3	98.91	3.042
155	95.03	101.2	100.4	99.06	100.3	99.97	3.011
166	96.48	100.5	100.5	96.48	100.5	100.5	3.000
152*	91.20	101.9	100.4	99.20	100.3	99.62	3.020
161	96.06	100.5	100.5	96.06	100.5	100.5	3.001
158	94.60	101.1	101.2	97.31	100.5	101.0	2.987
162	94.17	101.2	100.6	99.40	100.1	100.1	3.000
156	96.90	100.2	99.47	98.24	99.89	99.34	3.017
168	100.0	99.98	99.23	100.0	99.98	99.23	3.023
176*	89.86	102.0	100.5	99.38	100.1	99.59	3.016
151	95.46	100.9	100.9	95.46	100.9	100.9	3.000
150	100.7	100.2	99.97	100.6	100.2	99.97	3.006
153	96.99	100.5	100.4	97.99	100.5	100.4	3.005
146*	86.62	101.6	100.6	95.44	100.8	99.80	3.032
165	99.55	99.82	99.90	99.55	99.82	99.90	2.998
163	97.31	100.2	100.3	97.31	100.2	100.3	2.999
175	102.2	99.33	99.22	102.2	99.33	99.22	3.003
164	98.54	100.0	99.77	98.54	100.0	99.77	3.021
174	97.64	100.5	100.4	97.41	100.5	100.4	3.004
171	99.16	99.87	99.75	99.16	99.87	99.75	3.004
170	98.16	100.3	100.1	99.25	100.9	99.95	3.004

*Non Isothermal Reaction

TABLE 8.

SUMMARY OF PRODUCT DATA

ALUMINA CORE

Run No.	Concentration, Moles/Mole-ltr x 10^3									
	HCHO	HCOOH	CH_3OH	Acetone	MF	H_2O	O_2	CO	CO_2	CH_4
132	.0589	.0448	1.596	0	0	16.12	201.1	0	1.200	2095
126	.1655	.0709	2.063	0	0	17.29	190.7	0	7.404	2103
130	.1394	.0711	.5113	0	0	26.22	184.2	0	7.451	2109
128	.3446	.1068	4.805	0	0	118.7	90.99	25.69	34.27	2059
131	.2763	.1352	24.06	0	.2812	120.0	41.08	45.47		2080
116	.0089	.0291	.0721	.0235	0	11.38	186.0	0	2.176	2132
119	.0423	.0127	.2866	.0207	0	12.39	183.9	0	2.582	2125
121	.0371	.0197	.1216	0	0	14.09	181.2	0	3.683	2125
136	.0066	.0103	0	0	0	11.10	186.1	0	4.056	2129
122	.0369	.0150	.1725	0	0	17.12	177.0	0	6.073	2126
129	.1432	.0373	1.497	0	0	65.23	143.0	11.36	21.69	2085
127	.1385	.1472	4.373	0	0	179.8	20.44	20.00	72.32	2037
137	.1136	.5005	4.960	0	0	176.3	16.70	17.34	82.63	2027
125	.5129	.1594	35.42	.0408	.2289	180.3	15.65	62.79	35.63	2012
142	.6484	.3709	32.54	0	.2275	163.3	16.98	36.20	53.15	2018
120	.0408	.0617	.2385	.0251	.0038	12.10	179.6	0	1.235	2139
123	.0315	.0505	.1411	.0117	0	12.06	185.0	0	3.984	2133
140	.0124	.0063	.1369	0	0	13.34	161.5	0	13.98	2136
124	.1023	.0850	1.211	.0131	.0127	49.20	140.04	0	24.32	2134
143	.0165	.0568	.3815	.0103	.0089	18.64	169.3	0	6.997	2132
145	.0864	.1188	.9322	.0096	.0207	29.06	147.1	0	19.63	2126
141	.0711	.0775	1.356	0	.0192	47.00	124.6	0	26.08	2140
133	.1359	.1254	1.716	0	.0282	109.7	89.57	11.39	46.15	2074
144	.8169	.2960	33.62	.0293	.3516	145.2	18.27	29.46	50.77	2055

TABLE 8. (CONTINUED)

Run No.	Concentration, Moles/Mole-ltr x 10^3									
	HCHO	HCOOH	CH_3HO	Acetone	MF	H_2O	O_2	CO	CO_2	CH_4
172	.0120	--	.0060	0	0	7.658	200.9	0	0	2345
147	.0244	.0306	.0956	0	0	20.98	190.7	0	9.134	2317
154	.1465	.0740	.9671	0	0	47.69	156.8	14.12	18.91	2313
148	.1866	.1892	21.28	0	.0517	168.1	21.81	32.96	71.10	2224
157	.2625	.1368	2.925	0	0	121.1	98.20	23.62	30.77	2288
169	.2192	.1065	1.382	0	0	63.33	138.5	15.95	25.81	2308
159	.8419	.3607	33.39	.1126	.051	194.6	34.47	52.75	40.33	2198
173	.1644	.1004	1.230	0	0	64.52	136.5	0	24.61	2340
160	.0581	.0386	.3594	.1139	0	19.21	184.3	0	14.02	2334
149	.1861	.4792	17.68	0	.1260	149.4	17.57	11.40	96.17	2230
155	.1604	.1216	2.195	.0491	0	87.51	115.2	13.40	39.00	2297
166		.0910	.2742	.0937	0	17.64	187.6	0	7.462	2347
152	.6782	.2948	48.64	.1033	.3789	171.5	20.60	51.49	49.13	2200
161		.1026	1.320	.3504	.0370	35.71	166.2	0	18.27	2336
158	.1373	.0843	1.057	.0964	0	53.7	158.6	0	16.19	2338
162		.1447	2.119	.2126	.049	89.51	123.3	0	40.44	2299
156	.2190	.1581	2.497	.0643	0	99.5	88.38	12.59	48.05	2158
168	.2191	.1794	1.639	.0241	.0116	73.86	116.5	12.17	42.74	2298
176	.6767	.4673	57.72	.0960	.4644	245.4	18.08	35.53	55.75	2200
151	.0236	.0293	.3643	.0134	0	17.96	180.9	0	8.455	2355
150	.0357	.0350	.5540	.0092	0	28.66	171.8	0	19.50	2332
153	.0499	.0404	.3812	.0560	0	16.99	183.0	0	12.00	2344
146	.6817	.3594	46.17	.0607	.573	153.2	15.08	37.89	61.93	2221
165		.0937	.4378	.1691	0	17.80	194.7	0	6.653	2332
163	.1202	.0725	.6256	.0687	.0076	24.04	182.5	0	10.96	2337
175	.0690	.0427	.2768	.0413	.0022	14.28	191.3	0	9.154	2329
164	.1051	.0792	1.040	.0314	.0128	36.55	165.3	0	24.31	2319
174	.0497	.0313	.1940	.0141	0	13.24	181.7	0	9.463	2356
171	.0917	.0662	.3533	.0019	0	26.30	171.7	0	16.52	2334
170	.1272	.0922	1.021	.0205	.1131	50.01	147.6	0	28.44	2327

APPENDIX B

CALIBRATION OF CHROMATOGRAPHS

APPENDIX B

CALIBRATION OF CHROMATOGRAPHS

The calibration curves for oxygen, carbon monoxide and carbon dioxide in methane are given in Figures 44, 45 and 46. The gas samples were mixed in 500 cu. in. cylinders. Methane was added first and pressure was increased successively by addition of the other gases. The volume of each gas was taken to be equal to its partial pressure in the mixture. Each sample was analyzed three times, and the areas of the chromatogram were measured using a planimeter. The lines were determined by the method of least squares.

Calibration curves for methanol, methyl formate and acetone in water are shown in Figures 47, 48 and 49. The samples were prepared either by weight or by use of calibrated pipettes.

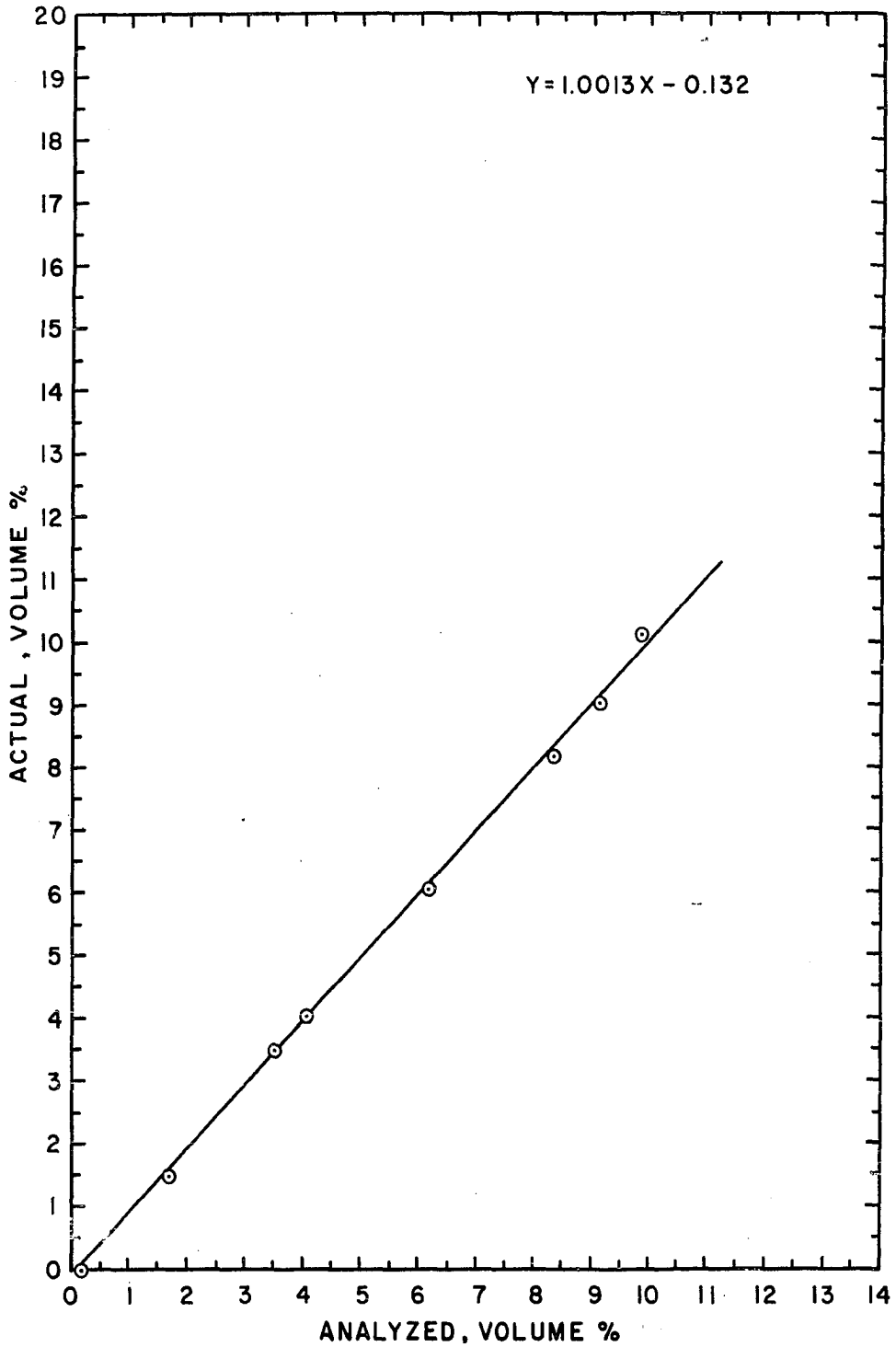


Figure 44. Chromatographic Calibration Curve for Oxygen.

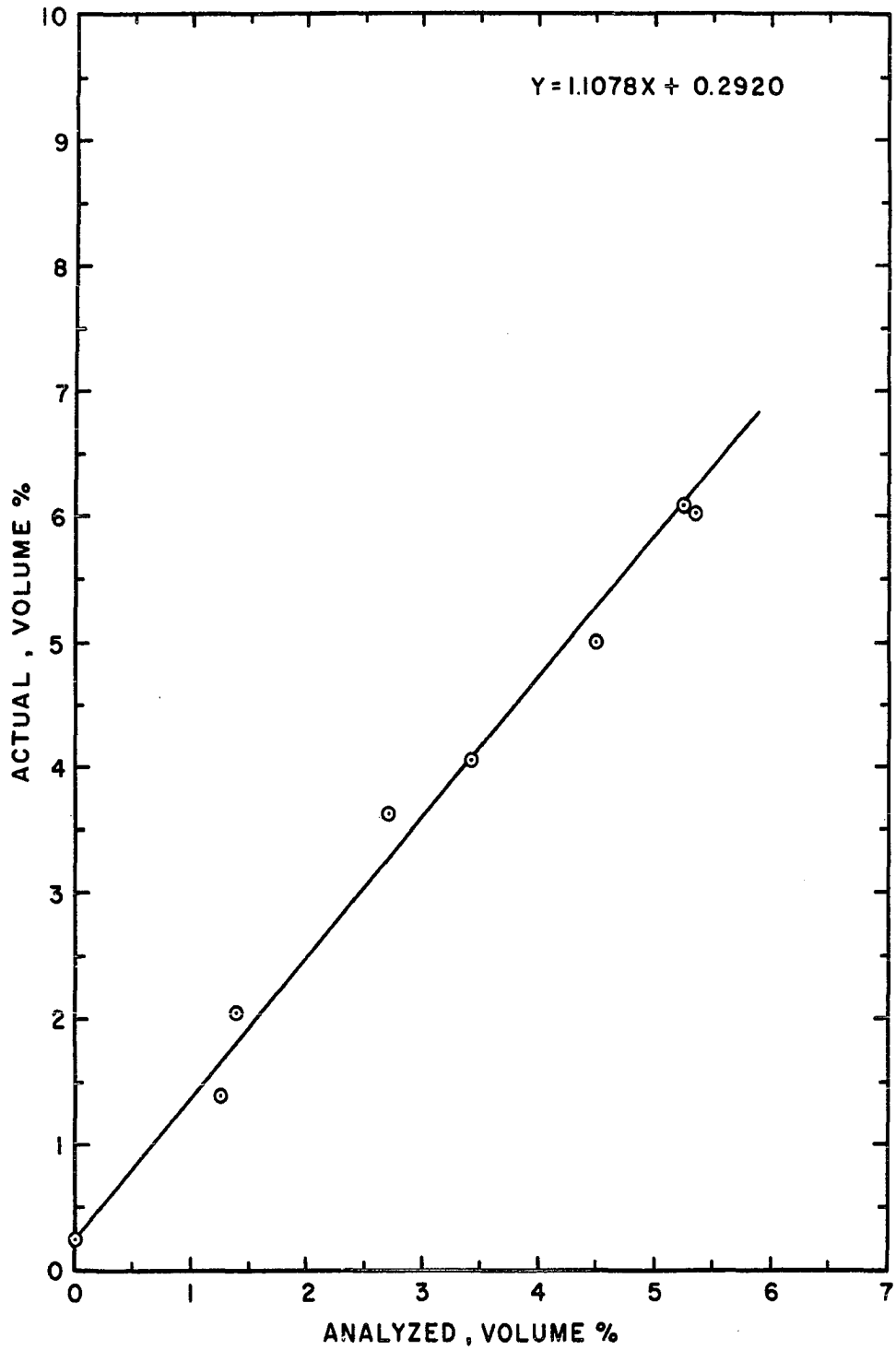


Figure 45. Chromatographic Calibration Curve for Carbon Monoxide.

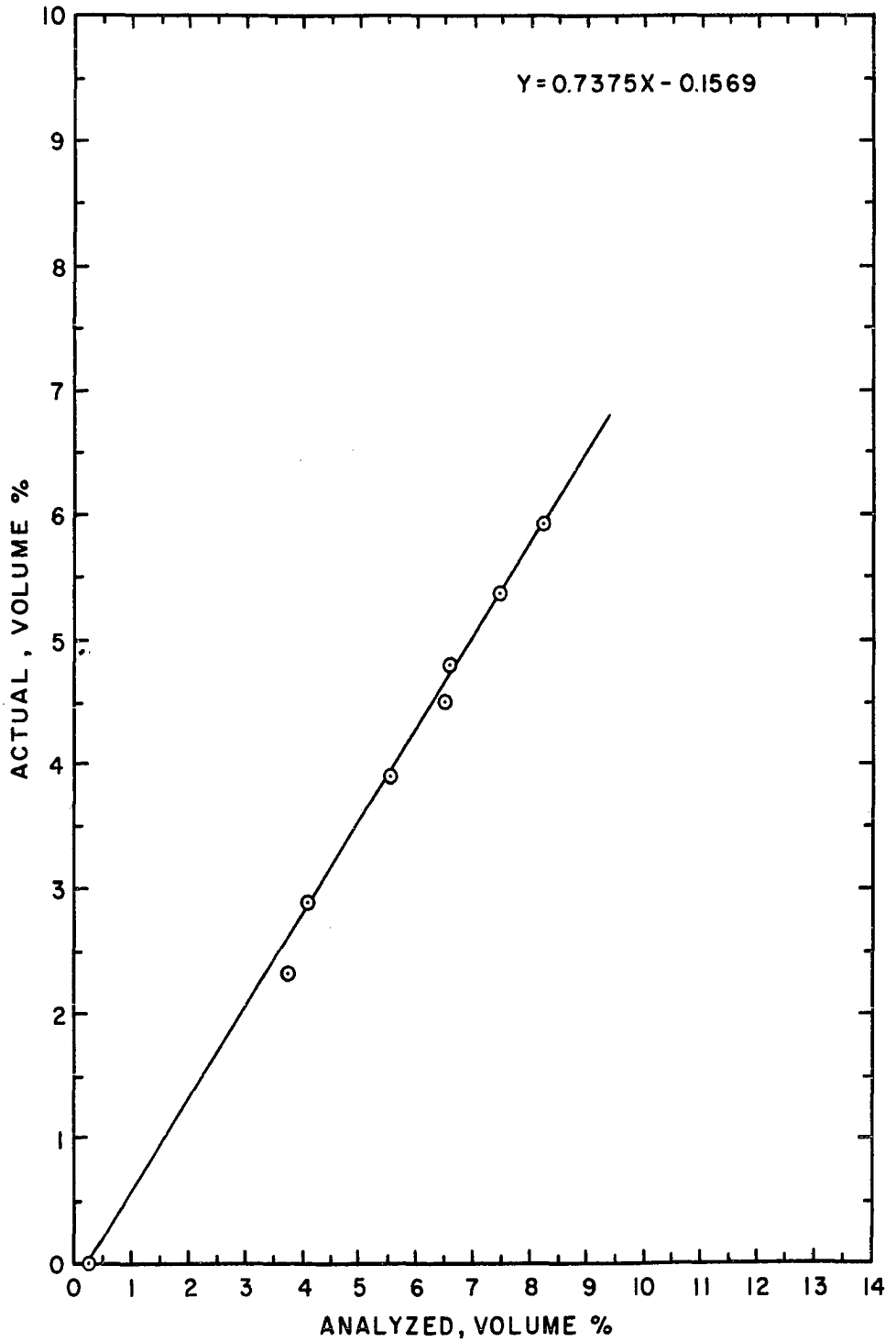


Figure 46. Chromatographic Calibration Curve for Carbon Dioxide.

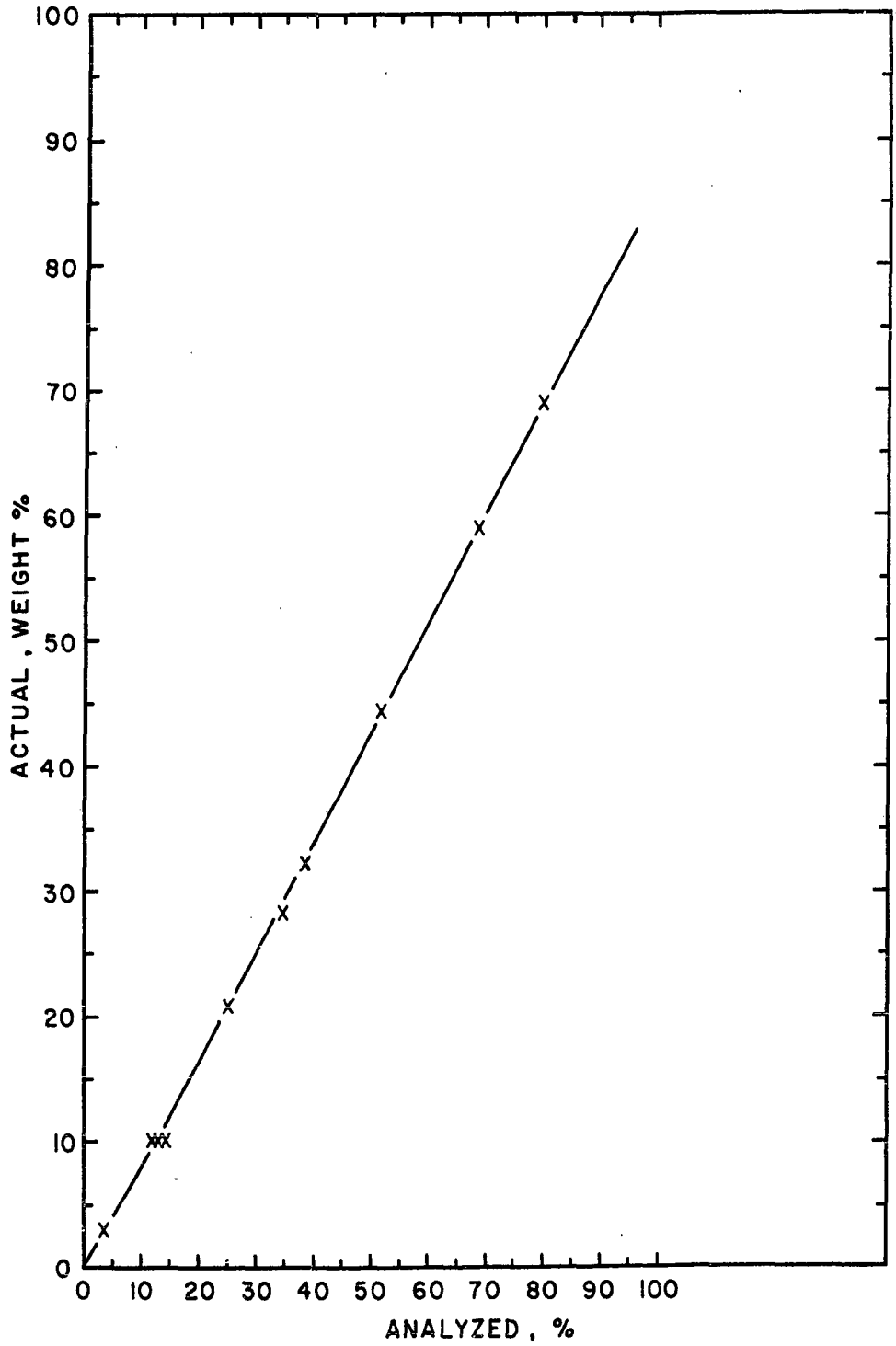


Figure 47. Chromatographic Calibration Curve for Methanol.

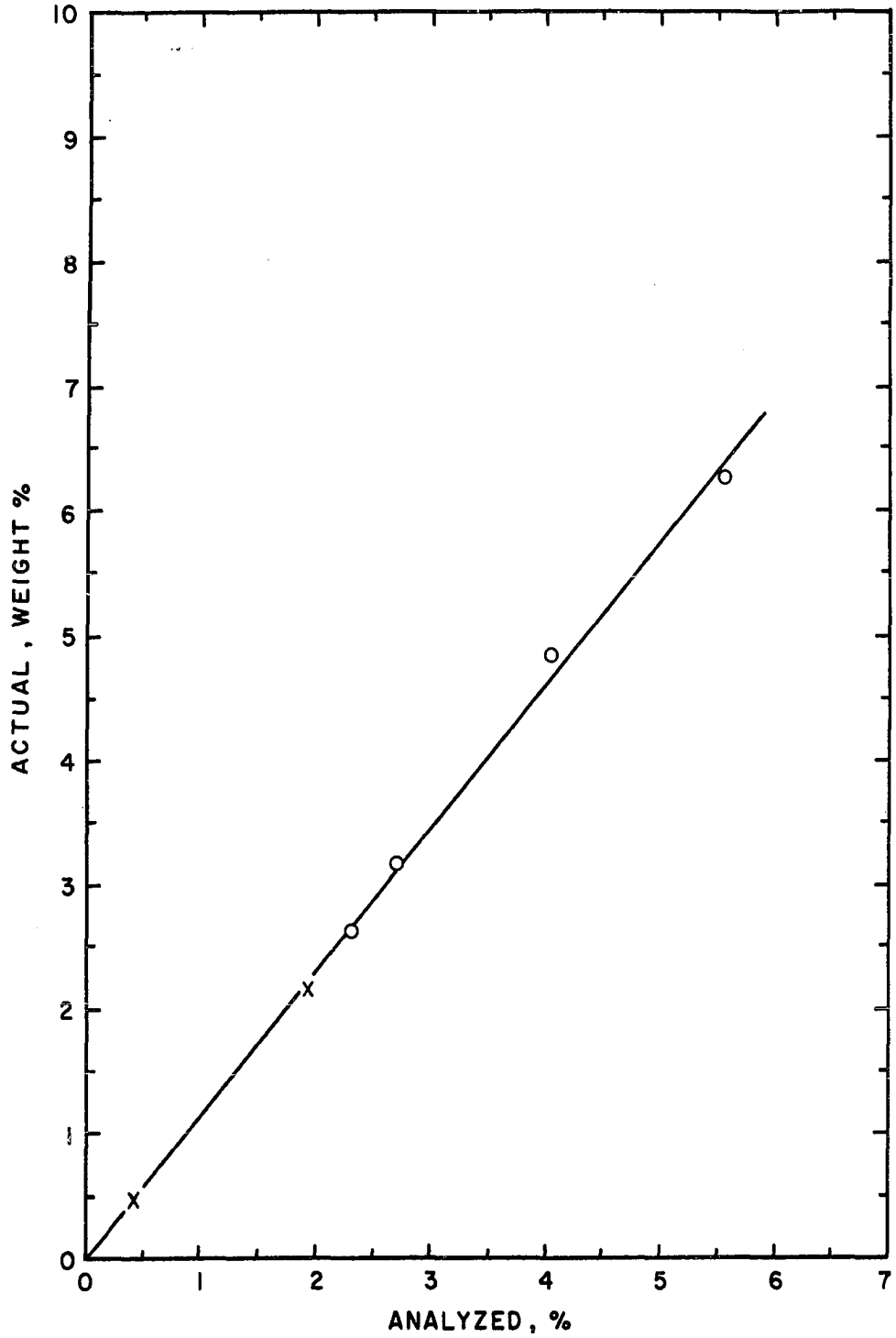


Figure 48. Chromatographic Calibration Curve for Methyl Formate

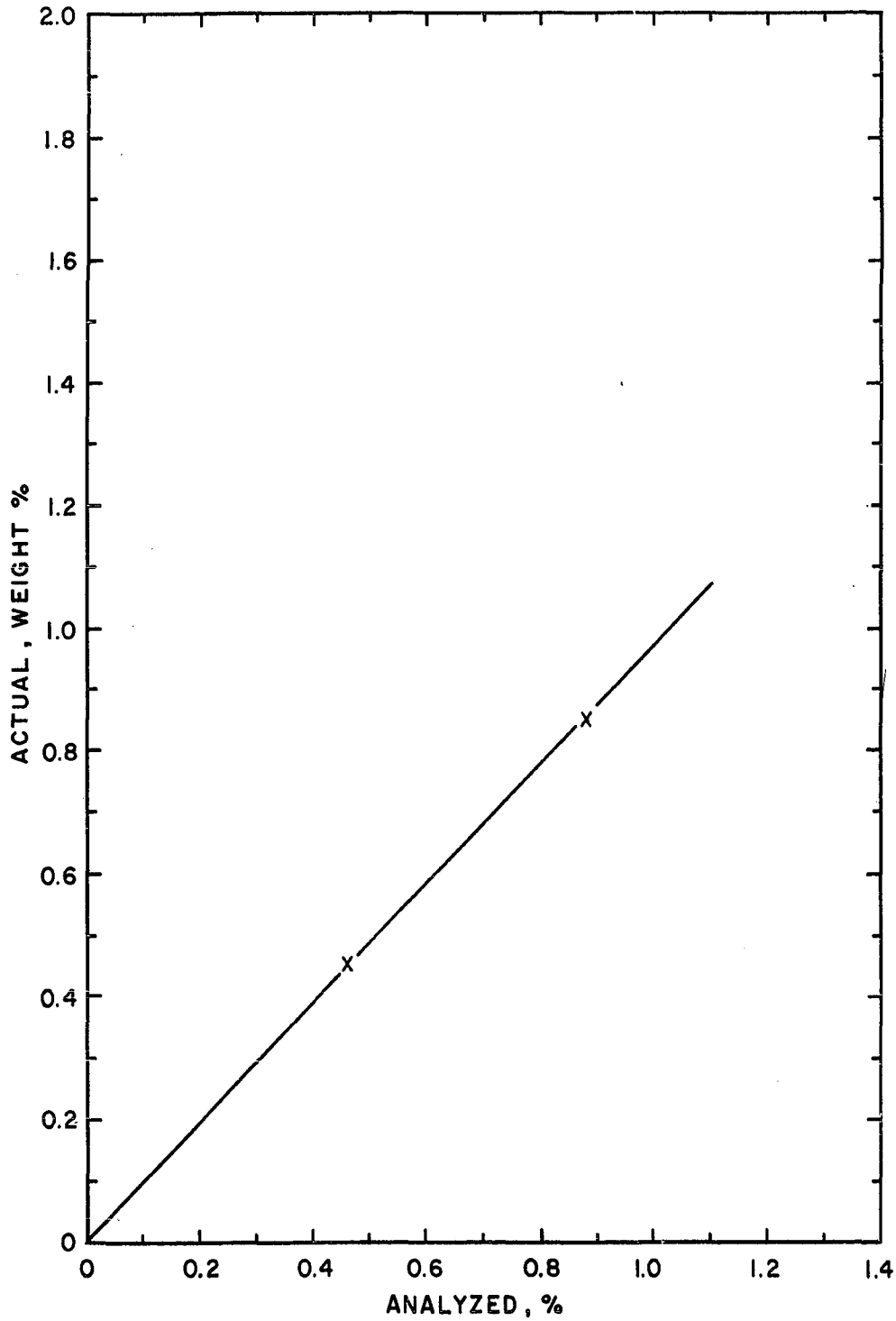


Figure 49. Chromatographic Calibration Curve for Acetone.

APPENDIX C

CHECK OF ANALYTICAL METHODS FOR FORMALDEHYDE, FORMIC ACID, AND METHANOL

APPENDIX C

CHECK OF ANALYTICAL METHODS FOR FORMALDEHYDE, FORMIC ACID, AND METHANOL

Three samples were prepared using calibrated pipettes:

	Wt. Percent
Formaldehyde	1.13
Formic Acid	3.00
Methanol	22.89
Water	72.98

Results of Analyses:

	Wt. Percent		
	Sample 1	Sample 2	Sample 3
Formaldehyde	1.24	1.11	1.20
Formic Acid	3.00	2.62	2.67
Methanol*	21.3	23.2	24.6
Water	74.5	73.1	71.5

	Average Error, Percent
Formaldehyde	+ 4.4
Formic Acid	- 8.0
Methanol	- 0.44
Water	0

*Determined from chromatographic analyses.

APPENDIX D

CURVE FOR CORRECTION OF FORMALDEHYDE CONCENTRATION IN THE PRESENCE OF ACETONE

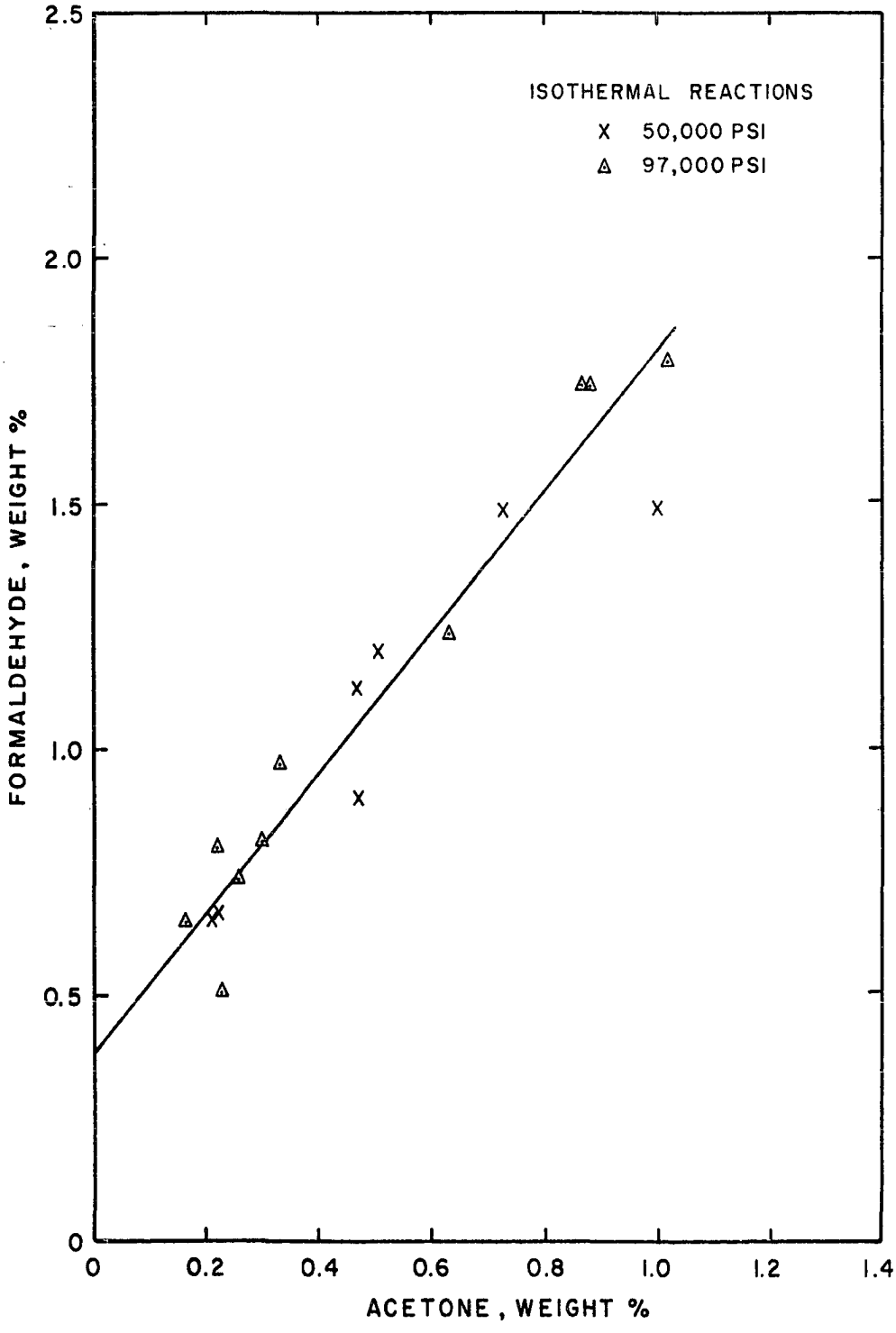


Figure 50. Curve to Correct Concentration of Formaldehyde in Presence of Acetone.

APPENDIX E

SAMPLE CALCULATION OF MATERIAL BALANCE

Experiment No. 129

PRODUCT LIQUID

Composition:	Wt. Fract.
HCHO	.0035
HCOOH	.0014
CH_3OH	.0390
Acetone	0
M. F.	0
H_2O	.9561

Weight 6.135 gm.

TOTAL PRODUCT

Weight: 204.7 gm.

Composition:

HCHO	.02147
HCOOH	.008589
CH_3OH	.2393
Acetone	0
M.F.	0
H_2O	5.866
O_2	22.86
N_2	2.740
CO	1.589
CO_2	4.766
CH_4	166.6

FEED

	Mole Fract.	Wt. gm/ mole	Wt. Fract.	Wt. gm.
O_2	.0859	2.749	.1575	32.24
N_2	.0080	.224	--	--
CH_4	.9061	14.498	.8300	169.9
		17.471		

PRODUCT GAS

Compositions:	Wt. gm/mole	Wt. Fract.
O_2 .0627 x 32 =	2.0064	.11510
N_2 .0086 x 28 =	.2408	.013813
CO .0050 x 28 =	.1400	.008031
CO_2 .0094 x 44 =	.4180	.023978
CH_4 .9142 x 16 =	14.627	.83908
	17.432	

Receivers:

Pressure = 19.055 atm.
temp. = 303.5°K
Z = .97004

Weight:

Receivers:

$$\frac{19.055 \times 173.04 \times 17.432}{.97004 \times 303.5} = 195.24 \text{ gm.}$$

RI:

$$\frac{19.055 \times 5.19}{518} = \frac{3.33 \text{ gm.}}{198.57 \text{ gm.}}$$

MATERIAL BALANCES

wt. gm.

	O	C	H
Feed:	32.24	127.4	42.47
Product:			
HCHO	.0115	.00860	.00144
HCOOH	.00599	.00224	.00037
CH_3OH	.1197	.0897	.0299
Acetone	0	0	0
MF	0	0	0
H_2O	5.215	0	.6511
O_2	22.86	0	0
CO	.9073	.6817	0
CO_2	3.465	1.301	0
CH_4	0	124.95	41.68
	32.59	127.0	42.27
% Recovery	101.1	99.67	99.52

APPENDIX F

CALCULATIONS FOR WET TEST METER

APPENDIX F

CALCULATIONS FOR WET TEST METER

A check on the calibration of the wet test meter was carried out using a 500 cu. in. sample of methane containing six volume percent oxygen and two volume percent carbon monoxide. Bomb pressure was 27.69 in. Hg gauge at 24.5°C. Barometric pressure was 28.73 in. Hg and wet test meter temperature was 20.8°C.

Wet test meter final reading	12.035 cu. ft.
Wet test meter initial reading	11.765 cu. ft.
Volume used	0.270 cu. ft.

Wet test meter corrected volume

$$= 0.270 \times \frac{28.73}{29.92} \times \frac{273}{293.8} = \underline{0.240} \text{ std. cu. ft.}$$

$$\text{Corrected pressure in cylinder} = 1 + \left(\frac{27.69}{29.92} \times \frac{273}{297.5} \right)$$

$$= 1.849 \text{ std. atm.}$$

$z = 0.9978$

$$\text{Cylinder Vol.} = \frac{(1.849 - 1)500 \times 16.31 \times 22.400}{.9978 \times 273 \times 82.06} = 6937 \text{ cc.}$$

$$= \frac{6937}{1728 \times 16.31} = \underline{0.246} \text{ std. cu. ft.}$$

An excellent check was obtained.

Sample calculations of feed gas weight for:

Experiment 150

Wet Test Meter

$$\text{Volume corrected} = 11.62 \times \frac{492}{543} \times \frac{28.37}{29.92} = 10.02 \text{ std. cu. ft.}$$

$$\text{Meter, moles} = \frac{10.02 \times 453.6}{359} = 12.66 \text{ gm. moles}$$

$$\text{Receivers, 0 to 1 atm.} = \frac{173.04}{.9904 \times 308} = .563 \text{ gm. moles}$$

$$\text{Reactor, 0 to 1 atm.} = \frac{4.74}{519} = .0091 \text{ gm. moles}$$

Total by wet test meter 13.23 gm. moles

Receiver Pressure

Calculated using computer 13.12 gm. moles

Experiment 152

Wet Test Meter

$$\text{Volume corrected} = 8.570 \times \frac{492}{543} \times \frac{28.69}{29.93} = 7.444 \text{ std. cu. ft.}$$

$$\text{Meter, moles} = \frac{7.444 \times 453.6}{359} = 9.408 \text{ gm. moles}$$

$$\text{Receivers, 0 to 1 atm.,} = \frac{173.04}{.9904 \times 308} = .563 \text{ gm. moles}$$

$$\text{Reactor, 0 to 1 atm.} = \frac{4.74}{526} = .0090 \text{ gm. moles}$$

Total by wet test meter = 9.980 gm. moles

Receiver Pressure

Calculated using computer 9.938 gm. moles

The check in both cases is excellent.

This dissertation has been
microfilmed exactly as received 67-3975

HARDWICKE, Norman Lawson, 1924-
THE MECHANISM OF PARTIAL OXIDATION OF METHANE AT HIGH PRESSURES.

The University of Oklahoma, Ph.D., 1967
Engineering, chemical

University Microfilms, Inc., Ann Arbor, Michigan